Design and control strategy of powertrain in hybrid electric vehicles

Alexandre Ravey

University of Technology of Belfort-Montbéliard
Graduate school SPIM (Engineering sciences and microtechnology)

THESIS

Presented at

The University of Technology of Belfort-Montbéliard
in order to obtain the title of
Doctor of Philosophæ

by

ALEXANDRE RAVEY
Engineer at University of Technology of Belfort-Montbéliard
Electric Engineering and Control Systems Department

CONCEPTION ET GESTION DE L'ÉNERGIE DES ARCHITECTURES POUR VÉHICULES HYBRIDES ÉLECTRIQUES

Thesis committee :

M. Mohamed EL Hachemi BENBOUZID	Université de Brest
M. Thierry-marie GUERRA	Université de Valenciennes
M. Mohamed GABSI	Ecole Normale Supérieure de Cachan
M. Pascal BROCHET	Université Technologique de Belfort-Montbéliard
M. Abdellatif MIRAOUI	Université de Cadi Ayyad
M. Srdjan Miodrag LUKIC	North Carolina State University
M. David BOUQUAIN	Université Technologique de Belfort-Montbéliard

Alexandre Ravey : *Conception et gestion de l'énergie des architectures pour véhicules hybrides électriques ,* Phd Thesis.

In the memory of Dr. Benjamin Blunier

ABSTRACT

Hybrid electric vehicle have known a quickly grow in the last 10 years. Between conventional vehicles which are criticized for their CO_2 emission and electric vehicles which have a big issue about autonomy, hybrid electric ones seems to be a good trade of. No standard has been set yet, and the architectures resulting of theses productions vary between brands. Nevertheless, all of them are design as a thermal vehicle with battery added which leads to bad sizing of the component, specially internal combustion engine and battery capacity. Consequently, the control strategy applied to its components has a lot of constraints and cannot be optimal.
This thesis investigate a new methodology to design and control a hybrid electric vehicle. Based on statistical description of driving cycle and the generation of random cycle, a new way of sizing component is presented. The control associate is then determined and apply for different scenarios : firstly a heavy vehicle : A truck and then a lightweight vehicle. An offline control based on the optimization of the power split via a dynamic programming algorithm is presented to get the optimal results for a given driving cycle. A real time control strategy is then define with its optimization for a given patterns and compared to the offline results. Finally, a new control of plug in hybrid electric vehicle based on destination predictions is presented.

RESUMÉ

Depuis une dizaine d'années, les constructeurs et les grands groupes du secteur de l'automobile se sont mobilisés autour de la recherche et du développement de nouveaux prototypes de véhicules économes (moins consommateurs d'énergie) et propres (moins de rejets de polluants) tels que les véhicules hybrides et tout électriques. C'est une nouvelle mutation. Elle fait profondément évoluer l'automobile, d'une architecture de propulsion thermique, devenue maîtrisée mais fortement polluante, vers une traction électrique ou hybride plus complexe et peu, voire pas du tout, maîtrisée ; le nombre de composants (sources d'énergie, actionneurs, contrôleurs, calculateurs, ...) devient important, de nature multidisciplinaire et possédant beaucoup de non linéarités. De plus, faute de maturité dans ce domaine, à ce jour l'industrie de l'automobile ne possède pas encore les connaissances suffisantes nécessaires à la modélisation, à la simulation et à la conception de ces nouveaux véhicules et plus particulièrement les dispositifs relatifs aux sources d'énergie et aux différents actionneurs de propulsion.

Les travaux de cette thèse visent à donner des méthodes de conception d'une chaine de traction hybride et d'en gérer la gestion de l'énergie. La thèse s'appuie sur l'exemple de la conception et la gestion de l'énergie d'un véhicule hybride basé sur une pile à combustible et des batteries.
Dans un premier temps, un méthode de dimensionnement des composants de la chaine de traction est présentée : Elle consiste en l'étude statistique de cycle de conduite générés pseudo aléatoirement représentatif de la conduite en condition réelle de véhicule. Un générateur de cycle de conduite à été crée et est présenté, et la méthode de dimensionnement de la source primaire, ici une pile a combustible, ainsi que le source secondaire de puissance, ici des batteries, est détaillée. Un exemple est pris pour illustrer cette méthode avec la conception d'un véhicule de type camion poubelle décrivant des cycles de conduites urbains à arrêts fréquents.
Dans un second temps, la gestion de l'énergie de la chaine de traction hybride série est étudiée : une gestion de l'énergie "offline" est présentée, basé sur l'optimisation par programmation dynamique. Cette optimisation permet d'avoir le découpage de la puissance par les deux sources de la chaine de traction de manière optimal pour un cycle précis. De part l'aspect déterministe de la programmation dynamique, les résultats servent de référence quant au futurs développements de gestion temps réel.
Un contrôleur temps réel basé sur la logique floue est ainsi exposé et les résultats sont comparés par rapport à la gestion "offline". Le contrôleur est ensuite optimisé et rendu adaptatif par un algorithme génétique et un algorithme de reconnaissance de type de profil routier.
Enfin, une introduction à la gestion de l'énergie dans les véhicules hybrides de

type : “plug in” est présentée : Elle repose sur le principe de la détermination de la distance restante à parcourir par la reconnaissance de la destination à l’aide d’une matrice de probabilité de Markov.

TABLE OF CONTENTS

LIST OF FIGURES

LIST OF TABLES

ACKNOWLEDGMENTS

At first, I would like to thank Dr. Mohamed EL Hachemi Benbouzid and Dr. Thierry-marie Guerra for accepting to review this dissertation, despite their very busy schedules, and for their helpful comments. I would also like to thank Dr. Pascal Brochet, Dr. Mohammed Gabsi and Dr. Srdjan Lukic for accepting to participate in my dissertation committee.

I am very grateful to Dr. Abdellatif Miraoui for giving me the opportunity to work in the hybrid electric vehicle topic with him. He has been always here for me even if his new opportunity at the Marrakech university away him from the lab. He gaves me responsibility and the opportunity to quickly integrate the electric vehicle international community.

I have a special thought to my co-advisor Dr. Benjamin Blunier. He is still an eternal source of inspiration for me even after he passed away in february. Our discussions had always lead on brilliants ideas, and his involvment in the team was so deep that his leaving still be felt today. He was also a good friend, and the link we created between together was unique. He is and he will miss me.

I want to specially thanks Dr. David Bouquain, Dr. Damien Paire and Dr. Daniel Depernet. All of them have been models for me during my undergrade studies, and working on their sides was an honor.

I am thankfull to my teammates who started the thesis in the same time as me : Mohammed Kabalo, Nicolas Watrin and Robin Roche. Working and progressing together has bring a lot of interestings meeting, discussions and fun in the coffee room. I would like to thanks all the persons that i met and worked with at UTBM : Dr. Fei Gao, Dr. Arnaud Gaillard, Mr Hugues Ostermann, Mr Mikeal Guarisco, Mr DonDong Zhao, Dr. Daniela Chrenko and all the technician and co worker. The enthusiasm of the team made these three years looks like three weeks.

I am thankfull to all the mobypost project members that i got the opportunity to work with, specially Sebastien, it has been a pleasure to work with you on the project and the prototype, and i hope i will be able to do it again in the future.

I am more than thankfull to Dr. Srdjan Lukic and his student : Mr Rui Wang, who welcome me during three months in North Carolina State University. This experience has been really rewarding for both personal and professional parts. I hope the link we started together is just the begining of a strong collaboration between our universities, and i welcome you to come to Belfort anytime.

I would like to thanks my two best friends for their supports during these three years, Thibaut and Philippe. Our casual meetings in the south of France are always a pleasure for me, even if the come back travel to Belfort is

hard most of the time. I thanks my familly for being supportive during all these years, specially my dad who has aroused my curiosity and is mostly responsible of my success of my many personal and professional project. Last but not least, my deepest thought goes to Anne, who illuminates all my days by being supportive and comprehensive.

GENERAL INTRODUCTION

In the beginning of the 21st century, the environmental dimensions of sustainable development became a key element of policy-making at international, regional and national levels. Indeed, the fear that current needs will compromise the ability of future generations to meet their requirements is omnipresent. The planet's natural resources are currently overexploited, and the constant increase of toxic emissions could result in an ecological disaster if no actions on the global scale are taken. The necessity to develop a production as well as a consumption model that spare natural resources while reducing toxic emissions is evident. However, it requires a tremendous degree of commitment from all parties involved whether it is government bodies, business firms or consumers.

The automotive industry, generally perceived as one of the main contributor to global warming, is well aware of such a responsibility. For many years now, car manufacturers have invested a colossal amount of money, time and human resources into Research and Development in order to reconcile mobility and sustainability. In the last 10 years, a numerous vehicle technology as emerged from manufacturers : Electric , hybrid or fuel cell vehicle are the most investigated technology todays. On the other hand, internal combustion engine based vehicle dominate drastically the automotive markets, and still evolve in term of fuel consumption and embedded electronics.

The last generations of cars has better engine efficiency, consequently their autonomy is increased, but also brings to the driver a comfort based on new technologies like air conditioning, global positioning system, reversing radar... On the opposite side, Electric vehicle (EV) has a lack of autonomy due to the battery technology who does not have a good Watts per kilogram ratio, and cannot embed a lot of electronics device, since their are power consuming which is already limited. In this scenario, fuel cell vehicle appears to be a good trade off since the autonomy can be closer to conventional vehicle while producing zero emission (assuming that the hydrogen is made using renewable energy). But, like EV, the main issue is the lack of charging stations : For electricity case, the autonomy of EV is so low that charging stations is required in almost all place (home, work, parking lots...). Nevertheless, some place are equipped with charging station coupled to renewable energy, specially photo voltaic panel because of the free space in the roof of industries/buildings. For hydrogen case, the storage of hydrogen is a big issue : the pressure of the tank is much higher than oil tank, and the hydrogen need to be kept at low temperatures to allow the flow when charging to be efficient. Consequently, Big changes need to be done to gasoline station to be able to provide hydrogen.

For all these reasons, hybrid electric vehicle appears to be the best solution for

shot-mid terms : the add of a electric drive train to the internal combustion engine allow to decrease fuel consumption while keeping the same autonomy. A lot of manufacturers focused on hybrid electric vehicle in the last ten years, with different architecture and technology. The best example is Toyota with the Prius, combining an electric drive to the gasoline motor without the need to charge the batteries. But the arrival of hybrid technology came during the internal combustion engine zenith. Consequently, manufacturers did not switch all their product to hybrid, and kept a huge conventional vehicle market which influenced a lot the research and development of hybrid model : Indeed, to reduce the cost of production and research, manufacturer tried to keep as more as possible the frame of the vehicle, its electronics and the internal combustion engine size. It leads to product the a big power of the internal combustion engine and small batteries, since the free space of the vehicle is limited. The control strategy of the vehicle, which control the power split between the engine, and the electric drive, also suffer of this conception. From this observation, this thesis investigates a new methodology to design the power train of hybrid electric vehicle and to control it.

The first chapter will draw up a state of arts of the electric and hybrid electric vehicle and its controls.

The second chapter will focus of the sizing of the components, by analyzing the vehicle's utilization, a.k.a the driving patterns that the vehicle do. A new approach of using this driving cycle is presented, analyzing statistically a family of driving cycle to build a generator in order to determine the size of the component on a representative sample of driving patterns rather than on a single one. The methodology of sizing is the explain and a second part focus on the optimal control of the vehicle knowing those cycles.

The third chapter will present the real time management of the power split of the vehicle designed, and new optimization and adaptation features : A fuzzy logic control for a Fuel cell hybrid electric vehicle is presented, and then optimized by a genetic algorithm method for a specific driving pattern. Some tool to implements this features while keeping good results on all patterns (urban,highway...) is then presented and results are shown experimentally using a lightweight fuel cell hybrid vehicle. Moreover, a control strategy based on distance prediction for plug in hybrid vehicle is then explain.

1

STATE OF ART : HYBRID ELECTRIC VEHICLE

1.1 INTRODUCTION

The automotive industry is well aware of its contribution to air pollution. Indeed, its estimates that road transportation in the Europe accounts for nearly a fifth of the Europe total CO2 emissions produced by man. In USA, transportation accounts for one third of greenhouse gases. In this context, manufacturers come with new technologies to replace the traditional internal combustion engine by electric drive, or fuel cell. FIGURE. 1 represents the CO2 consumption per kilometers using these different technologies in a vehicle : It clearly appears that improvement due to new technologies can radically change the CO2 emissions [1]. In this way, manufacturers began to investigate and develop new products like electric vehicle, hybrid electric vehicle or fuel cell hybrid electric vehicle to answer to this problematic. The followings section will described these technologies, pointing out their advantages and disadvantages. A state of art on energy management of hybrid electric vehicle is then drawn up and the possibility to increase its efficiency is discussed.

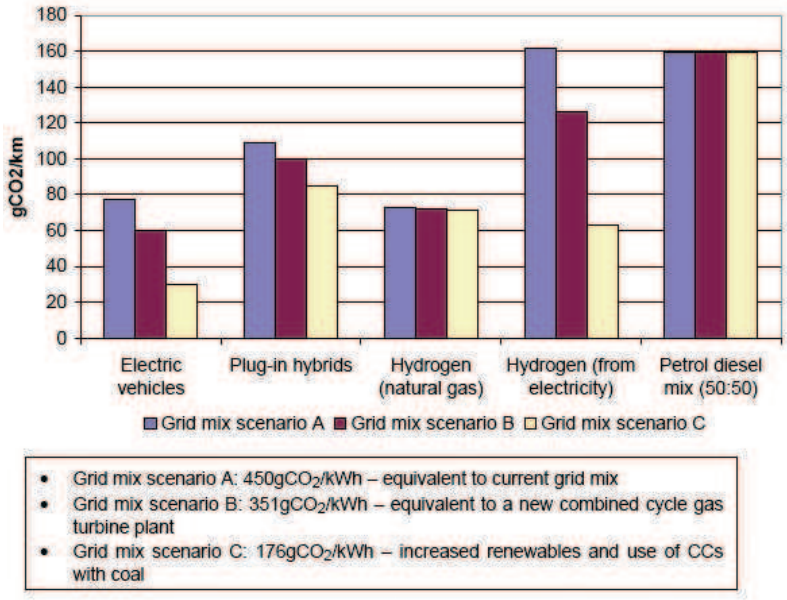

FIGURE 1. Comparison of CO2 emission for different vehicle's technology

1.2 ELECTRIC AND HYBRID ELECTRIC VEHICLES PRESENTATION

1.2.1 *Electric vehicle*

An electric car is composed of two main components : the electric motor and batteries. The principle of the electric motor has been discovered in 1821 by Michael Faraday, but electric motors became used in 1832, when the electromagnetic induction principle has been discovered [2]. The electric motor replace the traditional internal combustion engine and the power needed is provided by batteries. In the middle of the 19^{th} century, the electric car was popular but then decline when the internal combustion engine technology has been improved and the price of the gasoline became cheaper. Nowadays, environmental issue and the depletion of fossil fuel bring the renaissance of the electric vehicle.

Electric vehicle history

The first accumulator was created by Volta in 1800. This discovery allows to embed electricity into mobile application such as vehicles and open the door to electric car design. The first electric car made with lead acid batteries has been created in 1881 by G. Trouvé. The vehicle had an autonomy between 16 and 40 kilometers and a maximum speed of 14 km/h.
At the end of the eighteenth century, when the race to speed and distance records happened, electric vehicle growth in popularity. Among the most notable of these records was the breaking of the 100 km/h (62 mph) speed barrier, by Camille Jenatzy on April 29, 1899 in his "rocket-shaped" vehicle "Jamais Contente" [3]. During this time, electric automobiles were competing with petroleum-fueled cars for urban use of a quality service car : The companies Electric Carriage and Wagon built the first commercial application of electric cars for New York City taxis in 1897. They then built urban transportation vehicles such as buses and also trucks. The mobility generated by vehicle has created new needs, with greater distance. As a consequence, the internal combustion engine began to be predominant compare to electric motor. Moreover, the cost of thermal vehicle was three time lower than electric ones (the cost of Century Electric Roadster was 1750 dollars and the Ford T 500 dollars). Consequently, in 1920, electric vehicle almost disappear in favor of internal combustion engine vehicles [4].

It is only in the middle of the nineteenth, during the energy crises, that the electric vehicle got a renew. The major difference between electric and internal combustion engine power train was the autonomy (the evolution of the internal combustion engine coupled with high tank capacity allowed the vehicle to travel until 5 times the autonomy of an electric vehicle). Moreover, the weight of electric car was very big compare to thermal vehicle mainly due to the weight of the batteries which have a very small specific energy ration compare to gasoline. Consequently, only small quantity of electric

car for specific applications has been product during these years. In 1990, environmental issues due to gaz emission and the non fuel-efficiency of the internal combustion engine was point out by the California Air Resources Board (CARB), pushing for more fuel-efficient, lower emissions vehicles. This idea growth during the end of the century and became a major problematic in the vehicle industry during the 2000s. The adaptation of the thermal vehicle to electric such as Peugeot 106, Citroën AX have found their place only on very specific field like captive fleet (postal delivery) and didn't succeed in the consumer market [5]. The consumer was not ready to sacrifice the autonomy for gaz pollution saving. The industry focused the production for city car only and bring hybrid power train for standard vehicles. It leads to the design of small car mainly using lead acid batteries with small autonomy and directly focused for urban user. Nowadays, lithium-ion has replaced heavy lead-acid battery technology, and the autonomy reach 100km such has Citroën C-zéro, Nissan Leaf, Tesla Roadster, making electric vehicles attractive. Nevertheless, consumers still criticize the autonomy and the charging method which force the user to charge the battery almost everyday.

Power train

FIGURE. 2 represents a power train of an electric vehicle : The vehicle propulsion is provided by a DC or AC electric motor and the electricity source by batteries (lead-acid, Ni-Cd, Ni-Mh, Li-ion, Zebra ...). The speed regulation is controlled by an electronic device which interacts via the power converter. The connection to the grid is necessary to refill the batteries.

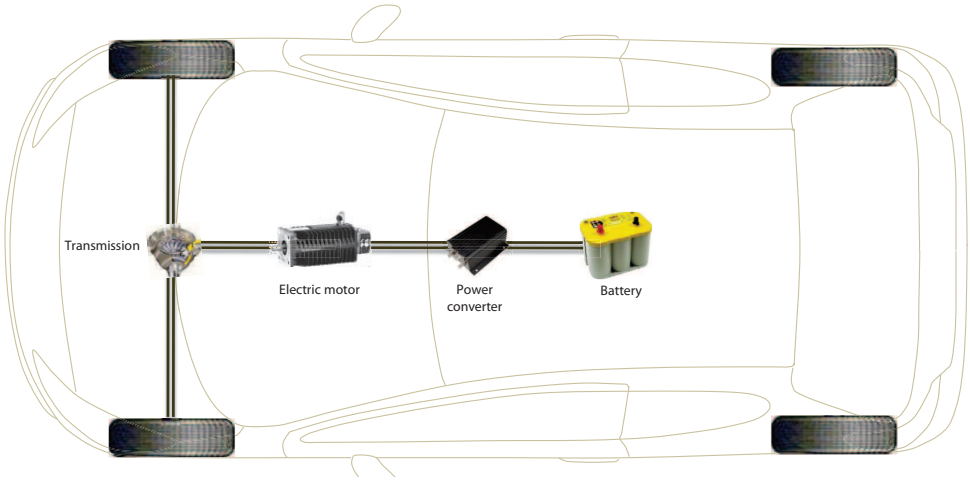

FIGURE 2. Electric vehicle power train

Existing Electric vehicles

LIST OF HYBRID ELECTRIC VEHICLES TABLE. 1 gives a list of sold electric vehicles in France with their autonomy and battery technology :

Manufacturer	Model	Autonomy	Battery technology
Citroën	C-Zero	150 km	Lithium ion
Mia Electric	Mia	130 km	Lithium iron phosphate
Mitsubishi	I-MiEV	150 km	Lithium ion
Nissan	Leaf	160 km	Lithium ion
Peugeot	iOn	130 km	Lithium ion
Piaggio	Porter	100 km	Lead acid
Renault	Fluence ZE	185 km	Lithium ion
Renault	Kangoo	170 km	Lithium ion
Smart	Fortwo	145 km	Lithium ion
Tesla	Roadster	390 km	Lithium ion
Venturi	Fetish	340 km	Lithium polymer

TABLE 1. List of produced electric vehicles

EXAMPLE : NISSAN LEAF The Nissan Leaf shown in FIGURE. 3 ("LEAF" standing for Leading, Environmentally friendly, Affordable, Family car) is an electric car produced by Nissan and introduced in Japan and the United States in December 2010. The electric power train with lithium ion battery allows the vehicle to have 160 km range (on NEDC driving cycle), corresponding to 2.4L per 100km gasoline equivalent. The vehicle has the following caracteristics :

- *Powertrain* : The Leaf uses an 80 kW and 280 N·m front-mounted synchronous electric motor driving the wheels.
- *Battery* : A 24 kWh lithium ion battery pack (presented in FIGURE. 4) divided in 48 modules where each module contains four cells, equivalent to a total of 192 cells.
- *Range* : The autonomy announced by the producer (Nissan) is 160km, recorded on ECE driving cycle but the United States environmental protection agency announced a range of 117 kilometers on US driving cycle.
- *Charge* : The Leaf can be charged by two methods : A standard 120/220volts AC charging and also a fast charging method using a 3.3 kW charger

(580 Volts). Consequently, the vehicle can be full charged in 8 hours.

FIGURE 3. Nissan Leaf

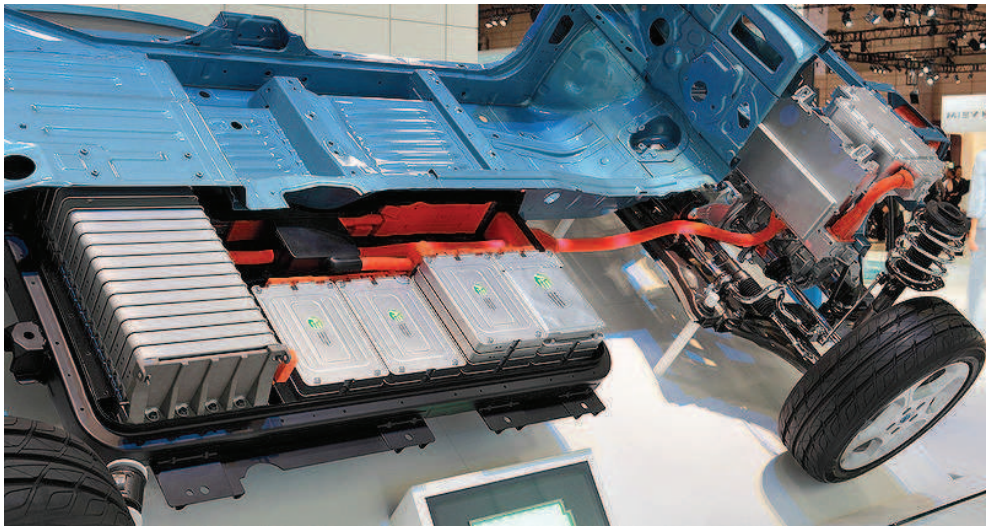

FIGURE 4. Battery pack of Nissan Leaf

1.2.2 *Hybrid electric vehicle : general presentation*

A hybrid vehicle is composed of two or more energy sources to provide the vehicle's power. One of these sources can be electric : in this case the

denomination of the vehicle is : Hybrid Electric Vehicle (HEV). For instance, a HEV can be made with internal combustion engine and electric motor with batteries. In this cases, the power can be provided either by thermal engine, electric motor or both. The control strategy (or energy management) is the method to control theses sources regarding the parameters and measures of the vehicle (speed, batteries's state of charge...). Due to the different types of energy included in the power train (mechanic, electricity), severals architectures of HEV exists [6].

History

The first hybrid power train appear in 1900, made by Ferdinand Porsche. The vehicle was composed of an internal combustion engine coupled with an electric motor with lead acid batteries. The torque provided by the electric motor was mechanically added to the thermal engine. The electric drive train was also able to run alone, which allowed the vehicle to run in pure electric mode (the autonomy was around 65 km). This vehicle has been presented in the Paris Auto Show in 1901. A second vehicle was exposed, based also on internal combustion engine and electric motor, but the internal combustion engine was coupled to a generator and the wheels was directly connected to the electric motor. Theses two motors described the two main type of architecture, parallel and series, which are still used today. The main drawback of these vehicles in this period was the electric motor control which were not mastered. As the same as electric car, HEV became investigated and produced in the end of the 20th century with the idea of fuel economy and environmental friendly cars. The main advantage between electric vehicle and HEV is that hybridization of the power train allows to keep a really good autonomy while reduce drastically the fuel consumption. The first mass-produced hybrid vehicle was the Toyota Prius, launched in Japan in 1997, and in 1999 in the United States.

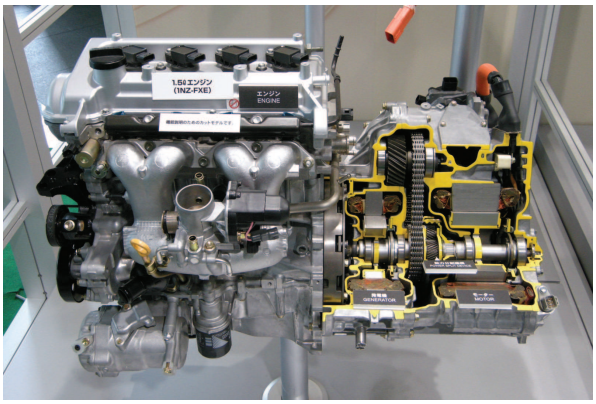

FIGURE 5. Toyota Hybrid System engine used in Toyota Prius

As shown in FIGURE. 5, the vehicle is based on hybridize a gasoline engine with two electric motor-generator : one between the internal combustion engine and the battery to charge it and one to provide the electric drive train. The vehicle has an estimated fuel economy of 4.5 l/100 km in the city and 5.2 l/100 km in highway driving. Between 1997 and 2010, the Prius global cumulative sales were estimated at 1.6 million units. In 2010, Peugeot introduces his hybrid powertrain called Hybrid4 in the 3008 Hybrid (12). The power train is split in one traditional thermal traction drive (front wheels) train and an electric propulsion with a 25 kW electric motor (rear wheels) coupled with 5 kWh nickel metal hydride batteries. A generator is linked between the internal combustion engine and the battery pack to charge it.

Produced HEV

TABLE. 2 represents a list of produced model of HEV with the different technology of hybridization used.

1.2.3 *Hybrid electric vehicle technology*

The varieties of hybrid electric designs can be differentiated by the structure of the hybrid vehicle drive train, the fuel type, and the operative mode :

Micro hybrid

Micro hybrid architectures are composed of a small electric motor (generally around 3 kW) doing a start and stop system (FIGURE. 6). This system automatically shuts down and restarts the internal combustion engine to reduce the amount of time the engine spends idling, thereby reducing fuel consumption and emissions. This is most advantageous for vehicles which spend significant amounts of time waiting at traffic lights or frequently come to a stop in traffic jams. This feature is present in hybrid electric vehicles, but has also appeared in traditional vehicle to help the internal combustion engine during starting phases. Fuel economy gains from this technology are typically in the range of 5 to 10%. Since vehicle accessories like air conditioners and water pumps have typically been designed to run off a serpentine belt on the engine, those systems must be redesigned to function properly when the engine is turned off. Typically, an electric motor is used to power these devices instead.

Mild hybrid

Mild hybrids are generally internal combustion engines equipped with an electric machine allowing the engine to be turned off whenever the car is coasting, braking, or stopped, yet restart quickly. Mild hybrids may employ regenerative brake and some level of power assistance to the ICE, but mild hybrids do not have an exclusive electric propulsion mode.

Manufacturer/technology name	Model	Power train Architecture
Audi e-tron	A1	Electric traction drive train (provided by Lithium ion battery pack) with range extender based on internal combustion engine
BMW Active hybrid	Series 3	Internal combustion engine coupled in parallel with electric motor and Lithium Ion battery pack
	Series 5	
	Series 7	
PSA Peugeot-Citroën Hybrid 4	3008	Internal combustion engine traction drive train coupled with electric propulsion drive train with Ni-Mh battery pack
	308	
	508	
	DS4	
	DS5	
Toyota Hybrid System (THS)	Prius	Power split drive train with two motor-generator
	Auris	
	Yaris	

TABLE 2. List of HEVs technology and models

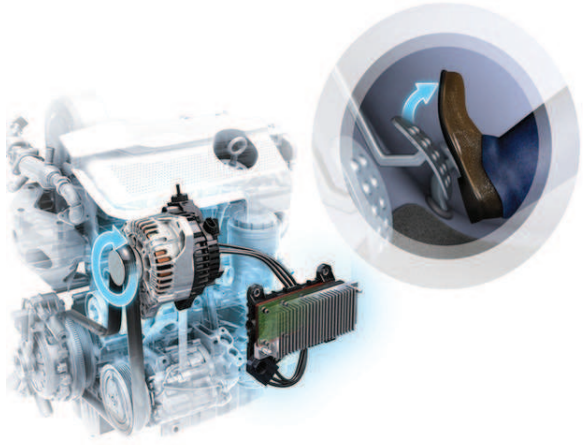

FIGURE 6. Start and stop system

These electric motors (around 20 kW or less) provide greater efficiency by replacing the starter and alternator with a single device which assists the power train and are called mild hybrids also don't require the same level of battery power and do not achieve the same levels of fuel economy improvement as compared to full hybrid models. One example is the 2005 Chevrolet Silverado (FIGURE. 7), The power train is a hybrid parallel architecture compose of a 7 kW electric motor coupled with the internal combustion engine by bell-housing. The fuel economy compare to the traditional thermal power train is estimate to 10 %. However, the vehicle cannot run in pure electric mode.

Full hybrid vehicle

Full hybrid vehicles are composed of a primary source of energy, ICE or Fuel cell, hybridized with electric drive. A full hybrid HEV is able to run in pure electric mode. Three categories can be distinguished :

SERIES HYBRID VEHICLE Series hybrid (FIGURE. 8) has the particularity to have the electric motor directly connected to the transmission. The internal combustion engine (in the case of FIGURE. 8, the ICE) runs as a range extender to increase the autonomy by charging the battery [7]. It running at a constant point, which can be set as the most efficiency point of the ICE if the vehicle is well designed, and the electric drive absorbs and provides power peaks. Series hybrid architecture has not very popular due to the major transformation of the architecture compare to thermal vehicle : The entire drive train is electric, and the control of electric motor is critical for a good behavior of the vehicle. Therefore, this architecture allows the ICE speed to be completely independent of the speed of the vehicle, allowing the motor to run at its

FIGURE 7. Chevrolet Silverado mild hybrid

best efficiency point. Consequently, this architecture offers the best fuel consumption compare to others.

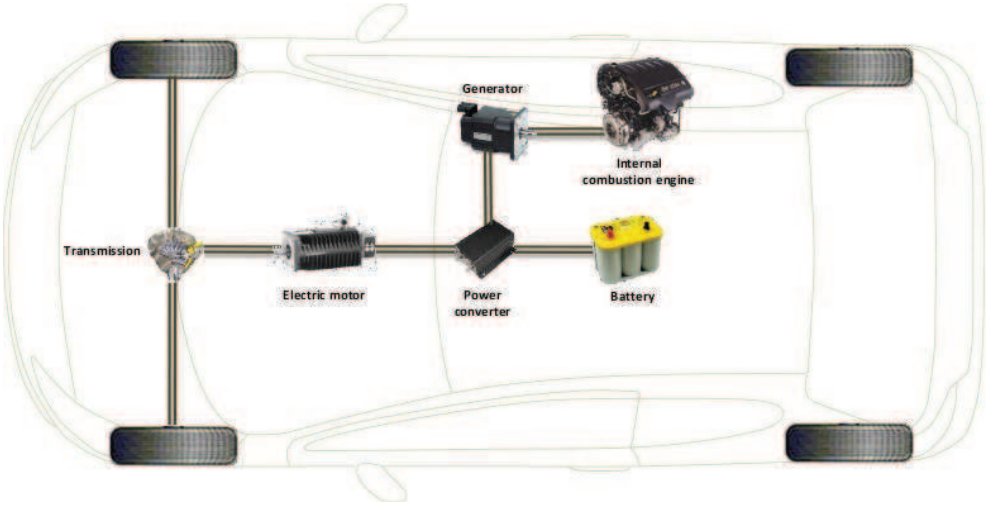

FIGURE 8. Series hybrid electric vehicle

FIGURE. 9 represents the power flow of the series power train for different scenarios :

- *Start* : Only the electric motor is used to start the vehicle : all the power come from the battery via the power converter.
- *Acceleration* : Both sources are used : the electric motor get power from the battery and from the ICE which gives electrical power by transforming the torque in electricity via a generator.
- *Steady speed* : When the speed is constant, the ICE can charge the battery by providing all the power needed to the electric motor plus the battery needs.
- *Brake* : During braking phases, the power is regenerated by the electric motor which is used in generator mode, the battery are then charged. It can be observed that the ICE can still charge the battery at the same time.

PARALLEL HYBRID VEHICLE Parallel hybrid systems (FIGURE. 10), add mechanically the ICE drive train and the electric drive train. The vehicle is able to run in pure electric mode, specially at low speed where the ICE is not efficient, the electric motor, which have a good torque at this speed provide the power needed by the vehicle. At constant speed, the ICE speed is linked to the speed of the vehicle. Consequently, its efficiency is the same as a conventional vehicle [8]. The gear adds the both torques to give it to the transmission. This type of architecture is mainly used by manufacturers because it enable to start from a thermal vehicle drive train and hybridize it by adding an electric part. Consequently, electric car model can be directly

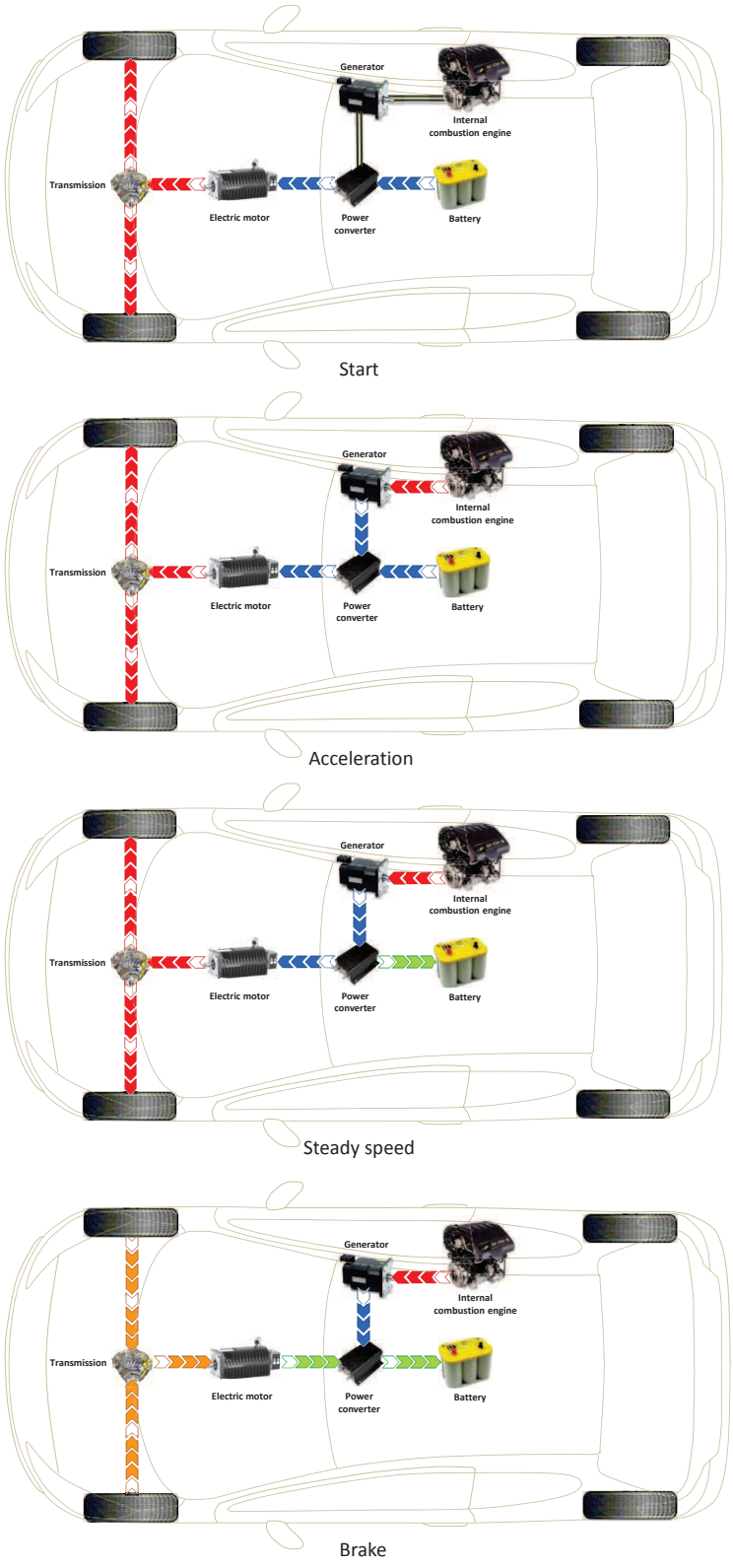

FIGURE 9. Series hybrid power train

derivated from standard one. The main drawback of this design is that the ICE is sized for standard use, which is over sized for an hybrid application.

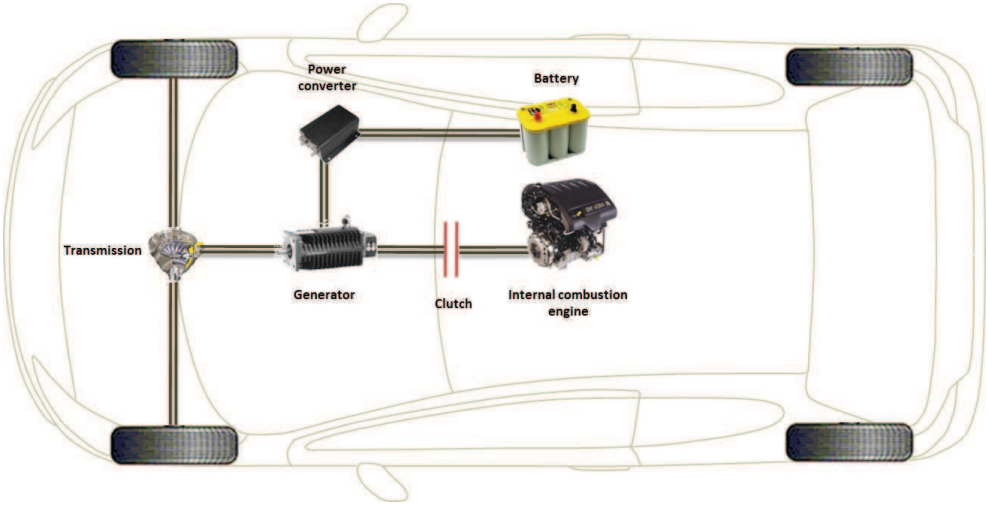

FIGURE 10. Parallel hybrid electric vehicle

FIGURE. 11 represents the power flow of the parallel power train for different scenarios :

- *Start* : Only the electric motor is used to start the vehicle : all the power comes from the battery via the power converter, the clutch prevents the ICE to be connected to the transmission .
- *Acceleration* : Both sources are used : the electric motor get power from the battery and the ICE is used : both torque are added to provide the vehicle power.
- *Steady speed* : When the speed is constant, the ICE can charge the battery by providing all the power needed by the vehicle plus the power needed to charge the battery via the electric motor which is used as a generator.
- *Brake* : During braking phases, the power is regenerated by the electric motor which is used in generator mode, the battery are then charged. It can be observed that the ICE can be disconnected via the clutch to prevent engine brake.

An alternative parallel hybrid layout is the ”through the road” type. The architecture is divided into two drive trains : A traction drive train generally used by ICE and a propulsion drive train used by electric motor. The batteries can be recharged through regenerative braking, or by loading the electrically driven wheels during cruise. Power is thus transferred from the engine to the batteries through the road surface. This layout also has the advantage of providing four-wheel-drive in some conditions, but the main drawback of this method is the road dependency : at high speed, the electric motor need to be disconnected from the road because its running point are not matching with the speed of the wheel. FIGURE. 12 shows the power train of the Peugeot

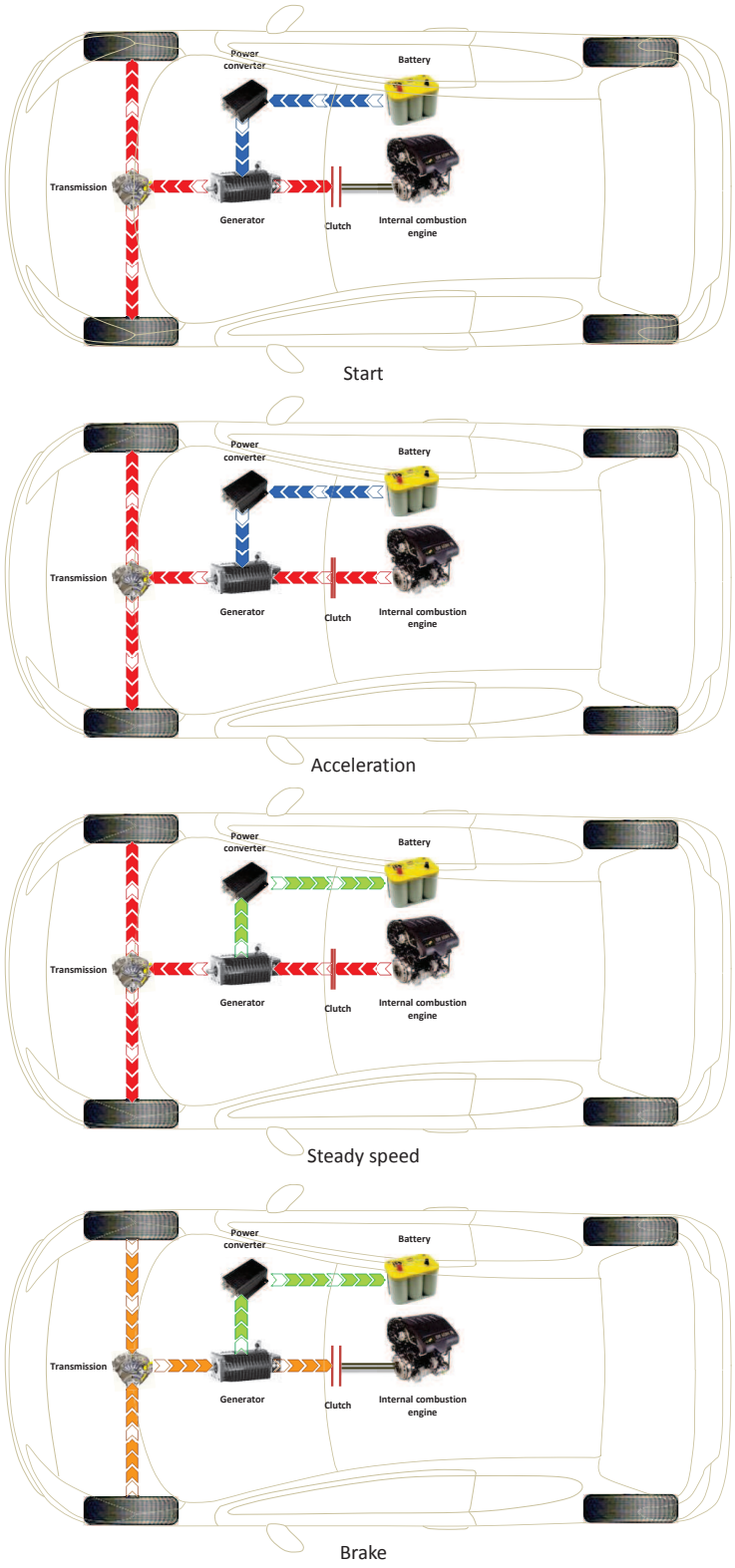

FIGURE 11. Parallel hybrid power train

3008 Hybrid4 made in France which has this type of layout. A generator is linked to the ICE to charge the battery during constant speed phases.

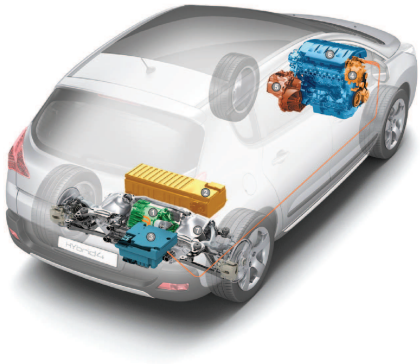

FIGURE 12. Peugeot 3008 Hybrid4

POWER-SPLIT VEHICLE Power-split hybrid or series-parallel hybrid (FIGURE. 13) are parallel hybrids. The architecture is made with two motor-generators : One between the internal combustion engine and battery which is used to charge them and another one to provide the electric power to the wheels. All three mechanical axis are linked with a planetary gear, which add each torque to give the power to the transmission. With this architecture, by designing wisely the size of both motor-generator, one of them can be used to run the vehicle at low speed (pure electric mode) [9], when the internal combustion engine cannot provide the power due to the lack of torque at these speed. The other one can be used to charge the battery while the internal combustion engine is running at its best efficiency point. The main advantage of this architecture is that gearbox and clutch are not needed since the electric motor provide the power when the internal combustion engine is not capable of due to its speed range limitation.

FIGURE. 14 represents the power flow of the power-split power train for different scenarios :

- *Start* : Only the electric motor is used to start the vehicle : all the power come from the battery via the power converter.
- *Acceleration* : Both sources are used : the electric motor gets power from the battery and the ICE is used : both torque are added to provide the vehicle power.
- *Steady speed* : When the speed is constant, the ICE can charge the battery by providing all the power needed by the vehicle plus the power needed to charge the battery via the generator. Compared to the parallel architecture, the use of the specific generator allows the ICE to run at its best efficiency points

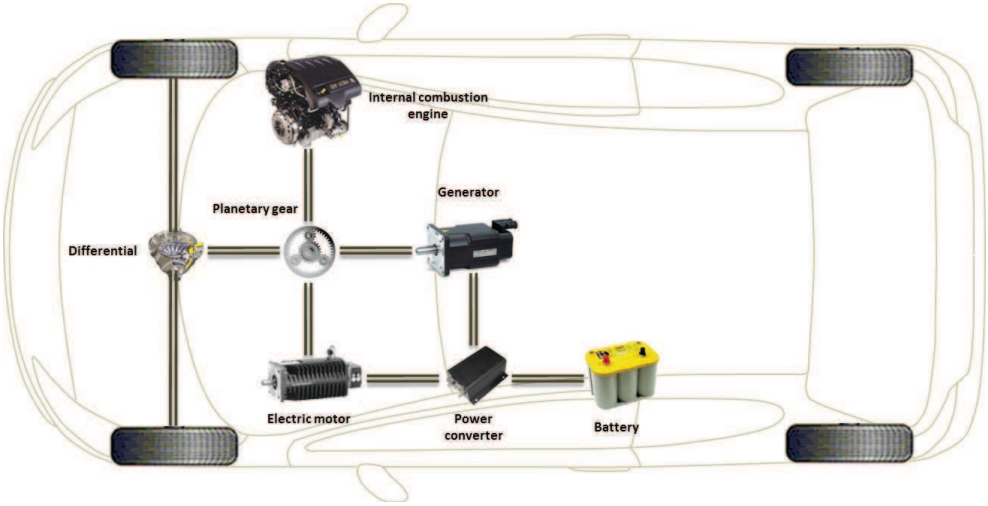

FIGURE 13. Power-split hybrid electric vehicle

– *Brake* : During braking phases, the power is regenerated though the generator and the battery are then charged.

The Toyota Prius was the first vehicle to used this architecture : A 18 kW generator motor is used to turn on the ICE and as a generator to charge the battery and a 33 kW electric motor provides the torque for low speed and high accelerations. This architecture has the advantage of series architecture : the internal combustion engine speed is not linked to the speed of the vehicle, it can run at its best efficiency point. It is also offer the advantage of the parallel architecture : the power provided to the transmission is mechanic. Consequently, commercial model can be directly adapted with this architecture.

POWER TRAIN COMPARISON TABLE. 3 shows a comparison with advantages and drawbacks of presented architectures. For each type of power train, the fuel consumption economy is directly linked to the driving cycle ran by the vehicle. When running urban pattern, the fuel economy is very good (around 35%), but for highway parts, almost all the power is provided by the ICE and the consumption is equal to conventional vehicles, since the electric motor is used only for accelerations [10].

1.2.4 *Fuel cell hybrid electric vehicle*

Build a vehicle which does not need gasoline to run is one of the most focused objective by car's manufacturers. That's why the fuel cell technology is highly studied.

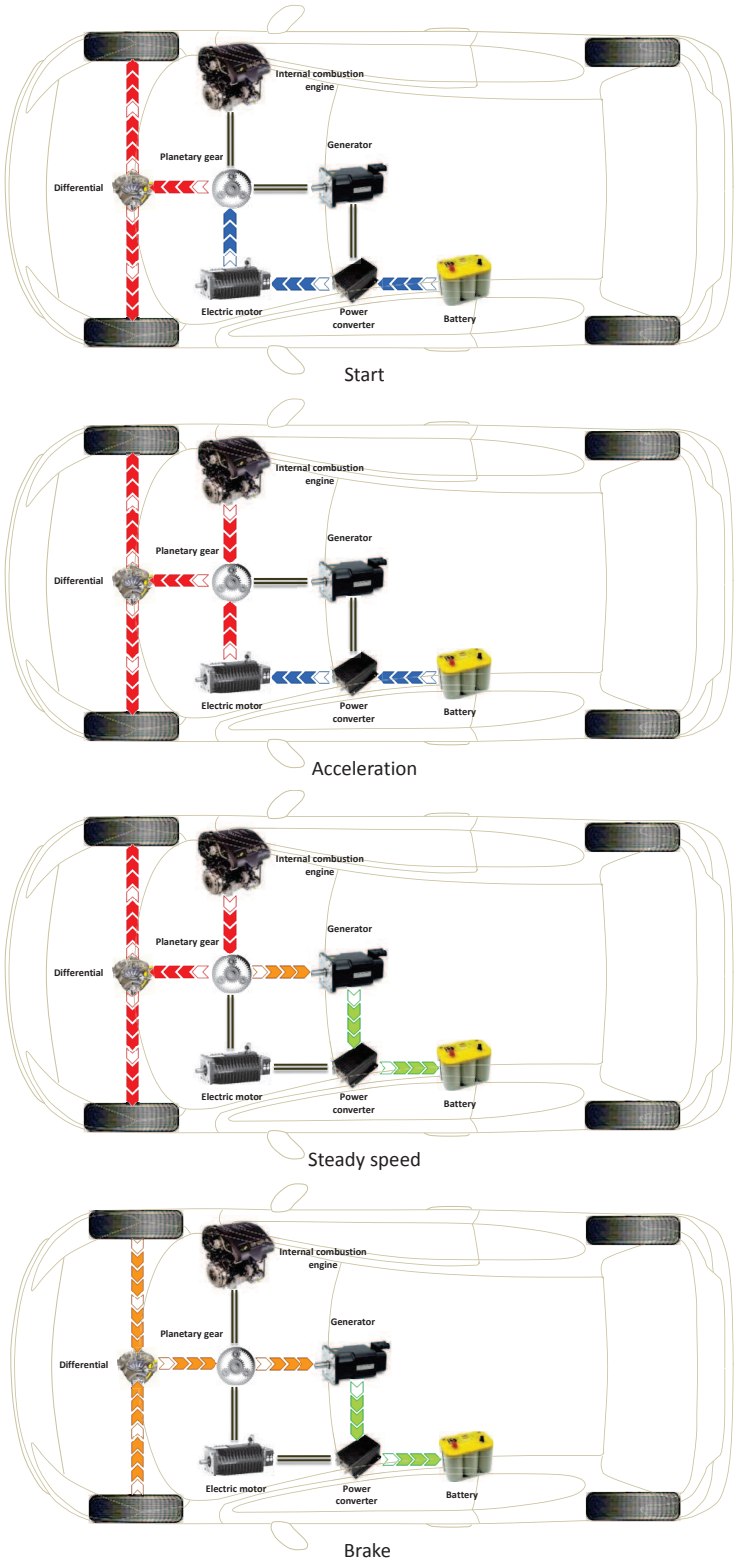

FIGURE 14. Power-split hybrid power train

Hybridization types	Pros	Cons
Series	Good efficiency at low speed	Low global energetic efficiency
	good control of ICE working points	can not run with ICE only
	Control strategy has low constraints	
Parallel	Good global energetic efficiency	The ICE may not work at the best working points
	One electric motor only	Complex mechanical parts
		Control strategy has more constraints
Power-split	Very good global energetic efficiency	More than one electric motor used
		Complex mechanical parts
	Very good control of ICE working points	Control strategy has a lot of constraints

TABLE 3. Pros and cons of different power train architectures

Fuel cell

The fuel cell is a potential candidate for energy storage and conversion. Indeed, a fuel cell is able to directly convert the chemical energy stored in hydrogen into electricity, without undergoing different intermediary conversion steps. In the field of mobile and stationary applications, it is considered to be one of the future energy solutions. The main difference between a fuel cell and a battery is that the fuel cell requires a constant source of fuel and oxygen to run. Therefore, the battery needs to be charged to provide energy.

HISTORY Welsh Physicist William Grove developed the first fuel cells in 1839. The first commercial use of fuel cells was in NASA space programs to generate power for probes, satellites and space capsules. Since then, fuel cells have been used in many other applications. Fuel cells are used for primary and backup power for commercial, industrial and residential buildings and in remote or inaccessible areas. Fuel cell are also used in mobile applications such as vehicle, bus, boats, airplanes... But the difficulty of hydrogen storage and fuel cell reliability bring heavy constraints to the democratization of the fuel cell into this type of application [11].

PRINCIPLE The fuel cell principle is the opposite to the electrolysis of water [12, 13] : The reaction between the fuel (H_2) and the oxidant (O_2) produce energy. At the anode, the dihydrogen is split in 2 protons of hydrogen and 2 electrons :

$$H_2 \longrightarrow 2H^+ + 2e^- \tag{1.1}$$

This reaction requires a catalyst. The catalyst use depends on the temperature of the reaction : The heater the temperature, the best the efficiency will be. Consequently, the material used could be made with lower quality. The free electrons allow to create a current if a load is linked between the anode and the cathode. The hydrogen protons go through the electrolyte to reach the cathode. At the cathode, the hydrogen protons and electrons merge to create water[14] :

$$\frac{1}{2}O_2 + 2H^+ + 2e^- \longrightarrow H_2O \tag{1.2}$$

PEMFC FUEL CELL Since automotive application requires low range temperature, the Proton Exchange Membrane Fuel Cell (PEMFC) is well suited [15] : PEMFC operates at temperature under 100 °C, with a stack efficiency of the order of 50 %. Its low-operating temperature enables the fuel cell to start up relatively quickly. The typical PEMFC power range is from a few milliwatts to a few hundred kilwatts [16]. The primary advantages of PEMFC are as follows :

- The electrolyte is solid : there is no risk of electrolyte leakage ;
- the operating temperature is low, which means that the cell does not need a long time to warm up before being fully operational ;

– the specific power is high, and be as high as 1 kW/kg.

However, it has its own drawbacks :

– The membrane must be kept in a good degree of hydration in order to transfer hydrogen protons. If this condition is not met, there is a risk of membrane deterioration, which would lead to the degradation of the fuel cell itself ;
– the necessity of platinium makes the fuel cells susceptible to contamination from carbon monoxide, which poisons catalytic sites ;
– the fuel cell is very temperature dependent, leading to cold-start in low temperature condition difficults ;
– heat and Air management of the fuel cell needs to be strictly regulated ;
– the durability of the fuel cell is limited, specially in mobile applications where environmental perturbations strongly disrupt the fuel cell system.

HYDROGEN STORAGE Three methods exist to store the hydrogen for fuel cell applications :

– Store the hydrogen in ambient temperature under high pressure ;
– Store the hydrogen in very low temperature as liquid or solid form ;
– Store the hydrogen by trap it into hydride metal.

For automotive applications, researchers and manufacturers tend to store the hydrogen into high pressure tanks composed of carbon fiber (superior to 300 bar. Nevertheless, hydride metal tank solutions are coming. This solution has the advantage to keep the tank at a low pressure (around 10 bars), but the temperature of the tank needs to be controlled and tanks are heavy.

FUEL CELL AND BATTERY VEHICLE The main issue of the PEMFC is its dynamic : The high variations of currents between the cathode and anode leads to high variation of membrane humidity. Consequently, dewatering or drowning of the membrane can happen which can be harmful. In automotive applications, where the dynamic caused by accelerations of the vehicle can be high, the hybridization of the PEMFC is necessary. The battery can provide the peak of power during high dynamic phases, letting the fuel cell runs at a constant current. Moreover, like a standard HEV, the battery allows to save hydrogen consumption and increases the autonomy of the vehicle. The following studies will investigate several solutions to design and control an efficient fuel cell hybrid electric vehicle.

1.3 CONTROL STRATEGY OF HYBRID ELECTRIC VEHICLE

The section 1.2.3 described the power flows for some scenarios of different HEV architectures. These power flows described a general situation and are not specific at a driving patterns/cycle. In order to determine in real time the power split between the first and the second sources in a HEV, a control strategy is determined. The control strategy is based on electronic components which interact with the power converter to control the electric parts (electric

motor/battery) or directly the ICE. Each power train architecture brings some constraints on the control : for example, the parallel architecture requires the same rotation speed for both ICE and electric motor while the series architecture allows the ICE to run at every working points [17]. Two kinds of control strategy can be found [18, 19] :

1.3.1 *Offline controls*

This type of control is based on optimization methods. The aim is to find the best power split profile for a selected trip. The driving cycle ran by the vehicle is assumed to be known, consequently, the power needed by the vehicle during all the trip is known. Based on this knowledge, optimization methods are run to find the optimal power split for this selected driving cycle. Some methods are based on Global optimization points like [20, 21, 22, 23, 24, 25, 26] where finding the best efficiency points of the ICE is investigated. The methodologies and controls used are really efficient for parallel architecture, since the control strategy interact to the electric drive to let the ICE runs the maximum of time to its best working point. Nevertheless, for series architecture, where the ICE can run at every speed independently of the vehicle speed, the optimization methods does not get the optimal results.

1.3.2 *Online controls*

Also called real time control, this control aims to finds a power split which fit to all situations without knowing the future demands of power. Several type of controls can be found in the literature [27, 28, 23, 29, 30, 31] which are simple to implement but specific to the vehicle driving style. Others controls like [32, 33, 34, 35] use fuzzy logic or neural network to determine the control of the electric drive based on the constraints of the power needed by the vehicle, remaining battery state of charge and architecture constraints.

Specific controls for fuel cell hybrid vehicle

Some control are also focus on fuel cell applications like [36, 37, 38]. As described in section 1.2.4, the fuel cell need slow dynamic to run efficiently. Consequently, the control has to be adapted with these constraints.

Predictive controls

Some predictive controls can be found in the literature [39, 40, 41, 42, 43, 44]. Most of them are based on the prediction of type of route that the vehicle will run. This type of control is very efficient for plug-in hybrid electric vehicle. Indeed, a plug-in vehicle allows to decrease the state of charge of the battery as far as possible during the cycle. Therefore, the conventional HEV need to keep the battery state of charge in a good zone, because of the lack of

connection to the grid to charge the battery. Consequently, the prediction of the power needed by the vehicle in future trip help the control to minimize fuel consumption by increasing the power provided by electric drive.

1.3.3 *Control used in commercial plug-in hybrid electric vehicles*

Most of the plug-in hybrid electric vehicle made by manufacturers runs with the same control : CD-CS mode. This control is composed of two parts :

- *Charge depleting (CD)* : The vehicle runs in all electric mode, the ICE is turned off and only the electric drive provide the power needed.
- *Charge sustaining (CS)* : The ICE is used to maintain the battery at a constant state of charge and to provide the power needed by the vehicle.

FIGURE. 15 shows the control strategy principle : The control is based on the state of charge of the battery : a first part, charge depleting mode, is run to decrease the state of charge of the battery. When the state of charge reaches a critical point, the ICE is turned on to maintain the state of charge constant and provide the power to the vehicle.
This control is really easy to implement, and really efficient when the driving distance is very small, since the vehicle will run in electric mode only and the fuel consumption will be null. Nevertheless, when the charge Sustaining mode is reached, the fuel consumption is higher than a standard HEV vehicle because the battery can not absorbs all peak of power due to its low state of charge. In this mode, two situations brings different results :

- The ICE is big enough to provide all the power needed by the vehicle while maintain the battery state of charge within working to its best efficiency point.
- The ICE needs to operate to different points to provide the power to the vehicle.

In the first case, the fuel consumption is minimized : The ICE runs at its best efficiency zone during all the charge sustaining mode until the end of the driving cycle. Nevertheless, this scenario requires to size the engine with a very good knowledge of the driving patterns. In the second situation, the ICE does not run at a constant point, the fuel consumption can be higher than a conventional thermal vehicle since the ICE need to provide the power needed by the vehicle and also charge the battery.

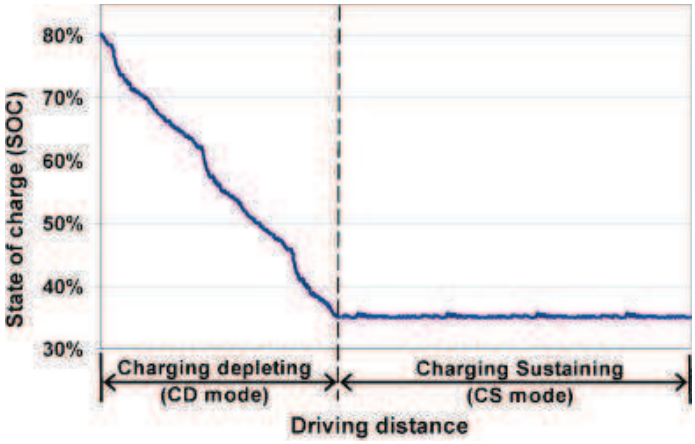

FIGURE 15. Charge Depleting - Charge Sustaining control strategy

1.4 CONCLUSION

In this chapter, hybrid electric vehicles has been presented focusing on the power train architecture and controls. Some vehicle architecture, like parallel or power-split, are mostly chosen by manufacturers to produce their cars. The choice is generally made to adapt a conventional thermal vehicle into an hybrid one. Moreover, the components sizing follows the same methodology : the ICE size is usually the same as the thermal vehicle, and the battery pack choice is limited by the free space in the vehicle.
The control strategy, which is directly linked to the architecture of the vehicle and the size of components, need to take into account the lack of energy of a small battery size and best working point of an over sized ICE. As described in the literature, severals solutions brings really good fuel consumption results but the control strategy is totally stuck with constraints resulting on this bad sizing. It leads to real times controls which are very efficient for urban patterns, but cannot reach offline controls results.
The work done in this thesis described a new methodology to size the component of an hybrid electric vehicle and the control associate to the vehicle with optimizations algorithm which allows to be efficient for all driving patterns.

2

HYBRID ELECTRIC VEHICLE CONCEPTION : SIZING SOURCES AND OPTIMAL CONTROL

2.1 DRIVING CYCLE ANALYSIS

A driving cycle is a series of data points representing the speed of a vehicle versus time. Most of the time, they are built using data collection : The procedure involves instrumentation of the test vehicle to collect information while driving on the test road. There are two major types of data to be collected, Driver behavior and vehicle vs Road data. The vehicle vs road data are used to prepare the road drive cycle and the driver data to prepare the Driver model. This part focus on the road drive cycle which will be used to determine the power cycle [45].

2.1.1 *Standard driving cycle*

Driving cycles are produced by different countries and organizations to assess the performance of vehicles in various ways, as for example fuel consumption and polluting emissions. Following up on an European Commission strategy adopted in 2007, the EU has put in place a comprehensive legal framework to reduce CO_2 emissions from new light duty vehicles as part of efforts to ensure it meets its greenhouse gas emission reduction targets under the Kyoto Protocol and beyond. The legislation sets binding emission targets for new car and van fleets. As the automotive industry works towards meeting these targets, average emissions are falling each year. In order to determine CO_2 emissions for each cars, standard driving cycles has been created [46, 47] :

FIGURE. 16 shows the ECE cycle which is an urban driving cycle, also known as UDC. It was devised to represent city driving conditions, e.g. in Paris or Rome. It is characterized by low vehicle speed, low engine load, and low exhaust gas temperature.

FIGURE. 17 shows EUDC (Extra Urban Driving Cycle). A segment has been added after the fourth ECE cycle to account for more aggressive, high speed driving modes. The maximum speed of the EUDC cycle is 120 km/h. FIGURE. 18 represent an alternative EUDC cycle for low-powered vehicles has been also defined with a maximum speed limited to 90 km/h.

FIGURE. 4 includes a summary of selected parameters for the ECE, EUDC and EUDC for low-powered vehicles cycles. Theses cycles are far away from real driving pattern in term of dynamic (acceleration and deceleration), stop time and maximum speed. That leads to very good fuel consumption and low CO_2 emissions when testing commercial cars. Nevertheless, it is still a

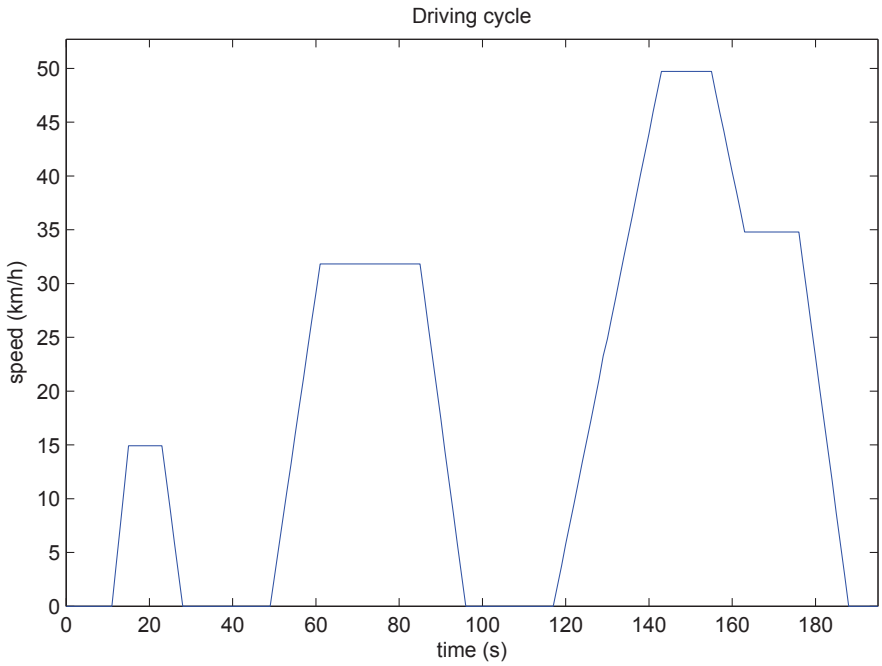

FIGURE 16. ECE 15 Cycle

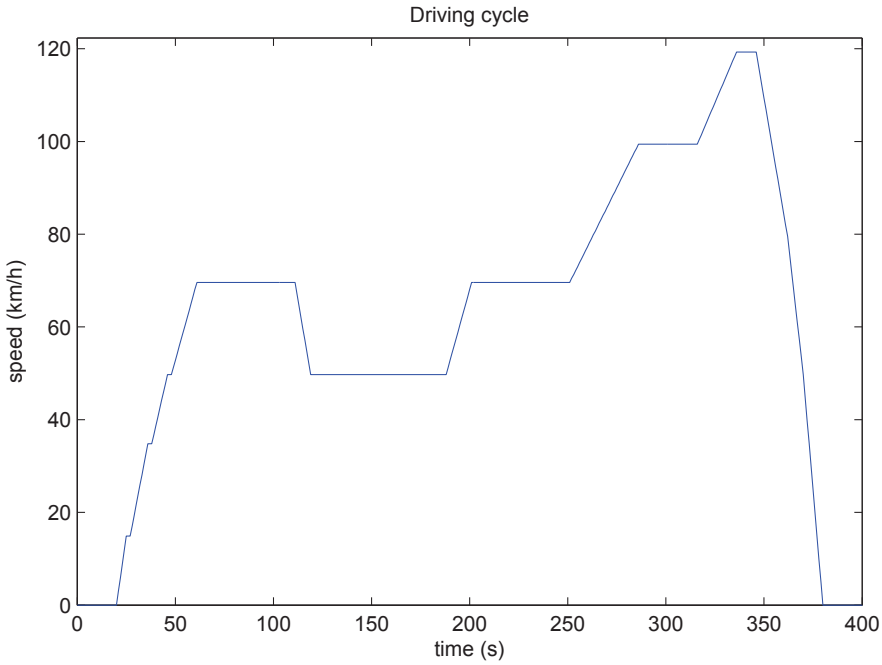

FIGURE 17. EUDC Cycle

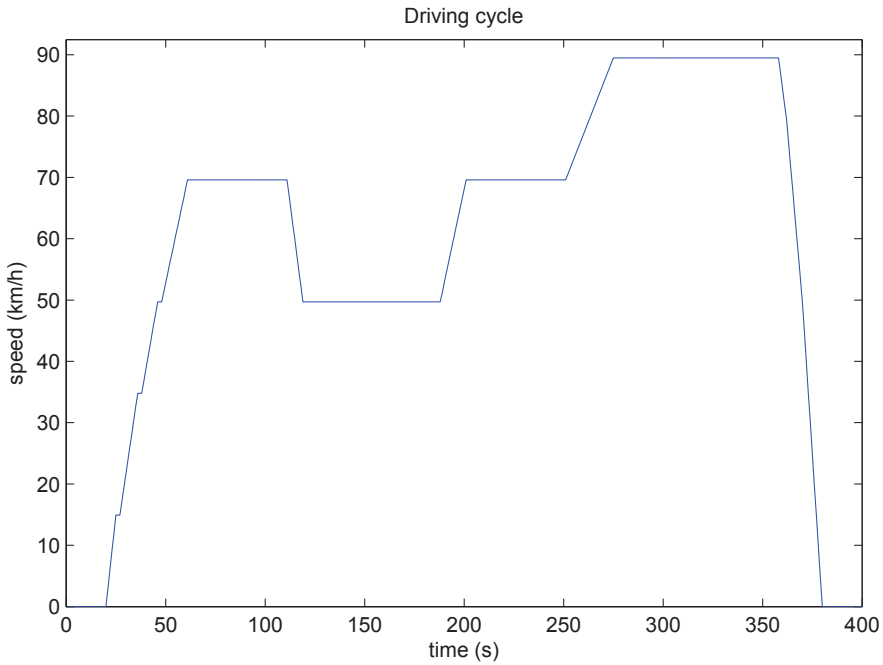

FIGURE 18. EUDC Cycle for Low Power Vehicles

TABLE 4. Parameters for the ECE, EUDC and EUDC low speed cycles

Characteristics	ECE 15	EUDC	EUDC low speed
Distance (km)	1.013	6.955	6.243
Duration (s)	195	400	400
Average Speed (km/h)	18.7	62.2	55.6
Maximum Speed (km/h)	50	120	90

good base to analyze and compare results between manufacturer and car models.

2.1.2 *Recorded driving cycle*

Some driving cycles are not created using approximate acceleration, deceleration and maximum speed, but are recorded from real driving condition [48]. The USA use real driving cycle in order to study the fuel consumption and gas emission. Severals driving cycle with different patterns are recorded : FIGURE. 19 shows a cycle recorded in the city of New York with a truck. This cycle emphasis the low speed and acceleration when driving an heavy weight vehicle. In the opposite part, FIGURE. 20 represents a cycle recorded in the area Cleveland composed of both urban and highway parts, where traffic jams are very rare compare to New York. Consequently, the vehicle recorded has less stops and can reach higher speeds.
The same methodology is used in India : FIGURE. 21 shows an urban driving cycle and FIGURE. 22 a highway recorded cycle. These driving cycles have strong different patterns than the USA's ones due to the speed limit in India, and also to the driving style of driver. Some driving cycle use blended mode : the cycle is made by both recorded and created parts : FIGURE. 23 represents the cycle used in the conception of the Toyota Prius : this cycle is recorded but the driving pattern is imposed to the driver. the driver try to follow the ECE cycle pattern : a first acceleration to reach 40 km/h is made, then the vehicle decelerate to 0 km/h. This protocol is repeated 2 times, then a new acceleration to reach 70 km/h is made to finally come back to 0. The advantage of this cycle is to take into account the performance of the car in terms of dynamic, so the results of fuel consumption and gas emission is closer to the reality than using simple ECE driving cycle. Nevertheless, it clearly appears that a single driving cycle cannot characterize the whole conditions of driving.

2.1.3 *Driving cycle generator*

Knowing the driving patterns is critical in the process of a hybrid electric vehicle conception. The process of sizing and control the sources of energy in the vehicle depends on it. The driving cycles describes previously are good to compare vehicles between them in terms of fuel consumption and gas emission but ,in the case of standard cycles, are not enough close to reality to characterize the power needed by the vehicle during a trip. In the other part, the recorded driving cycles are too specifics. Consequently, the analyses of this cycles leads to restrictive specification of the results. In this way, the study of a family of driving cycle regrouped by patterns (urban for example) leads to a better reflect of the reality. A driving cycle generator has been design to create multiple driving cycle from recorded one in order to get a representative sample of cycle for a family study. The following section will

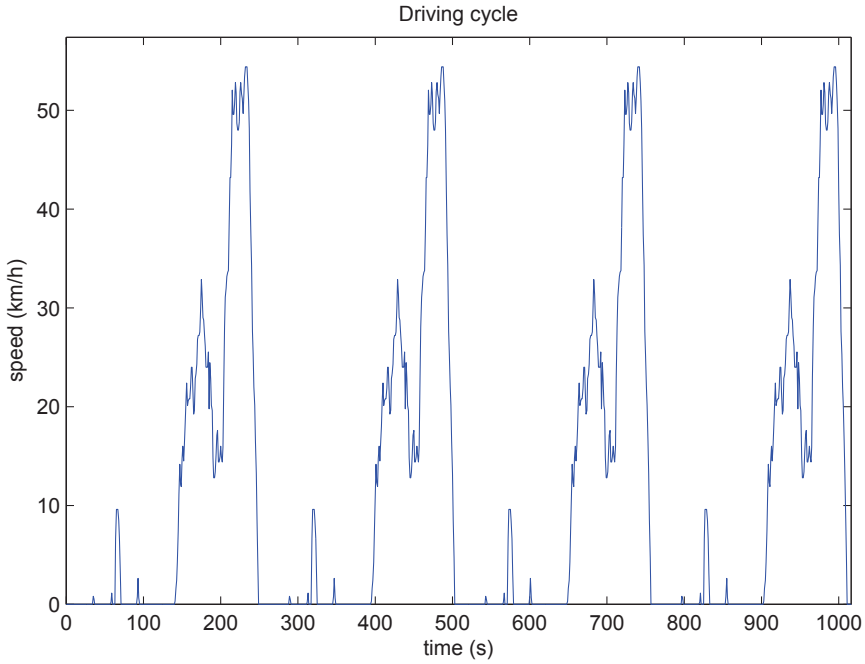

FIGURE 19. New York city recorded cycle with a truck

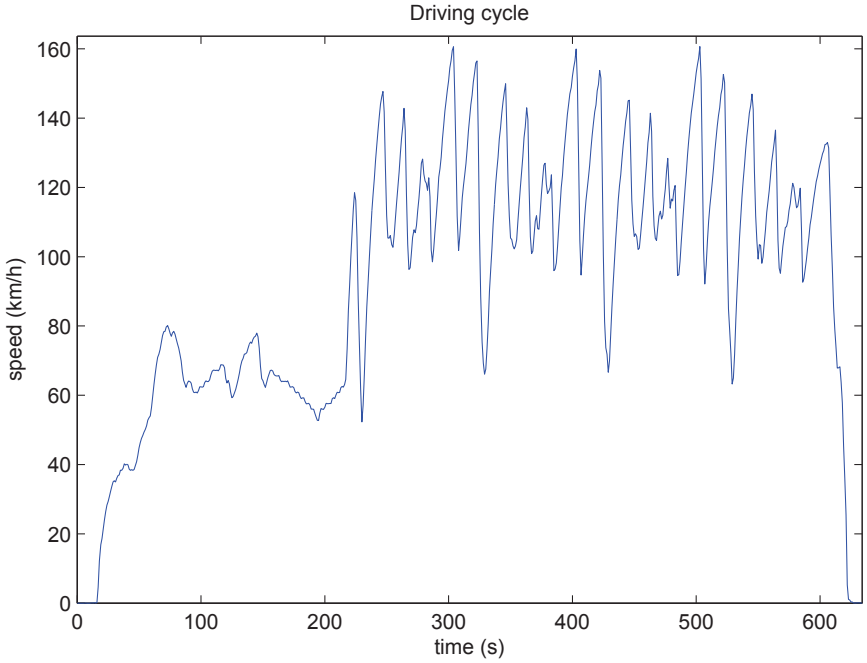

FIGURE 20. Cleveland highway recorded driving cycle

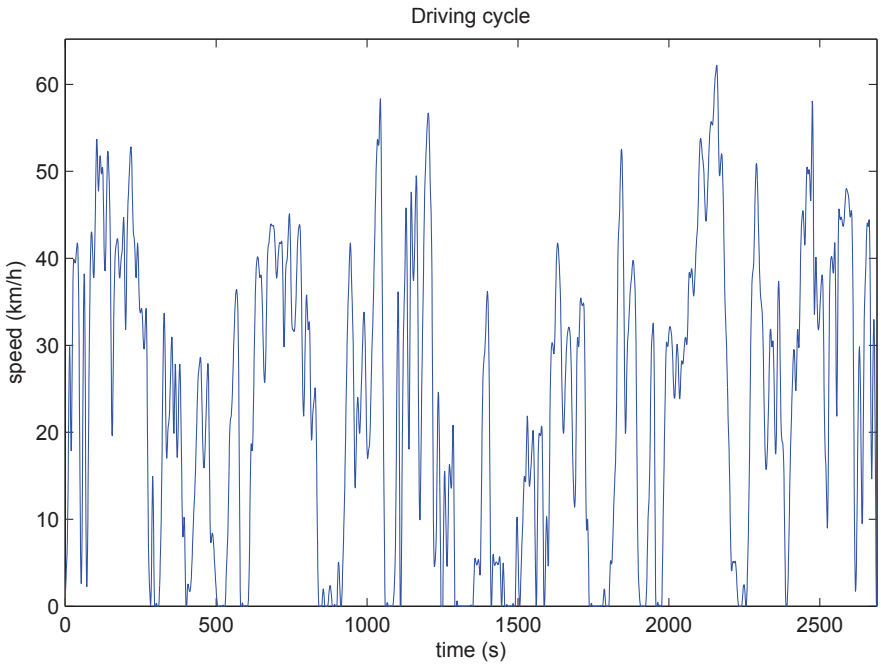

FIGURE 21. Urban part in India cycle

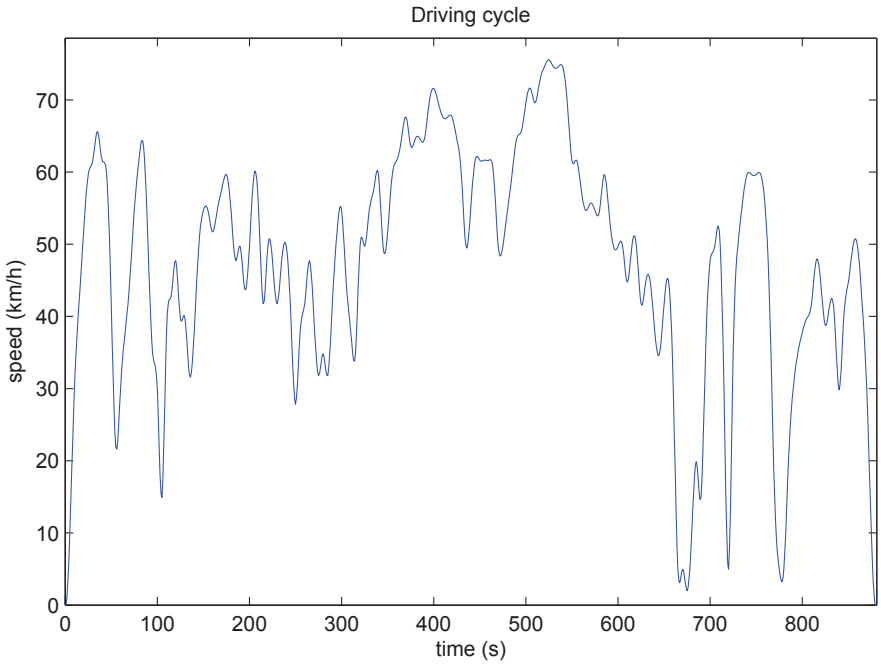

FIGURE 22. Highway part in India cycle

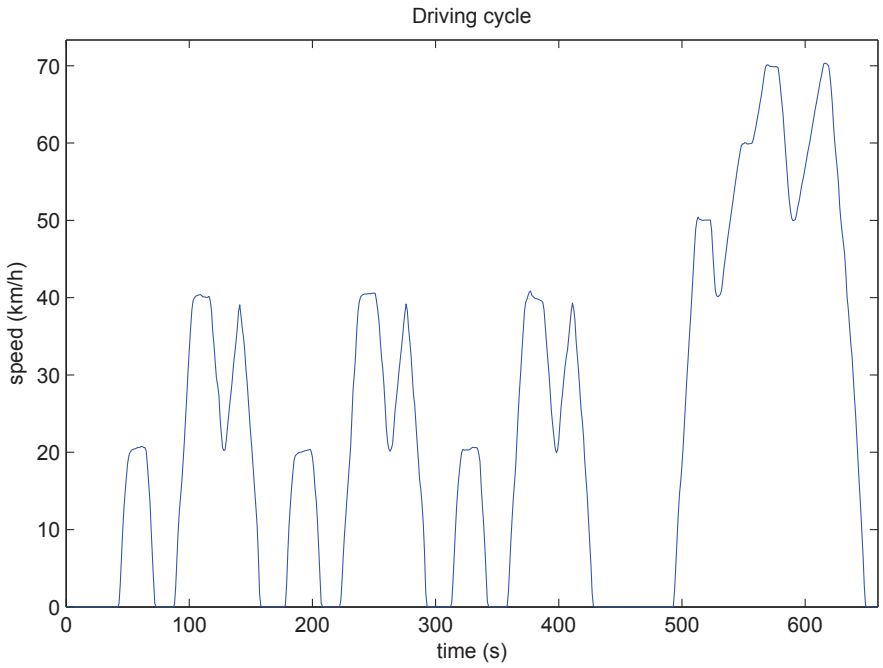

FIGURE 23. Toyota Prius blended cycle

describe the conception and utilization of this generator.

Data recording

The generated cycles are not totally random : They reflect statistically a set of data recorded. A first work has been made to collect data. The application chosen is a garbage truck of the city of Belfort, France. The general purpose of this truck is to do exactly the same trip every day to collect garbages from house and get it back to the garbage center. this leads to 2 observations :

- The cycle made by the vehicle is the same every day : The driving generated driving cycle cannot be random, they need to have the same pattern as the recorded one.
- The mass of the vehicle increases during the cycle : since the truck collect garbage, the mass of the vehicle increase until the truck is full.

Theses two parameters must appear in the data collected : A GPS logger is used to record the data of the truck for one week, corresponding to 6 driving cycle (one cycle every day). FIGURE. 24 shows the recorded used for this study : the GPS sensor gives information about position, speed, time and altitude. The frequency is set to 1 Hz. The logger as a memory of 4 Gb corresponding to more than 200 hours of record. Moreover, the mass of each garbage collected is weighted by the truck collect system in order to determine the total weight of the vehicle.

The following parameters are recorded :

FIGURE 24. ISAAC recorder

– *Position* ;
– *Time* ;
– *Speed* ;
– *mass of the vehicle* ;
– *altitude*.

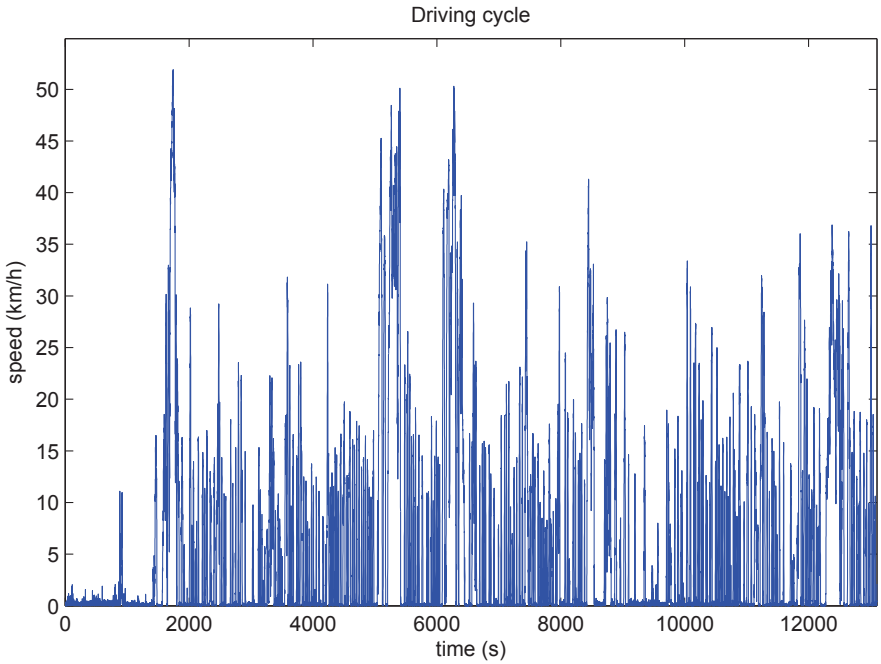

FIGURE 25. Recorded garbage truck cycle

FIGURE. 25 shows the driving cycle recorded for one day made by the garbage truck. The pattern is urban : the speed does not exceed 50 km/h and a lot of acceleration/deceleration phases can be observed. The 7 days of data will be analysed in order to collect informations to create new random driving cycles.

Statistical analysis of driving cycle

The garbage truck's driving cycle has a specific pattern as described in FIGURE. 26 :

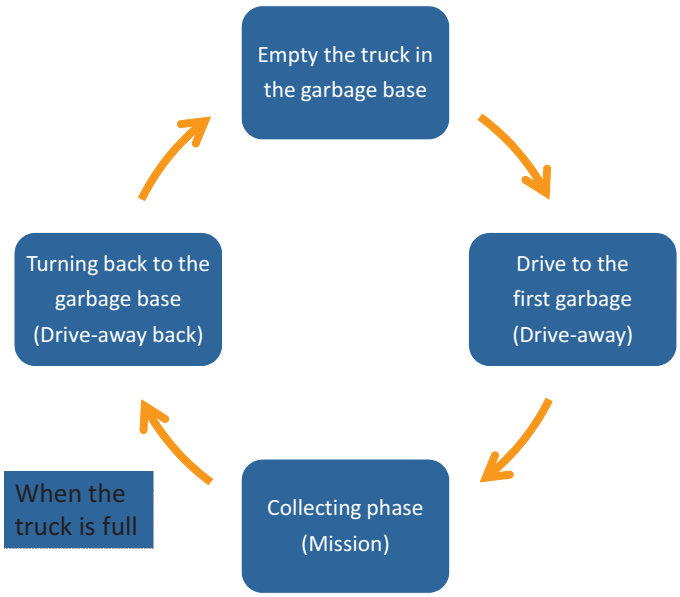

FIGURE 26. Truck Driving cycle pattern

- *Drive-away* The truck start empty and goes from base to the first house ;
- *mission/work :* The truck goes from house to house and stop at each house to collect garbage ;
- *Drive-away back :* When the truck is full, it goes back to base ;
- *Turnaround* : The Turnaround describes the whole cycle (drive-away, mission and drive-away back

The recorded driving cycle are analyzed and some parameters are extracted :

- *Drive-away distance :* distance between the garbage base and the first house ;
- *Drive-away speed :* mean drive speed from the base to the first house ;
- *Drive-away acceleration/deceleration :* mean acceleration/deceleration speed from the base to the first house ;
- *Working speed :* drive speed from one house to another ;

- *Working acceleration/deceleration :* acceleration/deceleration from one house to another ;
- *Working distance :* distance between two houses ;
- *Collection time :* time to collect the garbage of one house ;
- *Stop time :* time when the vehicle is stopped to collect garbage ;
- *Garbage weight :* weight of the garbage of one house that need to be collected in the truck ;
- *Road slope.*

Drive-away and driveway back parameters determination

The 3 phases of the cycle (drive-away, mission and drive-away back) cannot be strictly determined. In this way, a survey has been conducted on all turnarounds did by all the garbage trucks from the company to determine the distance between the base and the first house. FIGURE. 27 shows the statistical description of those results. The drive-away speed, acceleration and deceleration are extracted from the cycle within the mean drive-away distance. Since the truck goes back at the same base at the end of the cycle, the same results applies for the drive-away back.

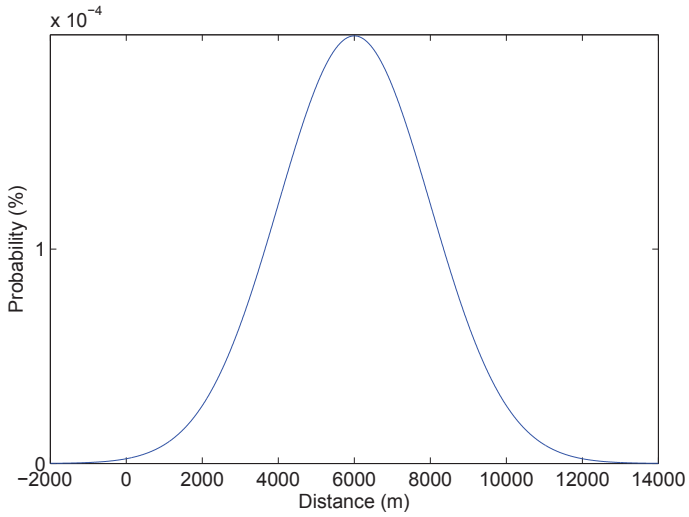

FIGURE 27. Drive-away distance distribution

Working speed distribution

In order to statistically describe the speed of the vehicle between two houses, each speed at each time step during the mission phases is analyzed, except when the speed is 0. FIGURE. 28 shows the working speed distribution : the distribution is not a Gaussian distribution because of the mission profile of the truck : it does a lot of stop and the mean speed is very low. It can

be observed that speeds inferior to 1 m/s does not appear.Those values are voluntary exclude because the distribution must represent the mean speed between two houses. Consequently, a speed lower than 1 m/s is to low to be considered as a mean speed (the distance run by the trucks will be to low to consider that it goes from one house to another).

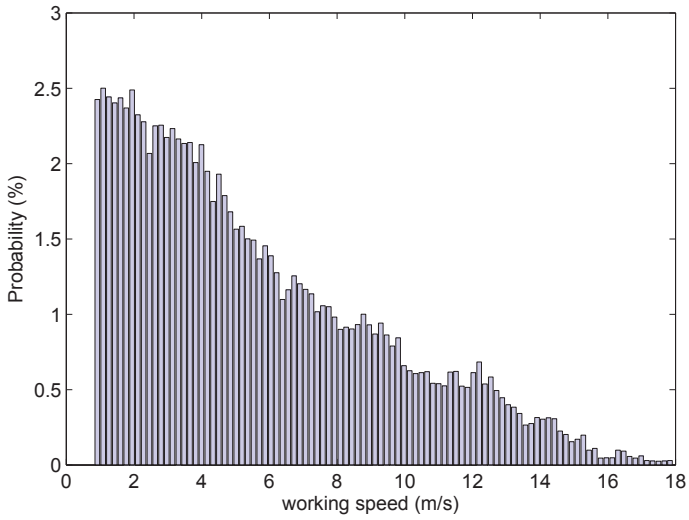

FIGURE 28. Drive-away distance distribution

Working acceleration/deceleration distribution

In order to determine the acceleration/deceleration did by the vehicle during the cycle, the acceleration profile has been created from the driving cycle using 2.1 :

$$\gamma(t) = \frac{dv}{dt} \tag{2.1}$$

FIGURE. 29 shows the acceleration profile derivate from the driving cycle. From this data, acceleration and deceleration profile are extracted and distributions are created FIGURE. 30 and FIGURE. 31.

Working distance

The working distance describe the distance made by the truck to get from a house to another. From the driving cycle, the driving distance can be determined by FIGURE. 32 where Ts is the sample time of the driving cycle (1 second) and Distancetot is the total distance between the 2 houses. FIGURE. 33 shows the statistical description of the working distance extracted. The majority of the distance are between 10 and 40 m and the distribution has a Gaussian shape.

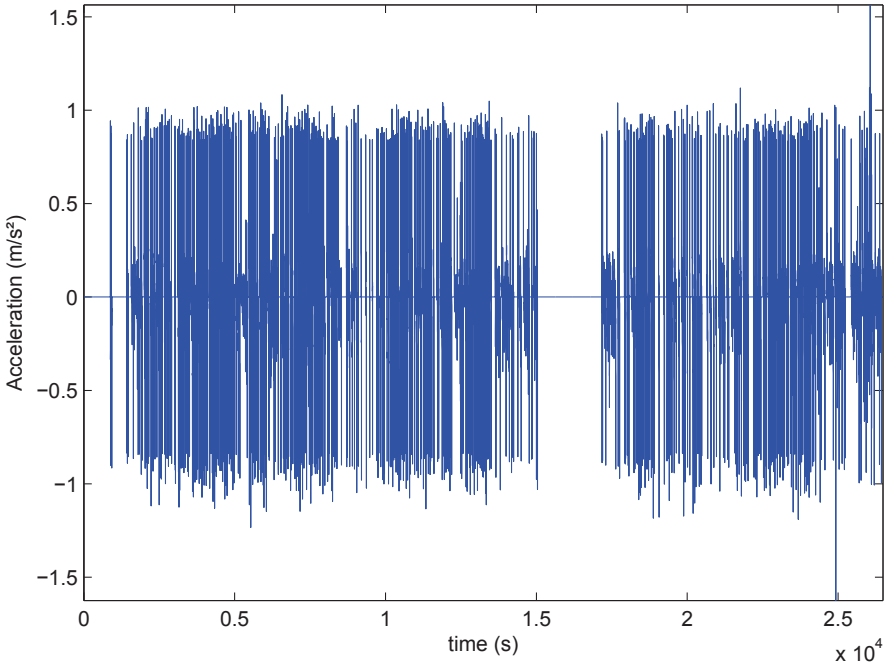

FIGURE 29. Acceleration profile

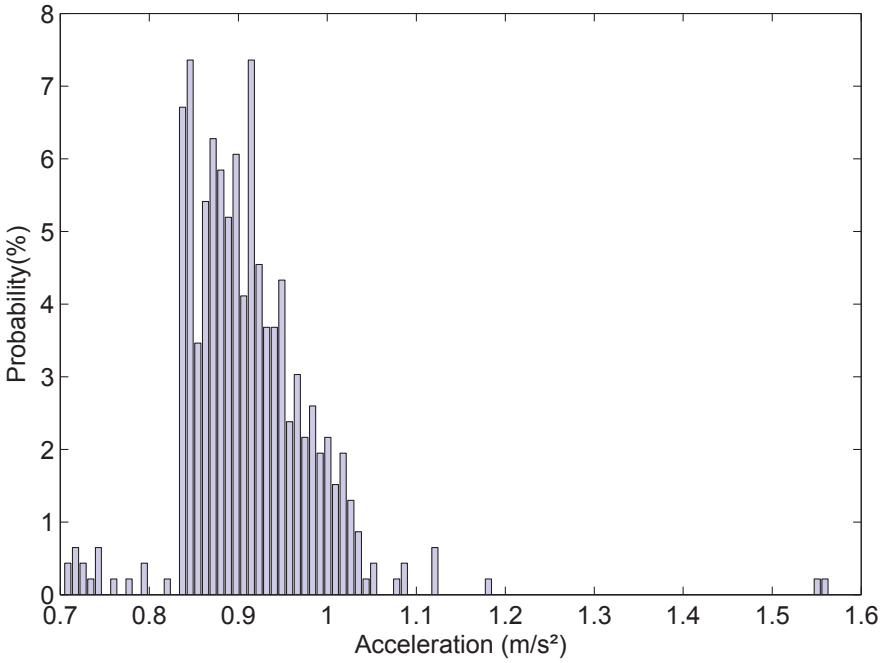

FIGURE 30. Working acceleration distribution

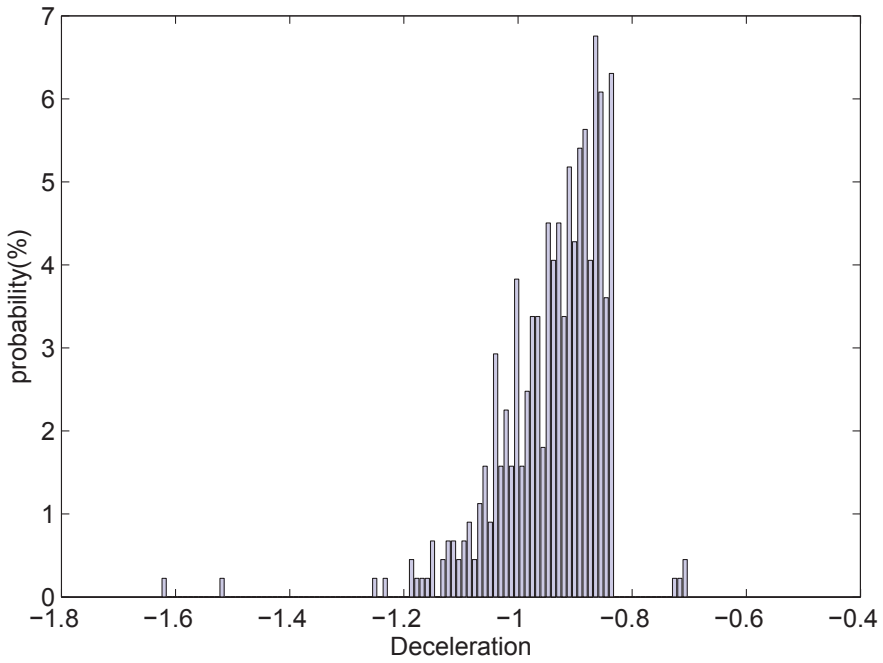

FIGURE 31. Working deceleration distribution

Stop time

The stop time is the amount of time spend by the vehicle when he is stopped to collect garbage between 2 houses. This information is extracted from the driving cycle using methodology described in FIGURE. 34where Ts is the sample time of the driving cycle (1 second) and Timestop is the total stop time. Results are drawn in FIGURE. 35. It can be observed that for a small amount of stop time (between 7 and 12 seconds), the probability is high (superior to 4 %). This part of the data does not reflect the time spend collecting garbage but the time stop by traffic light/jams. Indeed, since the driving cycle is the unique source of information : the algorithm cannot distinguish between stop caused by traffic or collecting phases.

Generate a driving cycle from statistical description of recorded data

As described in section 2.1.3, The truck runs a specific driving cycle called Turnaround. The generated driving cycle needs to have the same pattern as the Turnaround : Drive-away, mission and drive-away-back.
For each parts of the turnaround, the parameters are randomly generated using distribution as follow :

1. The empty truck goes out of the base : drive-away distance, drive-away speed and slope values are randomly picked up. As discuss in section 2.1.3, the speed picked corresponds as the mean speed of the vehicle

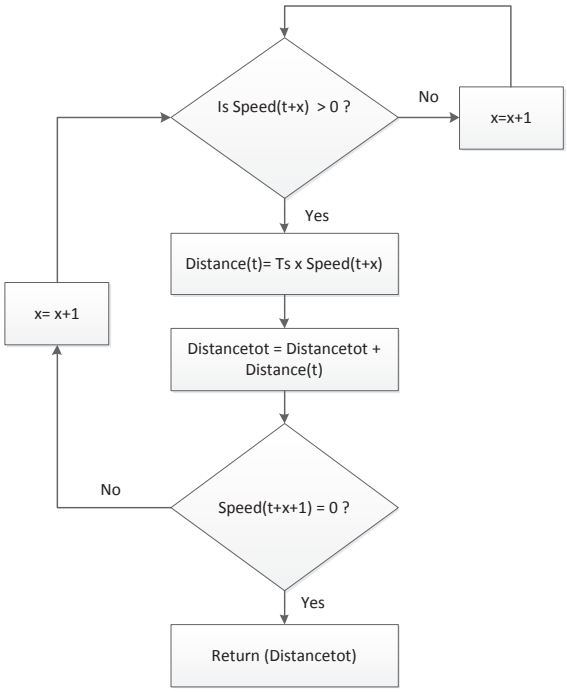

FIGURE 32. Algorithm flowchart to determine the distance between two house

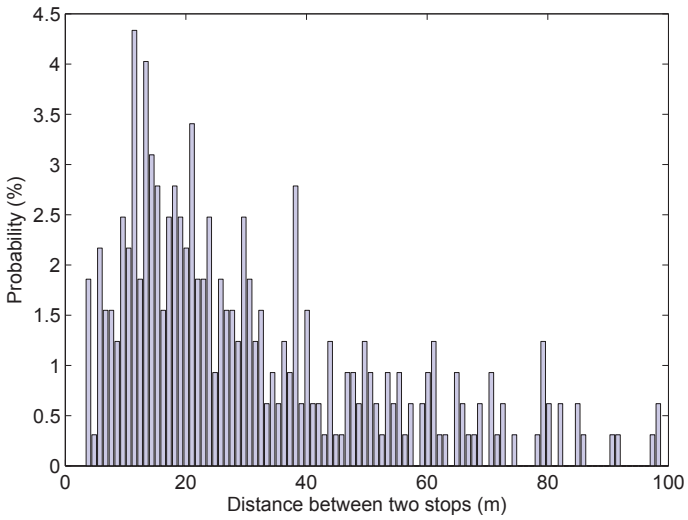

FIGURE 33. Working distance distribution

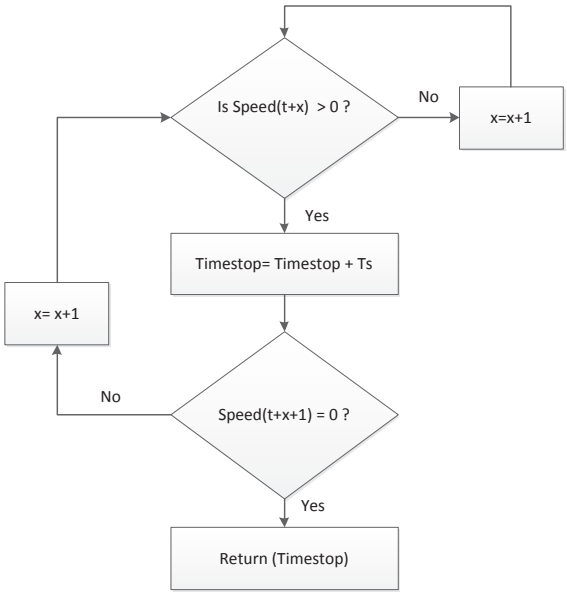

FIGURE 34. Algorithm flowchart to determine the distance between two house

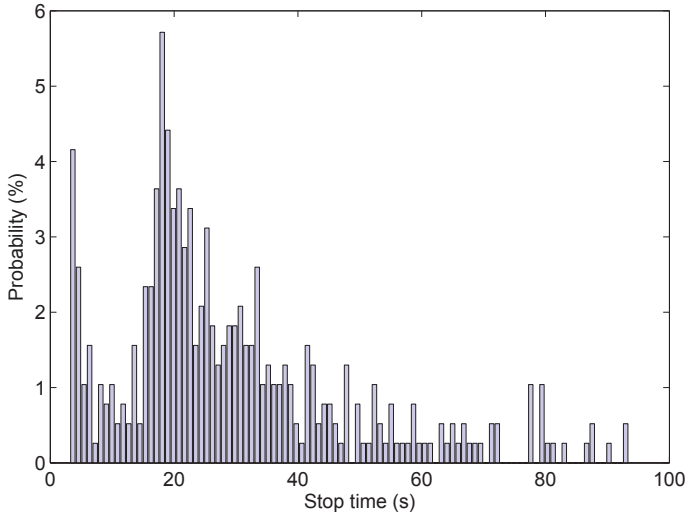

FIGURE 35. Working distance distribution

running from base to the first house ; the slope is also considered as the mean slope.

2. The truck collect the first bin : garbage weight and collection time values are randomly picked up.
3. If the truck is not full, working distance, working speed, acceleration/deceleration and slope values are randomly picked up : to ensure the coherence with FIGURE. 36 :

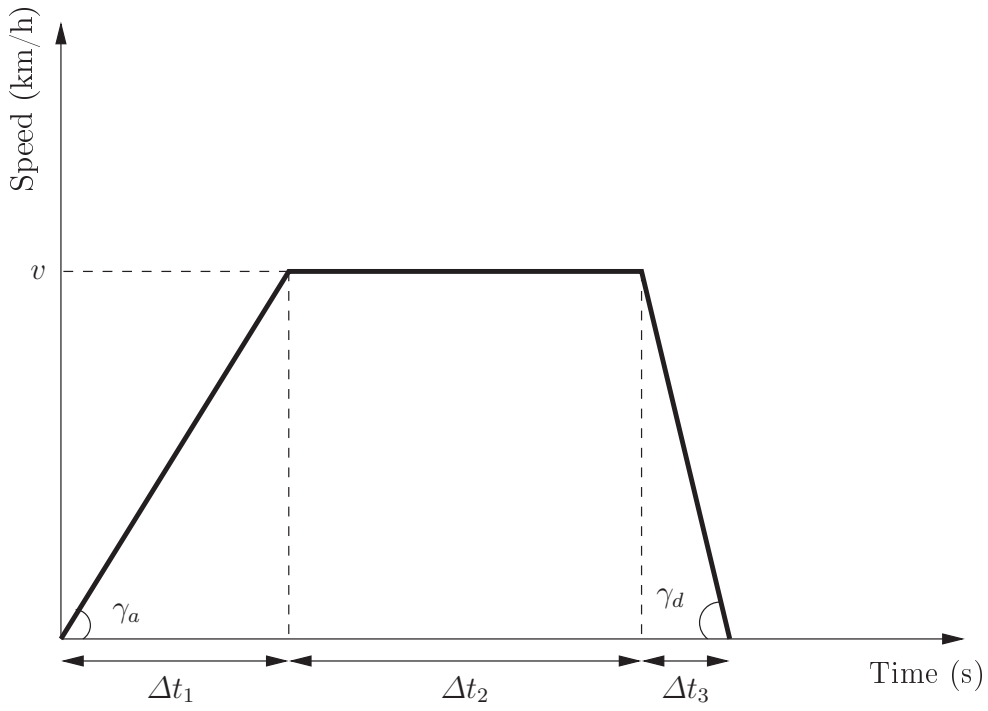

FIGURE 36. Determination of the time Δt_2 spent at speed v

Determination of the time spent at constant speed Δt_2 (2.2) :

$$
\begin{aligned}
d &= \frac{1}{2}\gamma_a \Delta t_1 + v \Delta t_2 + \frac{1}{2}\gamma_d \Delta t_3 \qquad (2.2)\\
d &= \frac{1}{2}\gamma_a \left(\frac{v}{\tan\gamma_a}\right) + v \Delta t_2 + \frac{1}{2}\gamma_d \left(\frac{v}{\tan\gamma_d}\right)\\
v\Delta t_2 &= d - \frac{v^2}{2\tan\gamma_a} - \frac{v^2}{2\tan\gamma_d}\\
\Delta t_2 &= \frac{d}{v} - \frac{v}{2\tan\gamma_a} - \frac{v}{2\tan\gamma_d}
\end{aligned}
$$

If $\Delta t_2 < 0$, the picked acceleration, deceleration and total distance does not fit with the speed chosen. In this case, a new speed v is calculated (2.3) :

$$\begin{aligned} \Delta t_2 &= 0 \qquad (2.3)\\ \frac{d}{v} - \frac{v}{2\tan\gamma_a} - \frac{v}{2\tan\gamma_d} &= 0\\ \frac{4\tan\gamma_a\tan\gamma_d - vd2\tan\gamma_d - vd2\tan\gamma_a}{v4\tan\gamma_a\tan\gamma_d} &= 0\\ v &= \frac{4\tan\gamma_a\tan\gamma_d}{d2\tan\gamma_d + d2\tan\gamma_a} \end{aligned}$$

The cycle continues from the step 2 until the truck is full ;

4. When the truck is full, drive-away distance, driveway speed and slope values are randomly picked up in the same way as step 1.

FIGURE. 37 and FIGURE. 38 show a generated driving cycle with the evolution of the weight of the vehicle. The 3 phases clearly appear on the driving cycle and the results in term off acceleration,deceleration,mean speed... respect the original recorded driving cycle.
Many driving cycle can be created with the generator, and the input parameters (statistical distributions) can be tweaked to generate specific scenarios : For instance, FIGURE. 39 shows the most power consuming driving cycle that can be generated : The acceleration/deceleration and speed are maximum and each weight of bin is minimum. Consequently, the vehicle does a lot of start stop (5 times more than in FIGURE. 37) with huge dynamics.

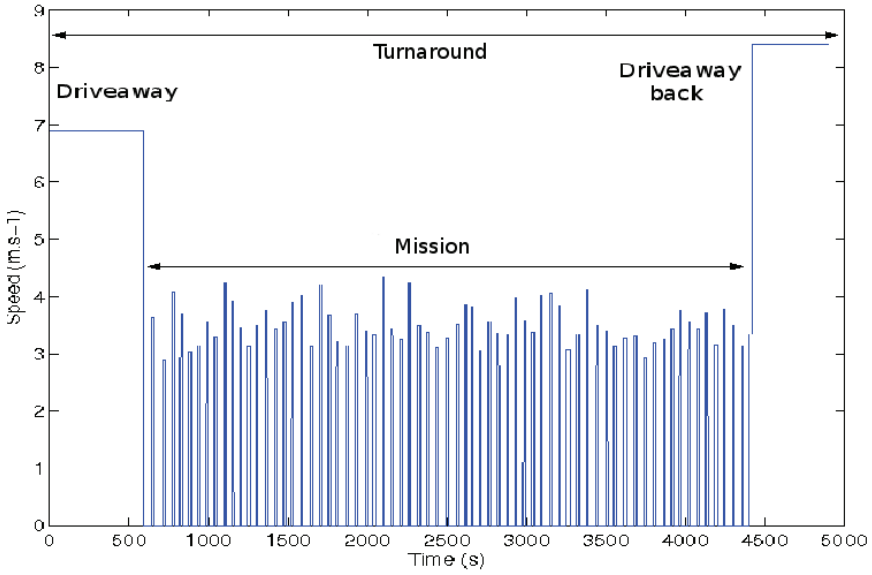

FIGURE 37. Generated driving cycle

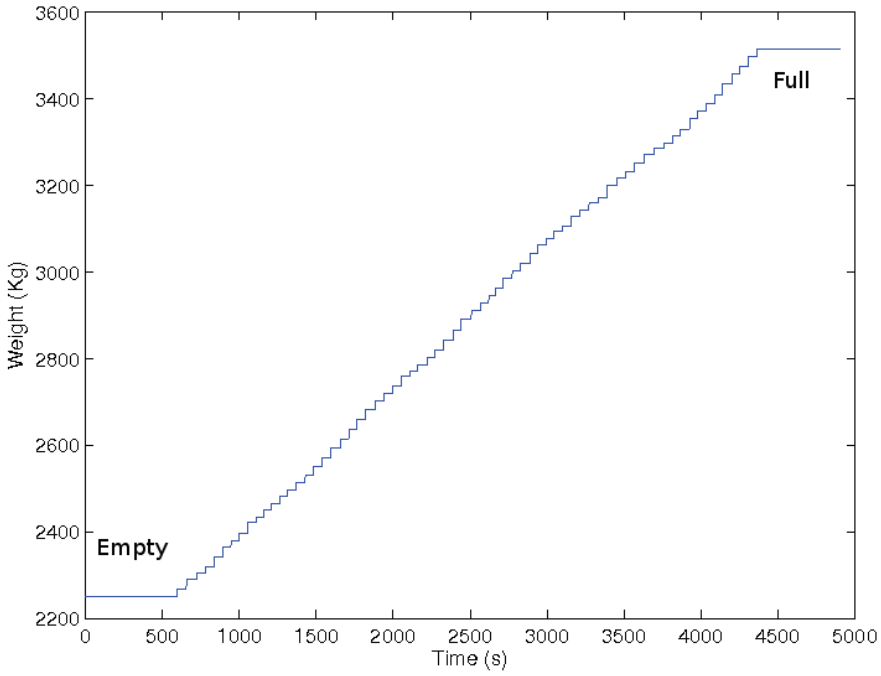

FIGURE 38. Generated weight driving cycle

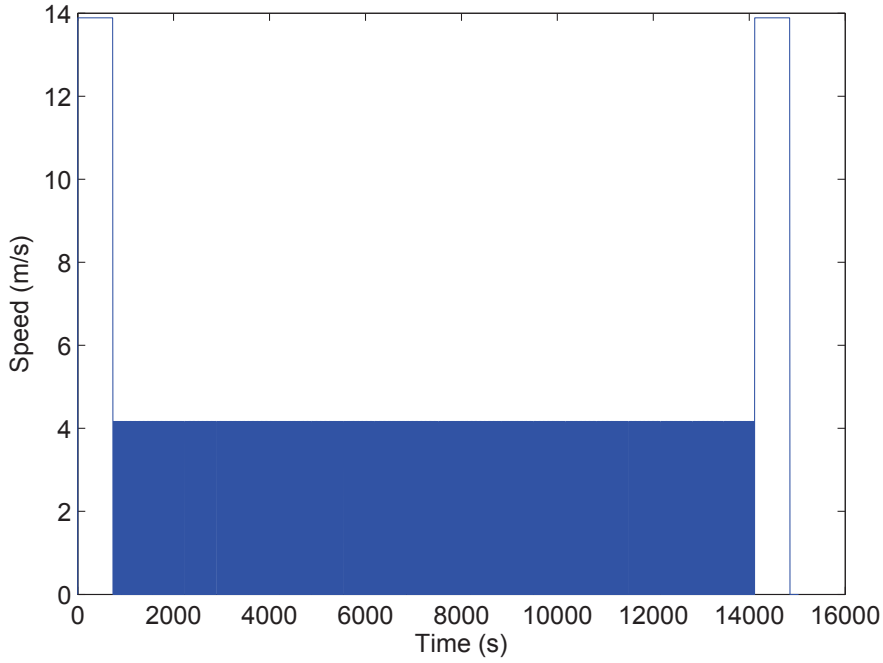

FIGURE 39. Generated most power consuming driving cycle

2.2 ENERGY SOURCES SIZING

2.2.1 *Power profile determination*

In a hybrid electric vehicle, the power needed at every time can be provided either by the primary source of energy (Fuel cell or Internal Combustion Engine) or by the batteries. The determination of the power needed by the vehicle during a driving cycle is crucial to determine the size of both energy sources [49, 50].

vehicle model

The power can be calculated by modeling the vehicle used [51] : The amount of mechanical energy consumed by a vehicle when driving a specified driving pattern depends on three effects :

- The aerodynamic friction losses ;
- the rolling friction losses ;
- the energy dissipated in the brakes.

The vehicle model can be describes using the Newton's second law (2.4) :

$$m_v(t)\,\frac{d}{dt}\,v(t) = F_t(t) - \Big(F_a(t) + F_r(t) + F_g(t) + F_d(t)\Big) \tag{2.4}$$

$$P_v(t) = v\,F_t(t) \tag{2.5}$$

where,

$$F_t(t) = m_v(t)\frac{d}{dt}v(t) + F_a(t) + F_r(t) + F_g(t) + F_d(t) \tag{2.6}$$

where F_a is the drag force, F_r the rolling friction, F_g the force caused by gravity when driving on non-horizontal roads, F_d the disturbance force that summarizes all other effects and F_t is the traction force which depends on speed and acceleration. FIGURE. 40 shows a schematic representation of this relationship :

- Aerodynamic Friction Losses : The aerodynamic resistance F_a acting on a vehicle in motion is caused on one hand by the viscous friction of the surrounding air on the vehicle surface. On the other hand, the losses are caused by the pressure difference between the front and the rear of the vehicle, generated by a separation of the air flow. For a standard passenger car, the car body causes approximately 65% of the aerodynamic resistance. The rest is due to the wheel housings (20%), the exterior mirrors, eave gutters, window housings, antennas, etc. (around 10%) and the engine ventilation (approximately 5%) [52]. Usually, the aerodynamic resistance force is approximated by simplifying the vehicle to be a prismatic body with a frontal area A_f. The force cause by the

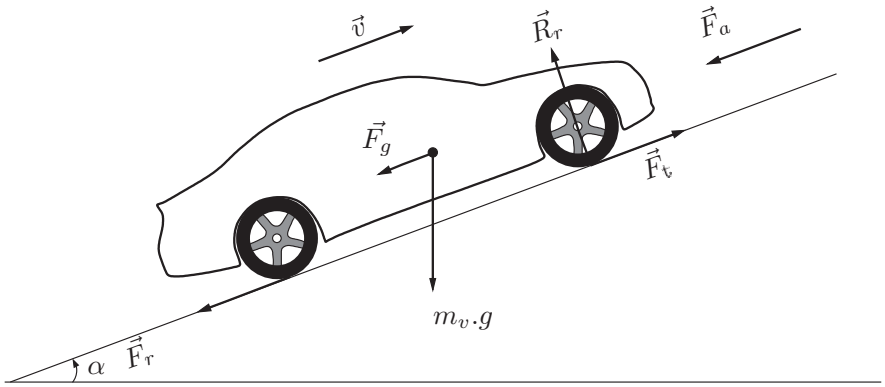

FIGURE 40. Schematic representation of the forces acting on a vehicle in motion

stagnation pressure is multiplied by an aerodynamic drag coefficient C_x that models the actual flow conditions (2.7) :

$$F_a = \frac{1}{2}\,\rho_a\,A_f\,C_x\,v^2 \tag{2.7}$$

Where v is the vehicle speed and ρ_a the density of the ambient air. The parameter C_x must be estimated using experiments in wind tunnels.

– Tolling Friction Losses : It is often modeled as (2.8) :

$$F_r = m_v(t)\,C_r\,g\,\cos(\alpha) \tag{2.8}$$

where m_v is the vehicle mass and g the acceleration due to gravity. The term $\cos(\alpha)$ models the influence of a non-horizontal road. However, the situation in which the angle α will have a substantial influence is not often encountered in practice. The rolling friction coefficient C_r depends on many variables : The most important influencing quantities are vehicle speed v, tire pressure p_t, and road surface conditions. The influence of the tire pressure is approximately proportional to $1/\sqrt{p_t}$. A wet road can increase C_r by 20% and driving in extreme conditions (sand instead of concrete) can easily double that value. The vehicle speed has a small influence at lower values, but its influence substantially increases when it approaches a critical value where resonance phenomena start.

– Uphill Driving Force : The force induced by gravity when driving on a non-horizontal road is conservative and considerably influences the vehicle behavior. In this text this force will be modeled by the relationship (2.9) :

$$F_g = m_v(t)\,g\,\sin(\alpha) \tag{2.9}$$

For our study, the truck is a hybrid electric vehicle made with fuel cell and batteries ; and has the following characteristics :

– Empty weight : 13,000 kg ;
– Mass when fully loaded : 19,000 kg ;
– Front surface (A_f) : 7 m² ;
– Drag coefficient (C_x) : 0.8 ;
– Rolling coefficient (C_r) : 0.015 ;
– Drivetrain efficiency : 0.72.

The aim of the study is to determine the power of the fuel cell and the batteries capacity.

Power profile

The generated driving cycles will be used as an input of the vehicle's model in order to determine the power profile at each time step of the cycle. The vehicle's model Matlab/Simulink is presented in Figure 41. The model parameters are : the speed, the slope, the acceleration and the weight of truck for each step of simulation.

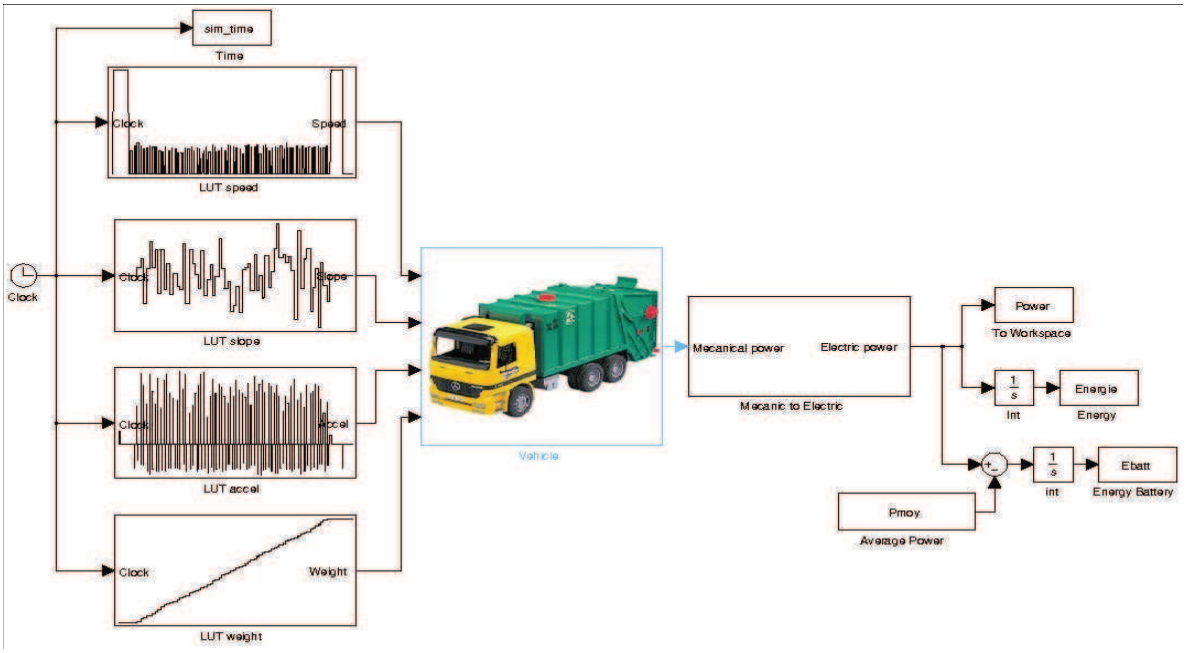

FIGURE 41. Simulink vehicle's model

The sequential algorithm used to run the simulation is presented in FIGURE. 42. Each generated driving cycle is simulated using the vehicle model and the instantaneous power $P(t)$ at each time step. FIGURE. 43 shows the profile power for the driving cycle recorded FIGURE. 25.

Then, the mean power $\bar{P}$ and the total energy E at the end of each cycle can

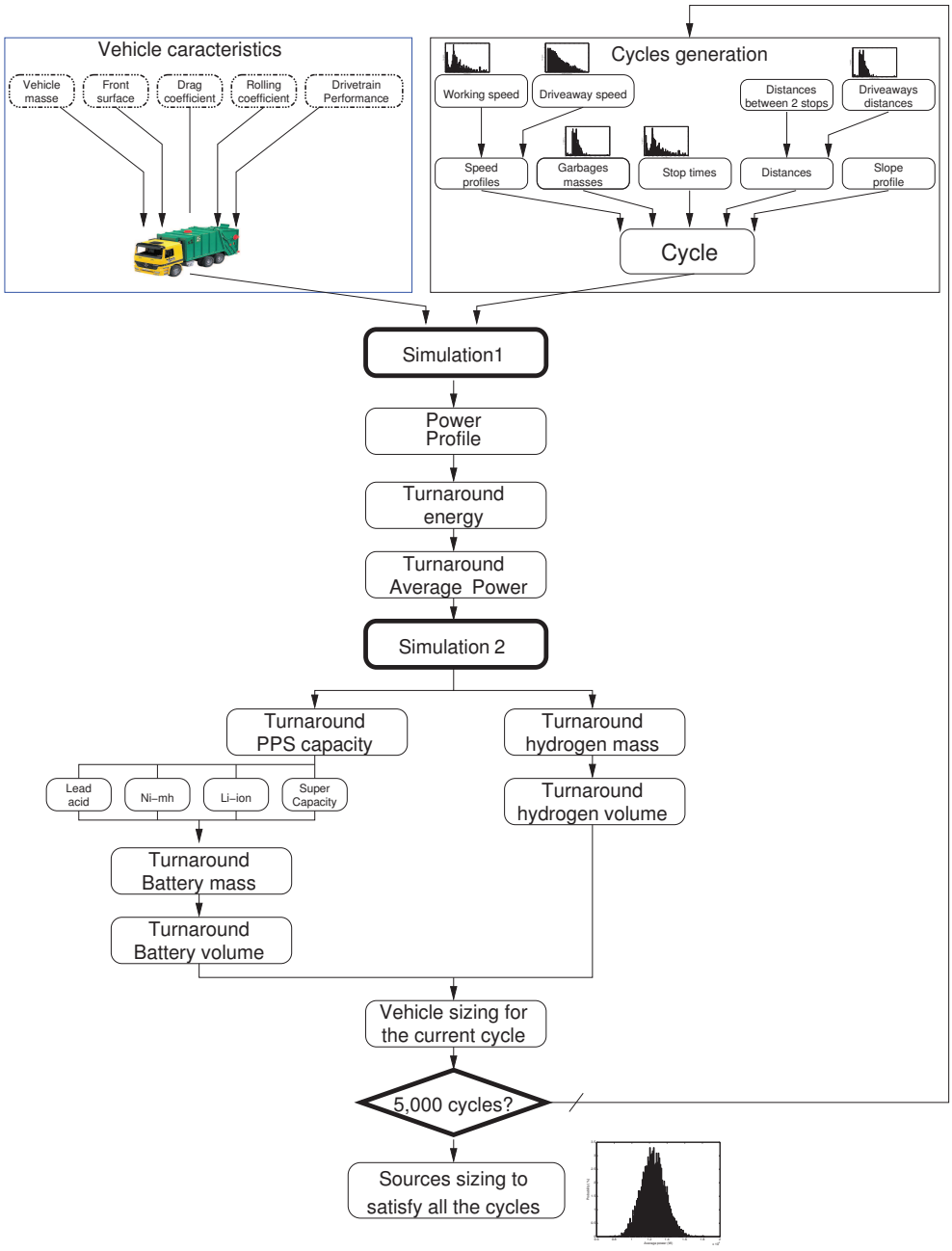

FIGURE 42. Algorithm flowchart

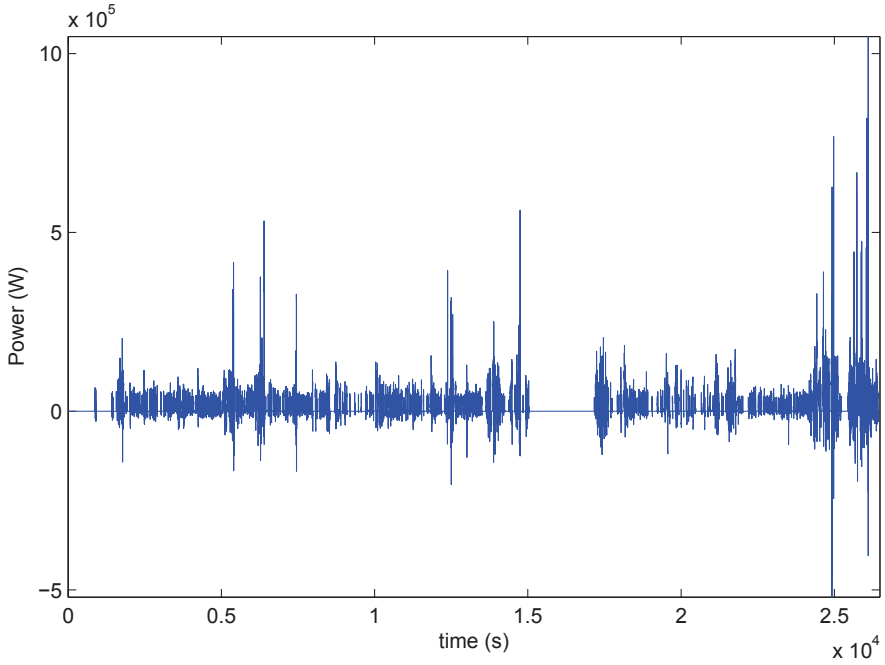

FIGURE 43. Power profile of a generated driving cycle

be computed using (2.10), (2.11) and (2.12), respectively :

$$P(t) = \frac{P_v(t)}{\eta_d} \tag{2.10}$$

$$\bar{P} = \frac{1}{T_{turnaround}} \int_0^{T_{turnaround}} P(t)\,dt \tag{2.11}$$

$$E = \bar{P} \cdot T_{turnaround} \tag{2.12}$$

where η_d is the drive train efficiency and $T_{turnaround}$ is the total time of the turnaround including all stops, working and drive-away times.

As each turnaround driving profile is different, the mean power and any other quantities such as the total time ($T_{turnaround}$) for each turnaround will vary. For example FIGURE. 44 represents the statistical distribution of the total time of a turnaround.

After the first simulation, a second simulation is run using the mean power obtained in the first one with the same driving profile. The second simulation determines the energy profile along the time of peaking power source(battery) (2.13) and its corresponding capacity (2.14).

$$E_{battery}(t) = \int P_{current}(t) - \bar{P}(t)\,dt \tag{2.13}$$

$$C_{battery}\,(Wh) = E_{battery\ max} - E_{battery\ min} \tag{2.14}$$

The results obtained from these two simulations are used to size the energy

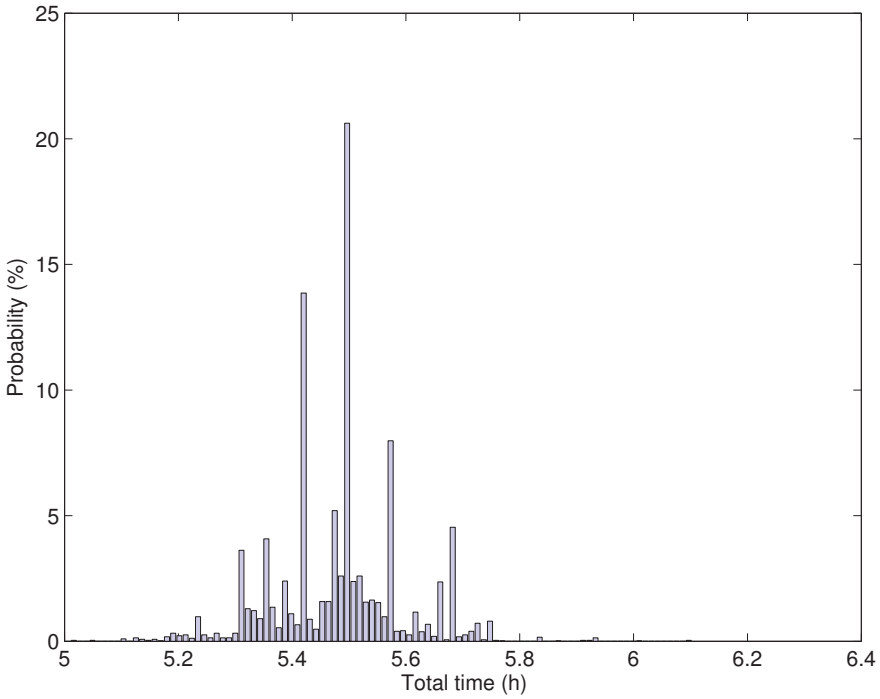

FIGURE 44. Total time distribution ($T_{turnaround}$)

storage sources (fuel cell power, hydrogen mass, battery power and energy capacity).

2.2.2 *Fuel cell stack power needs*

Mean power and energy distributions

After a simulation of 5,000 turnarounds, the mean power distribution is computed and given in FIGURE. 45. It can be clearly seen that the distribution of the mean powers is a normal distribution centered on 13 kW.

The high number of simulation (5,000) has been chosen to have more precise results keeping an acceptable simulation time (about 25 min for 5,000 simulation). However, it has been shown that from a number of 1,000 simulation the results are acceptable. The mean power distribution shows that the maximum mean power required for one turnaround does not exceed 18 kW. A 20 kW fuel cell stack will satisfy 100 % of the simulated cases based on the chosen parameters. These results allows the fuel cell stack and the hydrogen quantity to be chosen depending on how much turnarounds are planed for one day. Moreover, if the hydrogen infrastructure is equipped with a fast recharge station, the hydrogen tank does not need to be sized for the needs of one day but only for a few turnarounds.

Once the fuel cell power (*i.e., mean power*) is computed, it is assumed that

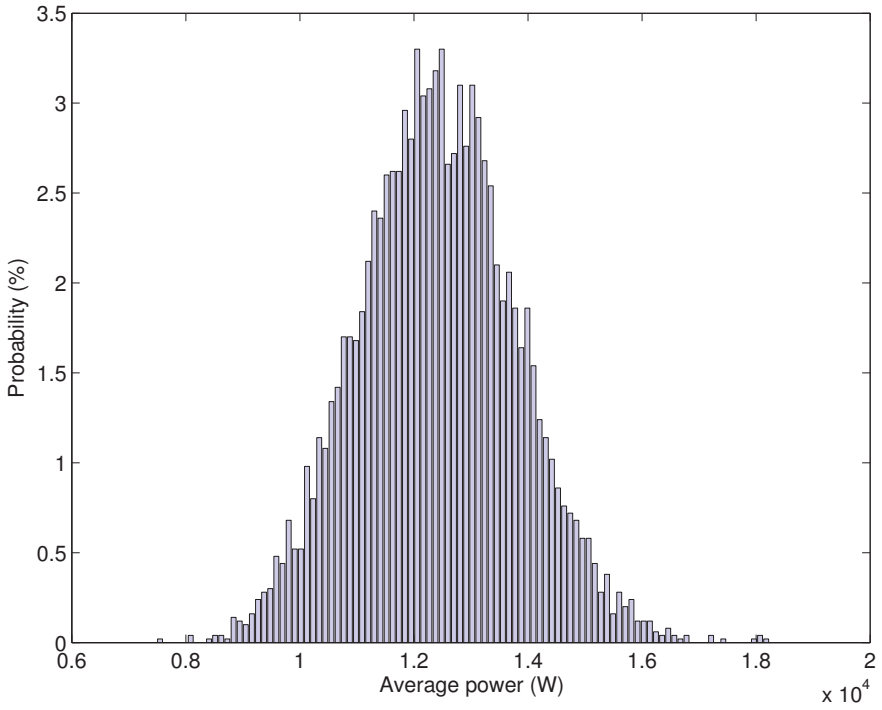

FIGURE 45. Turnaround mean power distribution

the fuel cell always output the mean power, also during stop phases, when the truck is collecting garbage. This mean power can be subtracted to the instantaneous power to determine the power needed by the peaking power source [53, 54].

2.2.3 *Peaking power source energy needs*

Once the mean power is determined, a second simulation is run to determine the energy (2.13) and capacity (2.14) of the second power source by integrating its power. The results are given in FIGURE. 46. It is assumed that the truck is not a plug-in vehicle : the initial and final battery's states of charges must be the same. The fuel cell recharges the battery when the power needed by the vehicle is below the mean power (*i.e.*, fuel cell power). The battery capacity has been calculated based on the battery state of charge constraints : depending on the technology, the state of charge should be between a minimum (15 % to 20 % for Lithium-based batteries and Lead-acid batteries) and a maximum (100 %). The battery capacity is calculated based on the fact that the fuel cell runs constantly at the mean power of the driving cycle and the battery gives or absorbs the remaining power. These results show that the maximum battery capacity does not exceed 23 kWh. A battery pack with 25 kWh will satisfy 100 % of the simulated cases based on the

chosen parameters.

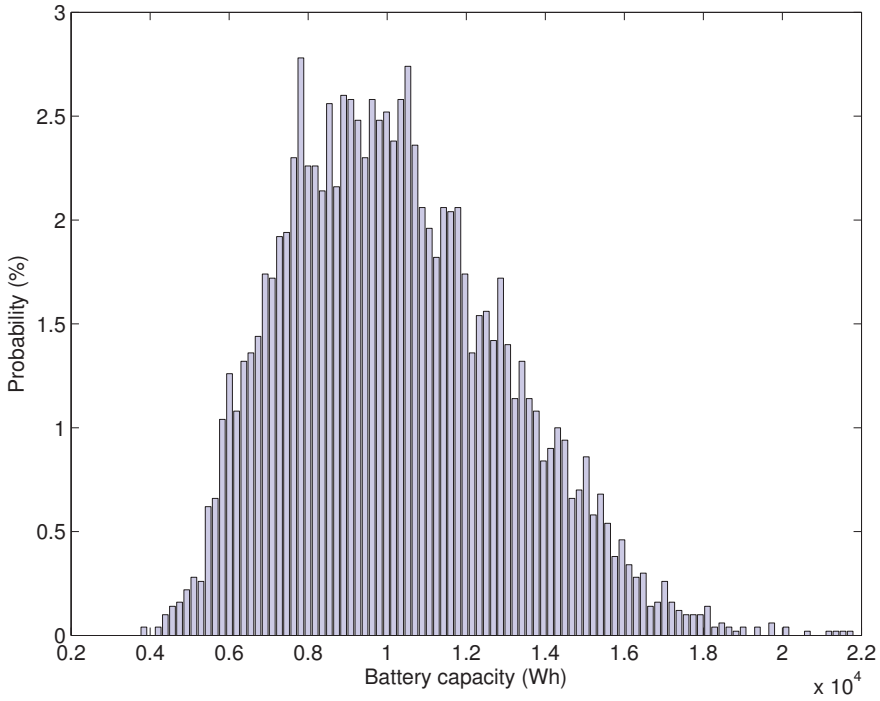

FIGURE 46. Battery capacity

2.2.4 *Practical sizing of both energy sources*

Fuel cell and battery capacity for several braking recovery rate

TABLE 5 shows the mean power of the vehicle and the battery capacity needed for the truck for several braking recovery rates. For this study due to repeated starts and stops, it is assumed that the recovery of braking energy rate is 60 % [55].

TABLE 5. Fuel cell and Battery capacity for several braking recovery rates

Braking recovery	Mean power (W)	Battery capacity (Wh)
0 %	21,600	24,800
30 %	19,900	23,100
60 %	18,300	21,900
100 %	16,400	20,600

2.2.5 *Size of the battery pack*

TABLE 6 shows the mass and the volume of different peaking power sources technologies based on the specific power and energy density given in [56]. This table is based on an energy recovery of 60 %.

TABLE 6. Size of the peaking power sources for several technologies assuming a 60 % energy recovery during braking phases.

Type	Mass (kg)	Volume (l)
Lead-acid	2,500	1,150
Nickel-metal	600	175
Lithium-ion	500	175
Ultracapacitors	2,000	1,000,000

Due to their very low energy density (10 Wh/kg) [57], it is shown that the ultra-capacitors are not suitable for this application. However, a triple hybrid vehicle including fuel cell (low dynamics, low power and overall energy), battery (medium dynamics and medium power, medium energy) and ultra-capacitors (high dynamics, high power and low energy) could be interesting but this would increase at the same time the vehicle complexity.

2.2.6 *Size of the hydrogen tank*

Once the fuel cell power is known, the quantity of hydrogen can be calculated to satisfy all the cycles. The mass and volume of hydrogen on board are deduced from the energy provided by the fuel cells. Currently, most of the hydrogen tanks are pressurized to 300 bar, with a minimum pressure of 30 bar (*i.e.*, empty tank). Knowing the power of the fuel cell and the duration of one turnaround, it is possible to calculate the energy needed. The distribution mass of hydrogen is then determined (Figure 47). The number of moles $n_{\text{turnaround}}$ and subsequently the volume of hydrogen can be deduced from the mass, as shown in Figure 48.

To ensure a proper hydrogen supply of the fuel cell, the pressure in the tank has to be higher than 30 bar for a 300 bar tank. Consequently, all the hydrogen in the tank cannot be used and an extra amount of hydrogen n_{extra} must be added. This extra amount must be taken into account to compute the final volume of the hydrogen tank.

From the ideal gas law, we have :

$$P_{H_2} \cdot V_{H_2} = n_{H_2} \cdot R \cdot T \tag{2.15}$$

where

$$m_{H_2} = \frac{E}{LHV \cdot \eta_{FCS}} \tag{2.16}$$

$$n_{H_2} = \frac{m_{H_2}}{2 \cdot M_H} \tag{2.17}$$

$$n_{H_2} = n_{turnaround} + n_{extra} \tag{2.18}$$

LHV is the lower heating value of hydrogen ($LHV = 120.1\,MJ/kg$), η_{FCS} is the fuel cell hydrogen efficiency and M_H is the hydrogen molar mass.

Combining equations (2.15) and (2.18) gives :

$$P_{H_2} \cdot V_{H_2} = (n_{turnaround} + n_{extra}) \cdot R \cdot T \tag{2.19}$$

The pressure at the end of the turnaround is P_{extra}, so n_{extra} is given by (2.20)

$$n_{extra} = \frac{P_{extra} \cdot V_{H_2}}{R \cdot T} \tag{2.20}$$

Each hydrogen volume can be obtained using (2.20) with (2.19).

$$n_{turnaround} + n_{extra} = \frac{P_{H_2} \cdot V_{H_2}}{R \cdot T} \tag{2.21}$$

$$n_{turnaround} = \frac{P_{H_2} \cdot V_{H_2}}{R \cdot T} - \frac{P_{extra} \cdot V_{H_2}}{R \cdot T} \tag{2.22}$$

$$n_{turnaround} = \frac{(P_{H_2} - P_{extra}) \cdot V_{H_2}}{R \cdot T} \tag{2.23}$$

$$V_{H_2} = \frac{n_{turnaround} \cdot R \cdot T}{(P_{H_2} - P_{extra})} \tag{2.24}$$

where P_{H_2} is the hydrogen tank pressure in Pascal (Pa), R is the ideal gas constant $\left(R = 8.314\,J \cdot mol^{-1} \cdot K^{-1}\right)$, T is the tank temperature in Kelvin (K), n_{H_2} is the number of moles of hydrogen for one turnaround and n_{extra} is the moles of hydrogen at the end of a turnaround.

2.2.7 *Conclusion*

This section presented a new methodology in the conception of an hybrid electric vehicle to determine the size of the energy sources. The driving cycle generator presented with the garbage truck scenario has been upgraded to be adaptive to every situation : A human machine interface has been created with Matlab/Simulink in order to use it easily (FIGURE. 49). This methodology has been presented on a conference : IEEE Vehicle Power and Propulsion Conference in 2010, Lille, France [58], and a journal article has been made : Energy sources sizing methodology for hybrid fuel cell vehicles based on statistical description of driving cycles : IEEE Transaction on Vehicular Technology, 2011 [59].

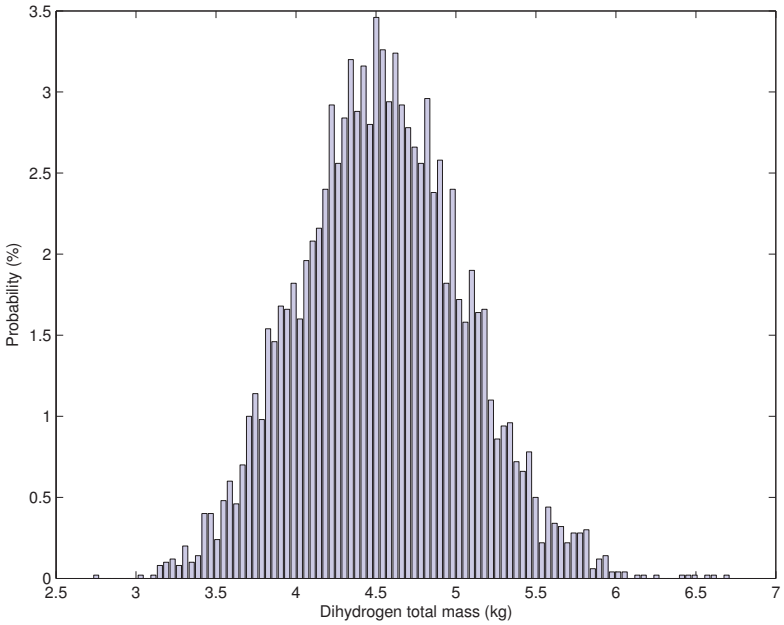

FIGURE 47. Hydrogen mass needed for one cycle with 60 % breaking energy recovery

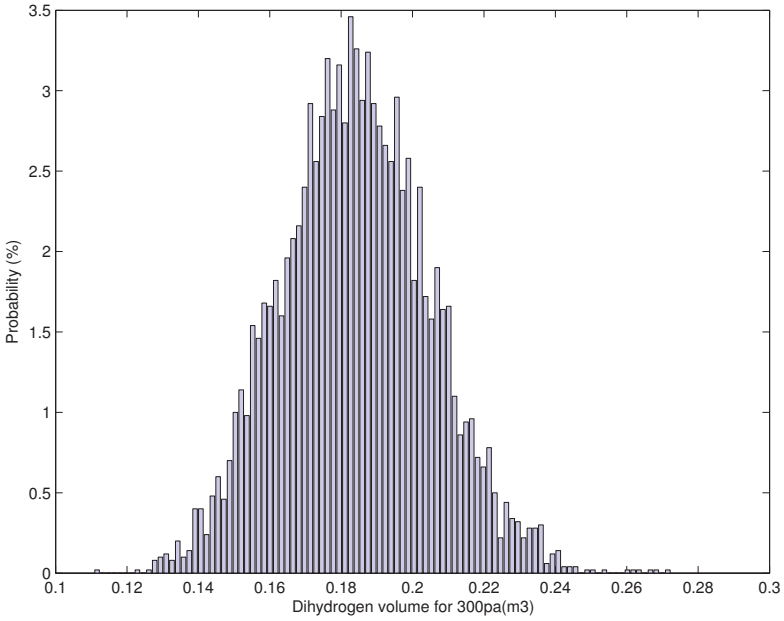

FIGURE 48. Hydrogen volume needed for one cycle with a 300 bar pressurized tank and 60 % breaking recovery

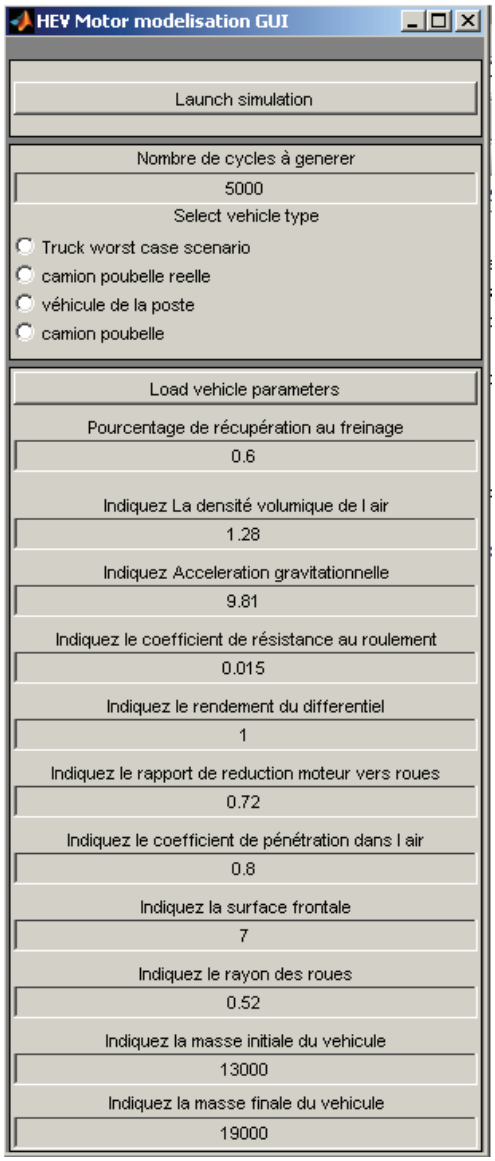

FIGURE 49. Driving cycle generator : User interface

2.3 OPTIMAL CONTROL OF A HYBRID ELECTRIC VEHICLE

In this section, the control of the vehicle will be discuss. After applying the methodology of sizing both energy sources on the truck, an optimization on the energy management will be made using dynamic programming. The energy management aims to get the lowest hydrogen consumption by the fuel cell for a given driving cycle. Consequently, optimizing it leads to the best hydrogen economy.

2.3.1 *Components model*

Architecture of the vehicle

FIGURE. 50 shows the drive train topology including the energy management system. The vehicle has a series architecture and the energy management controller will set the fuel cell current thanks to its associated DC/DC converter based on the battery state of charge.

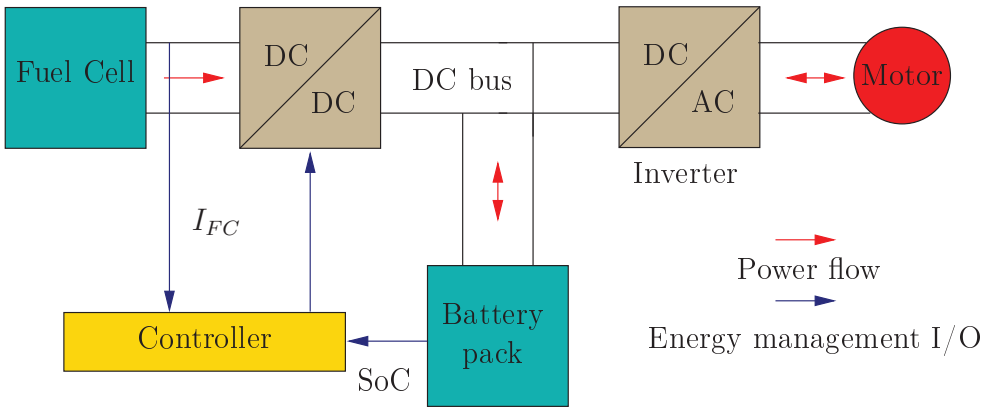

FIGURE 50. Drivetrain topology including energy management system

The power split between the fuel cell P_{FC} and the batteries P_b is given by (2.25).

$$P_v(t) = \eta_{FC}\, P_{FC}(t) + \eta_b\, P_b(t) \tag{2.25}$$

where η_{FC} is the fuel cell efficiency and η_b is the battery efficiency.

2.3.2 *Fuel cell model*

The fuel cell is used as the primary source of energy and the objective of the fuzzy rules is to minimize the hydrogen consumption given by (2.26)

[60, 12] :

$$m_{H2} = \int_0^t \frac{M_{H_2}\, n_c}{2\,F} I_{FC}(t)\, dt \tag{2.26}$$

where m_{H_2} is the hydrogen mass, M_{H_2} is the hydrogen molar mass, n_c is the number of cells, I_{FC} the fuel cell current and F the Faraday constant ($96,487\,C$). The fuel cell current I_{FC} permits the fuel cell power to be computed based on a simple fuel cell stack polarization curve FIGURE. 51. The fuel cell maximum power is set to 20 kW due to previous results.

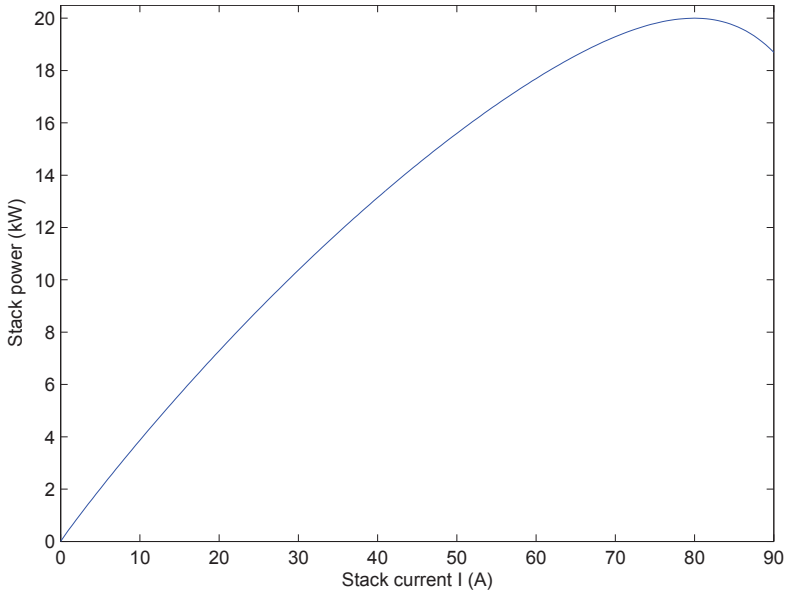

FIGURE 51. Fuel cell polarization curve

2.3.3 *Battery model*

The battery model is based on a simple current integration to know the battery state of charge at each instant time (2.27). The battery voltage is not considered in this model as the objective of the simulation is to obtain the energy to be stored in the battery for a turnaround.

$$SoC(t) = SoC_{init} - \frac{1}{C_{init}} \cdot \Sigma i(t) \cdot \Delta t \tag{2.27}$$

Where SoC is the battery state of charge, C_{init} is the initial battery capacity, which is set to 25 kWh due to previous results, and i is the current.

2.3.4 *Optimization : problem formulation*

The offline control strategy objective is to find the minimum hydrogen consumption for a known driving cycle [61, 62]. The consumption minimization problem can be written as a problem of optimal control for discrete system [63].

The battery's state of charge $x(k)$ can be considered as a dynamic system. The system can be written as :

$$x(k+1) = x(k) + P_b\,\eta_b\,T_s \tag{2.28}$$

$$\eta_b = \begin{cases} 0.95 & \text{if } P_b(t) < 0 \\ 1 & \text{if } P_b(t) \geqslant 0 \end{cases} \tag{2.29}$$

where P_b is the battery power level defined by (2.25), η_b the battery efficiency (0.95 for charge and 1 for discharge) and T_s the sampling time. The chosen criterion for N samples can be written as :

$$J = \sum_{k=0}^{N-1} \Delta\, m_{H2}(P_{FC}, k)\, T_s \tag{2.30}$$

where $m_{H2}(P_{FC}, k)$ is the hydrogen mass consumed for the power P_{FC} between two sampling times. According to fig 51, the fuel cell power is obviously limited :

$$\mu_{FC} = P_{FC_{min}} < P_{FC} < P_{FC_{max}} \tag{2.31}$$

where $P_{FC_{min}} = 0\,\text{kW}$ and $P_{FC_{max}} = 20\,\text{kW}$.

Moreover, the hybrid electric truck studied here is not plug in : the batteries cannot by charged by the grid. Consequently, the remaining state of charge at the end of the cycle needs to be the same as the one at the beginning [64], and the state of charge boundaries on x must be limited by the batteries charge, and discharge efficiencies. The discrete-time optimal problem can be then formulated as following :

$$\min_{P_{FC} \in \mu_{FC}} \quad \sum_{k=0}^{N-1} \Delta\, m_{H2}(P_{FC}, k)\, T_s \tag{2.32}$$

$$x(k+1) = x(k) + P_b\,\eta_b\,T_s \tag{2.33}$$

$$x_0 = SoC_{init} \tag{2.34}$$

$$x_N = SoC_{final} = SoC_{init} \tag{2.35}$$

$$x_k \in [0.4\,, 0.9] \tag{2.36}$$

$$N = \frac{T_{dc}}{T_s} \tag{2.37}$$

2.3.5 *Optimization problem solving using dynamic programming*

To solve this optimisation problem, a dynamic programming algorithm is used. This algorithm has been proposed by Sundstorm and Guzzella in [65]. The control input variable P_{FC} is discretized by step of 10 W such that $P_{FC} = [0, 10, 20... 19990, 20000]$ and the algorithm calculates the minimum cost-to-go function $C = \min(m_{h_2})$ at each node in the discretized state-time space with the constraint $x(k)$ given by (2.32) and the feasible inputs solutions give by (2.31).
The algorithm is composed of 2 parts : Firstly, a forward simulation described in FIGURE. 52 is run. The algorithm calculates all the possibility from $t = 0$ to $t = maximumtimeofthecycle$ with each discretized P_{FC}. All the results are stored in a 4D table including time, power, hydrogen consumption and batteries state of charge. Since the algorithm check for boundaries and if the results have not been already calculated from a different set of $P_{FC}, t, x(k)$; the time consuming is really slow compare to the methodology which calculate all the solutions of the problem. Nevertheless, the memory used is big and this kind of optimization cannot be applied in embedded system. Secondly, a backward simulation parse the memory table described in FIGURE. 53 from the last result respecting the constraint and find all the results from t_{final} to $t_{initial}$ by subtracting each time step the best hydrogen consumption calculated m_{h_2}.

2.3.6 *Results on the Hybrid electric truck studied*

The Dynamic programming optimization has been applied to the control of the garbage truck 2.32 : FIGURE. 54 shows the results for the driving cycle recorded : it can be observed that the final state of charge is the same as the initial (70 %), the constraint is respected. The fuel cell current is steady during most of the cycle but in the last part, it is increased a lot. It can be explained by observing the driving cycle pattern : the end of the cycle correspond to the drive-away back of the truck from house to the base, the mean speed during this phase is higher than the rest of the cycle. Moreover, the truck is fully loaded, and its weight linked with high speed and strong acceleration leads to huge peak of power that can be observed in the power profile. The optimized control results in these phase is a quick augmentation of the fuel cell current and then it remain steady. It can be explain by the fuel cell model : Indeed, the fuel cell high dynamic increase a lot the hydrogen consumption. Consequently, the control aim to keep the fuel cell current steady as most as possible. FIGURE. 55 represents the hydrogen consumption during the cycle. It reflects the results explained previously and the drive-away back phase clearly appears.

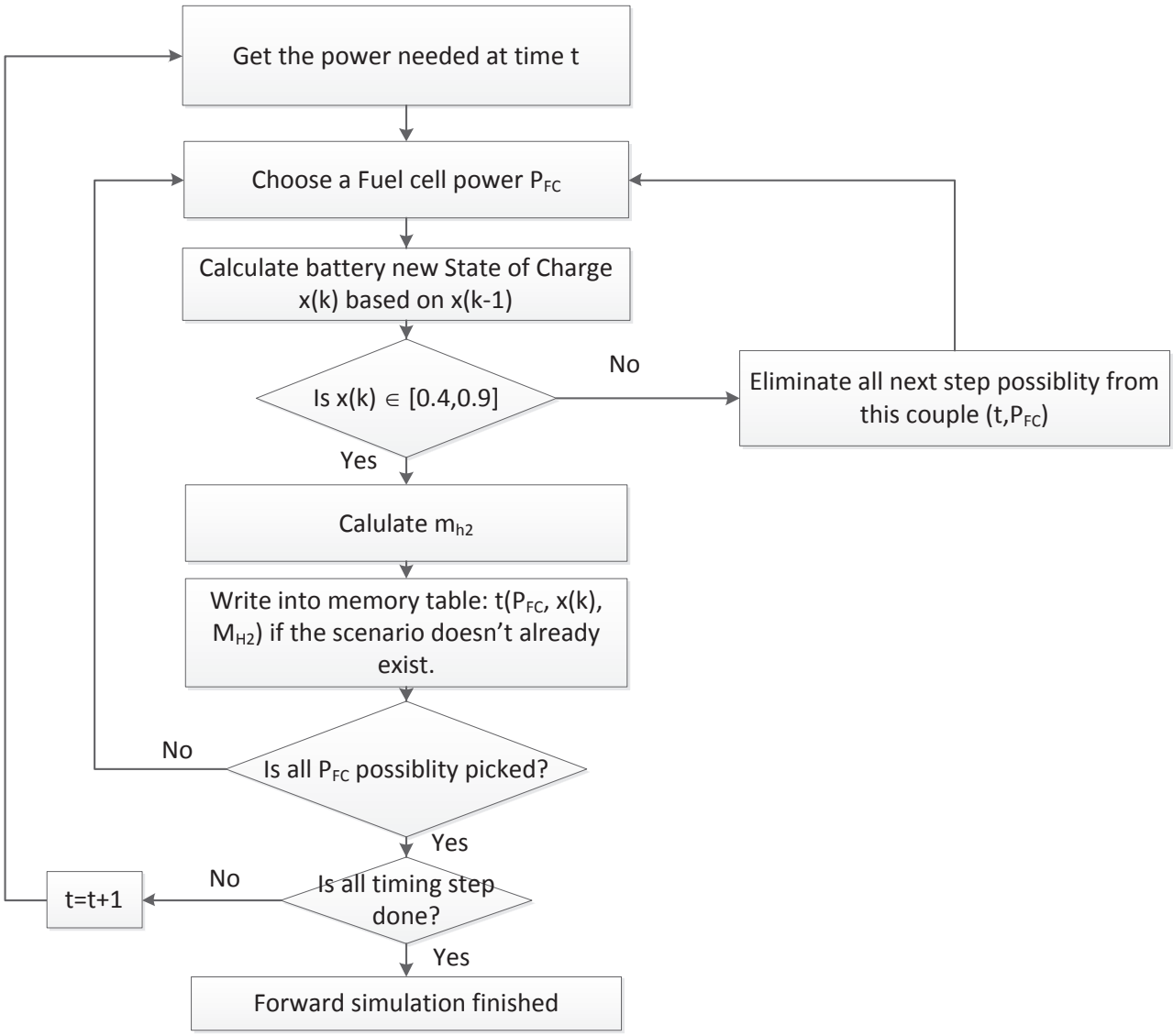

FIGURE 52. Dynamic programming forward simulation

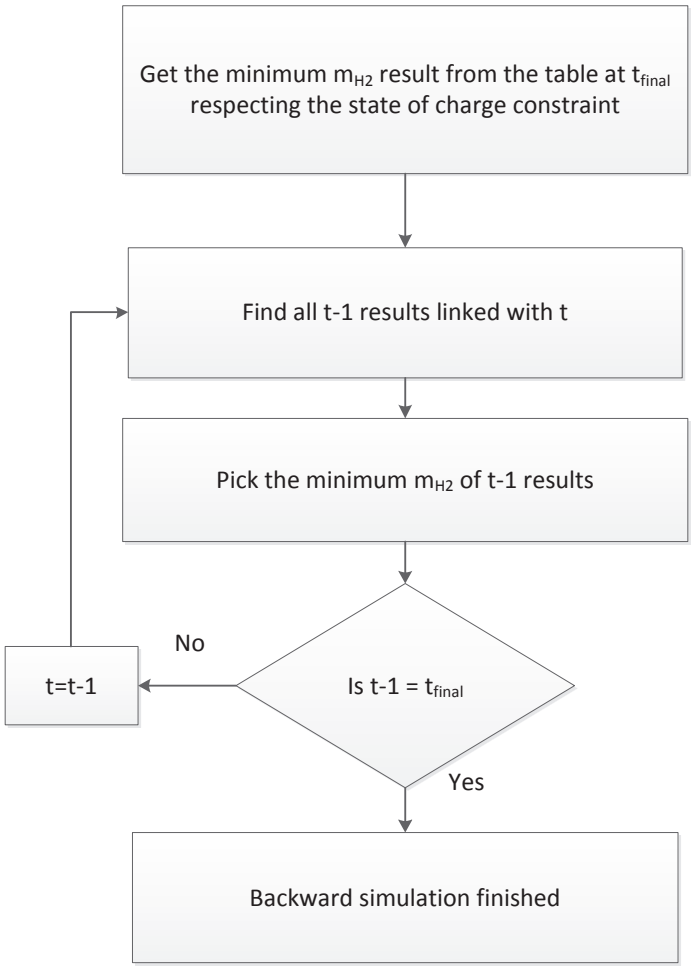

FIGURE 53. Dynamic programming backward simulation

2.3.7 *Conclusion*

This section has presented an optimal control strategy based on dynamic programming for hybrid electric vehicle with an application on a garbage truck. This "offline" control strategy allows to get an optimal results of the powersplit between the primary source and the peaking power source by minimizing the hydrogen consumption, in case of a fuel cell as primary source. The results of this optimisation will be used as reference when building real time controller. This study has been presented in a conference : Electronique du Futur 2011, Belfort, France [66].

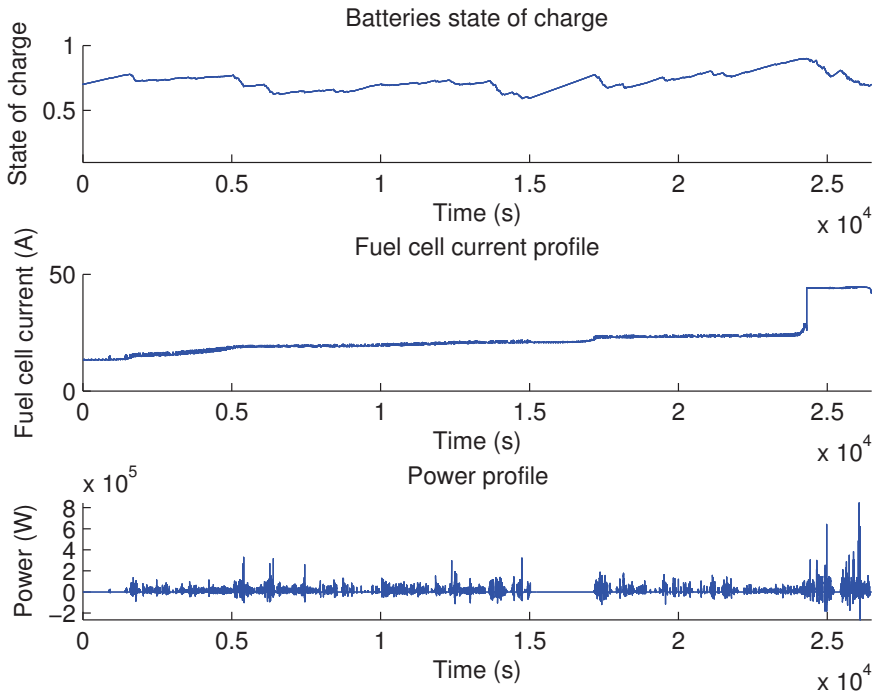

FIGURE 54. Dynamic programming results of the truck on the recorded driving cycle

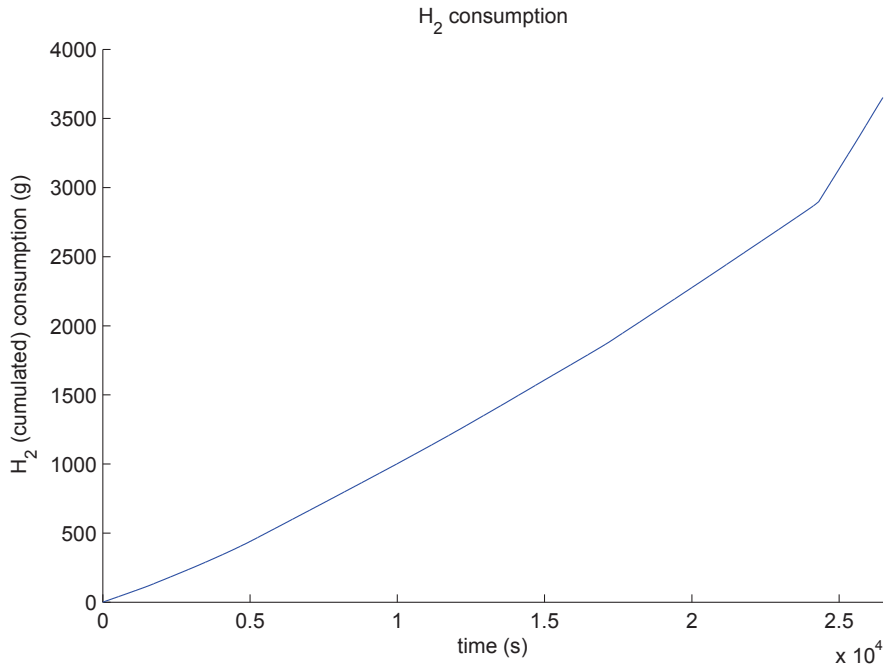

FIGURE 55. Dynamic programming results : hydrogen consumption of the truck on the recorded driving cycle

2.4 COMBINED OPTIMAL SIZING AND ENERGY MANAGEMENT

The methodology of sizing discussed in section 2.2 is really efficient when working with a family of driving cycle. Nevertheless, since it is assumed to choose the primary energy source as the mean power of the driving cycle. For a single driving cycle study, this type of choose can not be the optimal one. Indeed, the control strategy and the sizing of the component are directly linked : the control defines the power provided by the primary source at each step time of the cycle. The results can be far from the mean power. On an other hand, the control needs the vehicle parameter, a.k.a. the size of component to calculate the power split. The following section presents a new methodology to determine the best sizing and control for a specific driving cycle. The vehicle used in this study is a lightweight vehicle presented in section 3.

2.4.1 *Interlinked optimization problem*

The aim of this study is to find the best sizing for the fuel cell (rated power) and the battery (capacity), assuming an optimal power split and for a specific driving cycle. Two interlinked optimization loops are run simultaneously, as shown in Fig. 56. A first optimization is run on sizing, and chooses various

couples of fuel cell rated power and battery capacity. Each couple is then used as an input to the vehicle model used in the second optimization, which determines the optimal energy management strategy that results in the lowest total hydrogen consumption. In the end, the algorithm returns the best found sizing and the corresponding optimal energy management strategy and consumption.

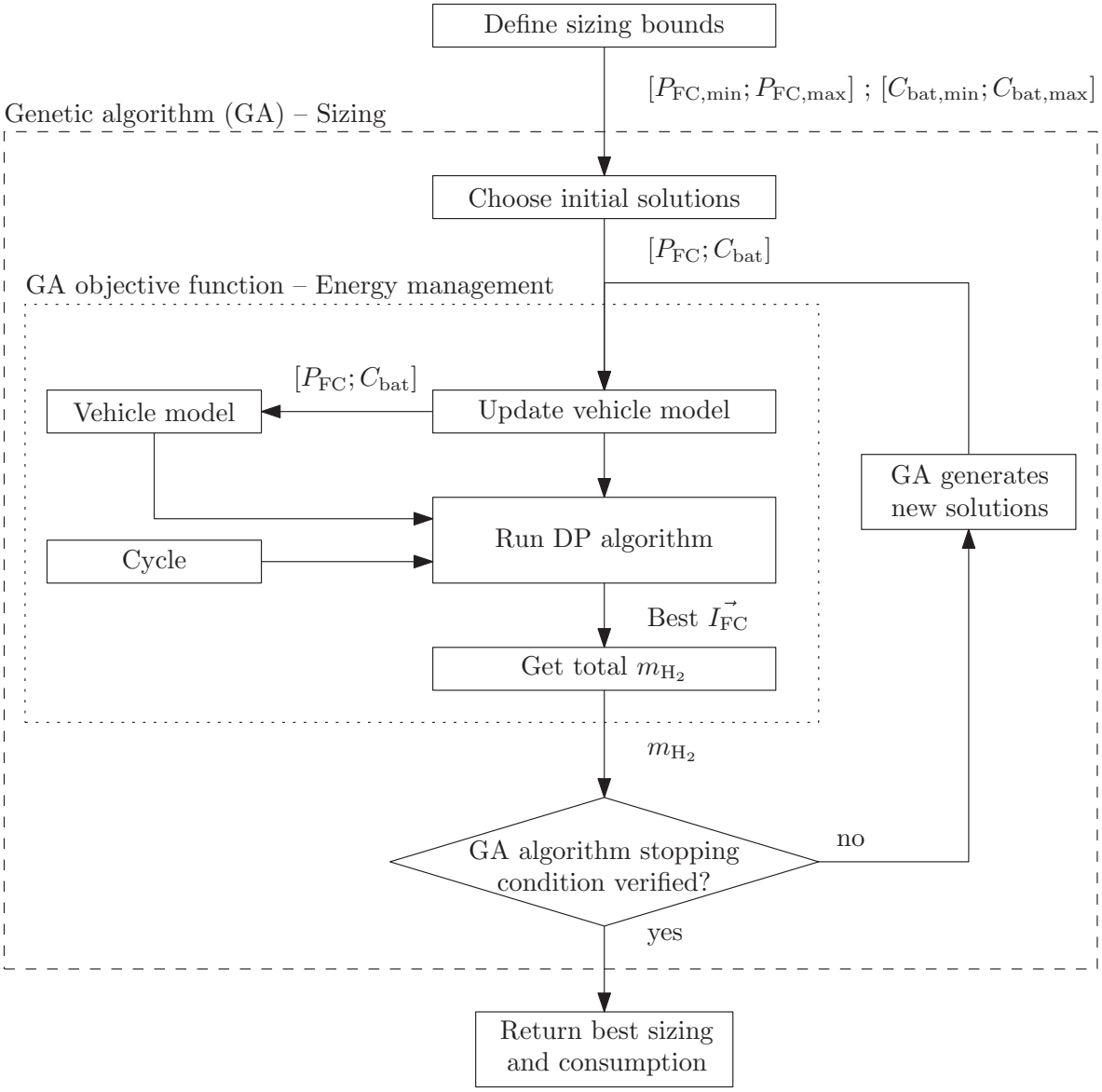

FIGURE 56. Architecture of the algorithm. The objective function is used to evaluate each solution provided by the genetic algorithm.

Sizing optimization

The sizing optimization tries to find the best set of fuel cell rated power and battery capacity, resulting in the lowest total hydrogen consumption. The total mass m_{tot} of the vehicle is obtained using (2.38) :

$$m_{tot} = m_{HEV} + \frac{C_{bat}}{N_{bat}} + \lambda(P_{FC}) \tag{2.38}$$

where m_{HEV} is the vehicle mass without batteries, C_{bat} is the battery capacity selected by the sizing algorithm, N_{bat} is the energy density of the batteries and λ is the function giving the mass of the fuel cell as a function of its rated power. This function is determined using data extracted from several constructor data sheets (Fig. 57), and leads to a quadratic relationship between mass and rated power. The value of P_{mot} is recomputed for each sizing couple, as the algorithm would otherwise tend to choose over-sized batteries. The vehicle model is thus customizable and adapts to the solutions proposed by the optimization algorithm.

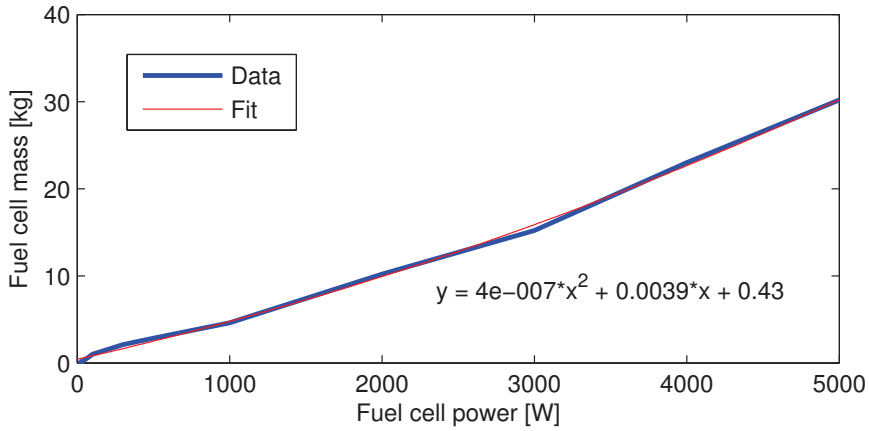

FIGURE 57. Fuel cell mass as a function of its rated power

The discrete state-time problem is then formulated as follows :

$$\min_{S_{FC}\in\psi_{FC}, S_{bat}\in\psi_{bat}} m_{H_2}(S_{FC}, S_{bat}, m_{tot}) \tag{2.39}$$

where $\psi_{FC} \in [0, 20000]$ and $\psi_{bat} \in [0, 30000]$ are the fuel cell rated power and battery capacity search domains in W and in Wh, respectively.

The problem is solved using a genetic algorithm, with a population of 30 individuals and 50 generations. Genetic algorithms [67] are a type of meta-heuristic based on the principles of natural evolution, and that use the concepts of inheritance, mutation, selection and crossover to make a population of solutions evolve through a given search space toward the best solutions. MathWorks's Matlab's genetic algorithm function `ga` is used for solving this problem.

Optimal energy management strategy

Using the solutions input by the sizing optimization, the second optimization loop tries to find the optimal control strategy by minimizing the hydrogen consumption on the selected driving cycle [61, 62]. The optimization algorithm is the same as explained in section 2.3.4 and the constraints are :

$$x_0 = 0.7 \tag{2.40}$$
$$x_{N-1} = x_0 \tag{2.41}$$
$$x \in [0.4; 0.9] \tag{2.42}$$
$$P_{FC}(t) \in [P_{FC_{min}}; P_{FC_{max}}] \tag{2.43}$$
$$P_{FC_{min}} = 0\,W \tag{2.44}$$
$$P_{FC_{max}} = P_{FC} \tag{2.45}$$

2.4.2 *Results*

In order to analyze its performance, the proposed methodology is tested on two standards driving cycles, the ECE and LA92 driving cycles, and results are then compared with another sizing methodology.

Results on standard driving cycles

As shown in Fig. 58 and 59, the dynamic programming algorithm is able to find the optimal fuel consumption while ensuring the final SOC is equal to its initial value at the end of the cycle, as required.

In terms of sizing and consumption, for the ECE cycle, the algorithm finds that the best sizing is obtained for a 6.5 kW fuel cell and a 75 Wh battery. It then returns a total hydrogen consumption of 3.0 g. For the LA92 cycle, the algorithm obtains a 9.0 kW fuel cell and a 72 Wh battery, for a total hydrogen consumption of 15 g.

Having data available on the entire driving cycle thus enables the control strategy to maintain an almost fuel cell current that minimizes the hydrogen consumption and to re-charge the battery during stop phases. Not being able to access all this information, an on-line control strategy would not be capable of it.

Comparison with another sizing method

In order to evaluate the performance of the algorithm, results are compared with sizing method based on a statistical description of driving cycles [**?**]. For the ECE driving cycle, this method gives a 3.6 kW fuel cell and a battery capacity of 96 Wh, with a fuel consumption of 3.3 g. For the LA92 driving cycle, it returns a 2.6 kW fuel cell, a battery capacity of 221 Wh and a fuel consumption of 53 g.

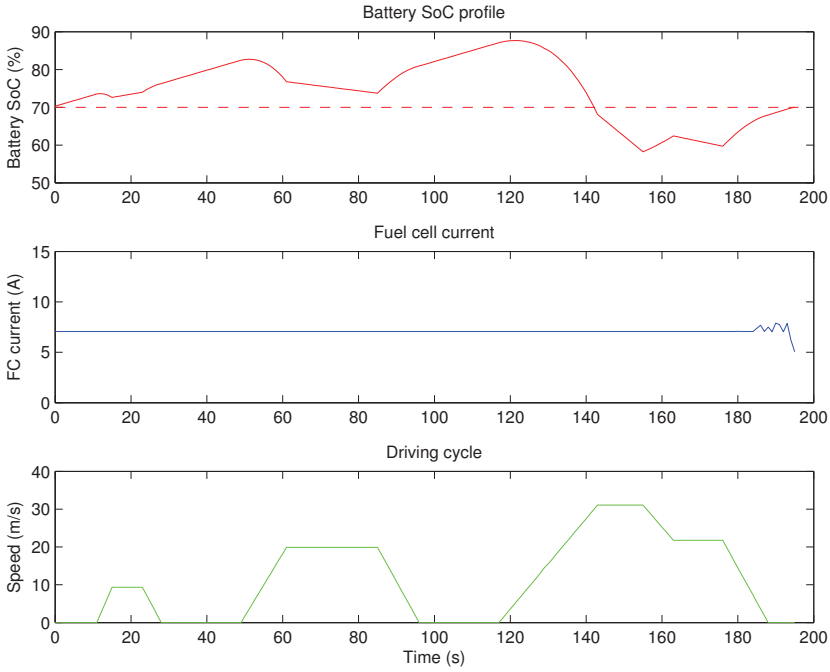

FIGURE 58. Simulation results for the ECE driving cycle

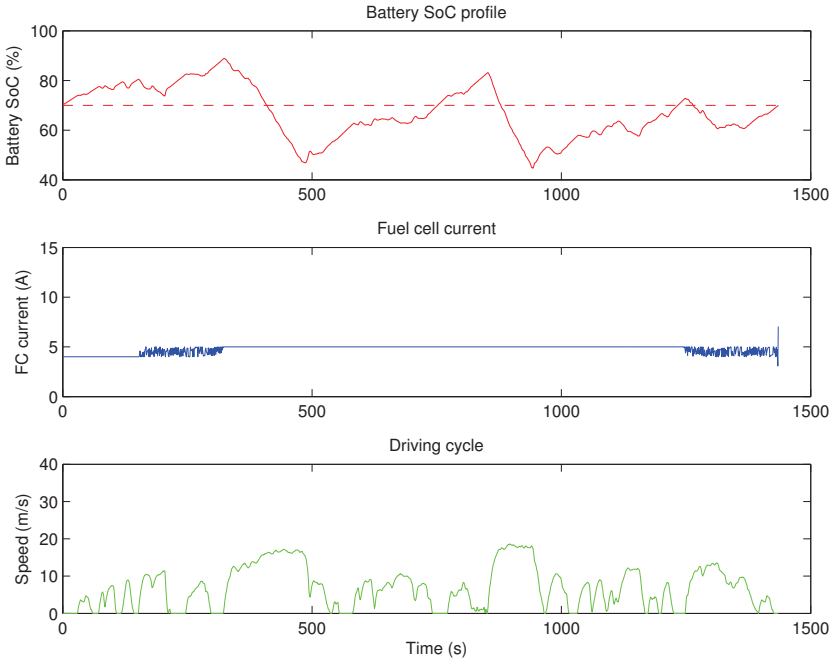

FIGURE 59. Simulation results for the LA92 driving cycle

A comparison of both methodologies (Table 7) shows that the proposed algorithm gives a smaller battery (by 22 % for ECE and 67 % for LA92) and a lower fuel consumption (by 9.1 % for ECE and 72 % for LA92) than the other one. However, the size of the fuel cell is increased in both cases. Results are particularly spectacular for the LA92 cycle, as a totally different sizing strategy is adopted by both algorithms.

Increasing the size of the fuel cell enables the fuel cell system to operate closer to its optimal operation point, without much impact on the mass of the vehicle, as fuel cells are much lighter than batteries. This also indicates that the fuel consumption and the fuel cell size (and the corresponding price) are contradictory objectives. A compromise could then be found to try to accommodate both objectives.

TABLE 7. Comparison of the results obtained by the proposed method with another one based on the statistical description of driving cycles

Driving cycle	Result	Unit	Reference method	Proposed method	Comparison
ECE	Fuel cell	kW	3.6	6.5	+80 %
	Battery	Wh	96	75	−22 %
	Hydrogen	g	3.3	3.0	−9.1 %
LA92	Fuel cell	kW	2.6	9.0	+246 %
	Battery	Wh	221	72	−67 %
	Hydrogen	g	53	15	−72 %

Feasibility map

In order to try to determine how the hydrogen consumption evolves when selecting different sizing solutions (especially for real applications), a feasibility map is traced. This map is obtained by computing the optimal hydrogen consumption for a given driving cycle for a wide range of fuel cell sizes and battery capacities.

Fig. 60 shows this map for the ECE driving cycle. A color map is used to indicate the value of the total hydrogen consumption : blue indicate a low consumption and red a high one. White areas indicate that the algorithm could not find a feasible solution, e.g. because the SOC cannot be maintained. Results indicate that choosing a small battery with a large fuel cell returns the lowest fuel consumption because the fuel cell runs with the best efficiency.

2.4.3 *Conclusion*

The proposed combined optimization algorithm enables finding the optimal sizing for a given HEV architecture and driving cycle, resulting in the lowest fuel consumption and enabling to maintain the SOC of the battery.

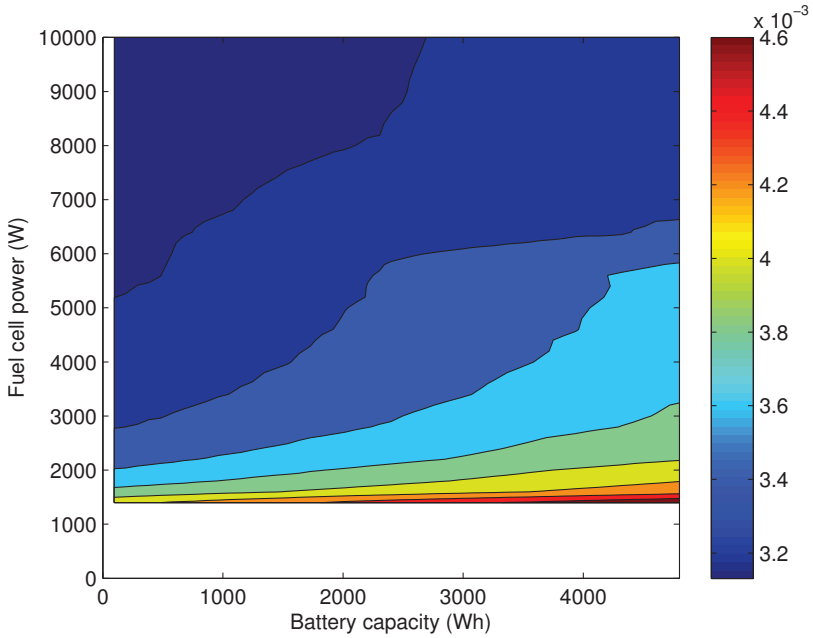

FIGURE 60. Hydrogen consumption map for the ECE driving cycle

This methodology also enables to reduce the size of the energy sources (here mostly the battery), and consequently the vehicle mass, by selecting their minimal size so that the lowest fuel consumption is obtained, compared to other methodologies that often rely on simpler control strategies that tend to give higher fuel consumptions. However, this methodology is cycle oriented, and the results can be applied only if the vehicle is used with a predefined driving style, as for postal services or garbage collection.
This study has been presented on a conference : IEEE Transportation Electrification Conference and Expo (ITEC), 2012, Dearborn, USA [68].

2.5 CONCLUSION

This chapter has focused on the conception of the hybrid electric vehicle and its control knowing the driving cycle. The methodology proposed allows to reduce the size of the component, and consequently the cost of the vehicle. It also permits to save study the impact of building an hybrid electric vehicle rather than a standard one (with Internal Combustion Engine) for specific driving patterns. Hydrogen consumption, size of the component and tanks can be determined and compare to standard vehicle's fuel consumption.
Optimal control strategy gives the best results of the power split control for a specific driving cycle. it can be used as a reference when building real time control strategy.

3

REAL TIME CONTROL STRATEGY FOR HYBRID ELECTRIC VEHICLE

3.1 INTRODUCTION

This chapter focus on control strategy of hybrid electric vehicle : in a first time, a real time controller based on fuzzy logic will be presented : the controller will be used in 2 scenarios :

- The garbage truck studied in section 2.2
- A lightweight vehicle : This vehicle is an electric vehicle from GEMCAR manufacturer and has been transformed into a hybrid electric vehicle based on fuel cell and batteries : FIGURE. 61 shows the original vehicle : it is a lightweight vehicle based on lead acid batteries who is built to run urban patterns. The System and Transport Laboratory modified this vehicle by adding a fuel cell, tanks, DC/DC converter and controllers to transform it into a series hybrid. FIGURE. 62 andFIGURE. 63 shows the transformed vehicle which will be used for this study.

FIGURE 61. GEMCAR electric vehicle

Two sections are then presented aiming on optimizing the controller for a specific driving cycle with genetic algorithm ; and a layer to the control is added to distinguish different driving patterns and adapt the controller. Finally, a study on predictive controller is presented based on a plug-in hybrid electric vehicle with Global Positioning System (GPS).

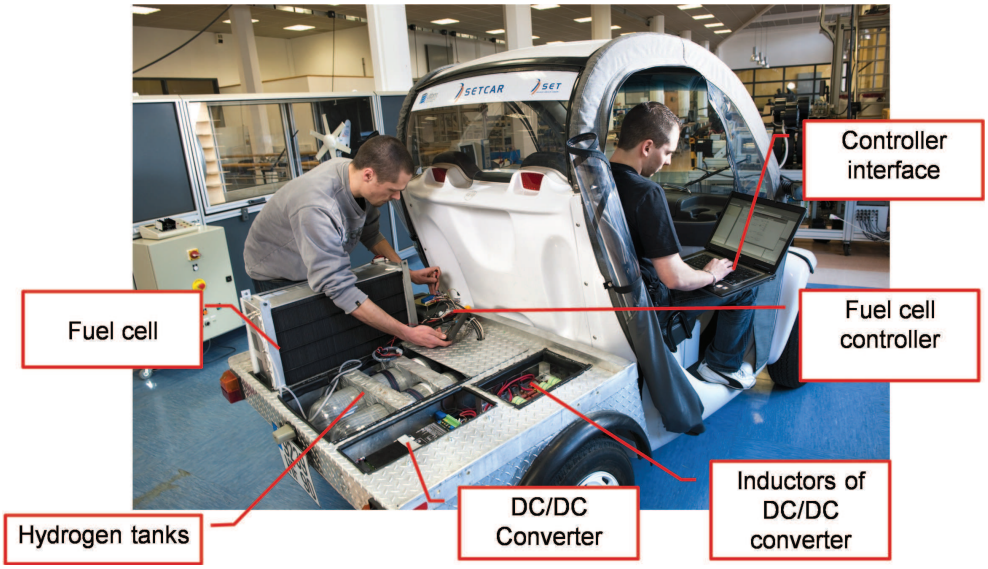

FIGURE 62. SeTcar : hybrid electric vehicle based on a fuel cell as a primary source of energy

FIGURE 63. SeTcar : Zoom on the fuel cell system

3.2 REAL TIME CONTROL STRATEGY USING FUZZY LOGIC

Section 2.3 presented a control based on an optimization with dynamic programming. This offline control gives the optimal results but require the knowledge of the driving cycle done. In real application : the control cannot predict precisely the driving cycle used. Consequently, a real time control must be adaptive and be enough robust to face all type of driving patterns [69, 70, 71]. Applying this to our study, the control strategy has to take into account the following constraints :

1. The fuel cell dynamics and voltage cycling (low voltages) are limited to increase its lifetime. Ideally, the fuel cell should work at a constant power corresponding, in this case, to the driving cycle mean power ;
2. The fuel cell should work around its optimal working points, where its efficiency is the highest. The fuel cell has been designed for that in the section 2.2 ;
3. The battery State-of-Charge is maintained in a given edge and limits the cycling (the final state of charge must be as closest as possible as the initial one) ;
4. The energy is recovered during braking phases.

3.2.1 *Fuzzy logic controller*

A real time control based on fuzzy logic controller has been chosen to control the fuel cell : FIGURE. 50 shows the implementation of the controller in the vehicle andFIGURE. 64 shows the input and output of the controller : The controller imposes the current reference of the fuel cell to the DC/DC converter. It can be observed that only the state of charge is taken into account by the controller to determine the current reference. Indeed, since it is assumed that the vehicle is built with the methodology proposed in section 2.2, the battery can provide enough power to absorb the peaks needed by the vehicle.

FIGURE 64. Fuzzy logic controller principle

The parameters of the fuzzy controller are tunable by the user and are represented by trapezoidal functions :FIGURE. 65 shows these functions applied to the 20 kW fuel cell used in the truck study.

4 memberships functions can be distinguished :

– *Ze : electric zone* : the fuel cell is stopped ;

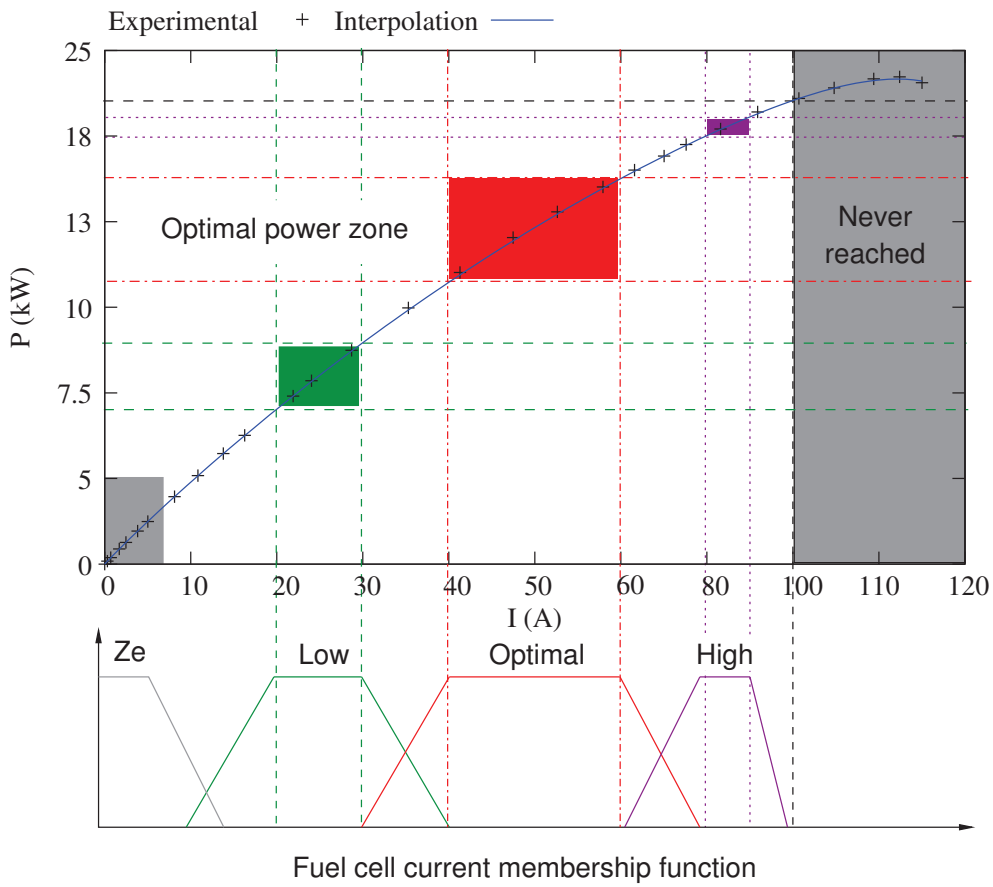

FIGURE 65. Working zones of the fuel cell system

– *Low zone* : the fuel cell work under its optimal zone, the efficiency is not optimal but the fuel cell current is low ;
– *Optimal* : the fuel cell run in its optimal zone (in case of the truck study, 13 kW ; corresponding to the results presented in section 2.2) ;
– *High zone* : Fuel cell maximum current is allowed.

In the same way, the input state of charge is divided into 4 functions :
– *Low state of charge* : the output needs to operate higher than its optimal running point ;
– *Optimal state of charge* : the output can run within its optimal power zone, the batteries absorb or provide the peaks of power ;
– *High state of charge* : the output can work under its optimal running zone ;
– *Very high state of charge* : the output reference can be switch to 0, the batteries can provide enough energy to run in electric mode.

To link input and output functions, fuzzy logic rules are sets :

1. If (SOC is low) then (I_{FC} is high)
2. If (SOC is good) then (I_{FC} is opt)
3. If (SOC is high) then (I_{FC} is low)
4. If (SOC is very high) then (I_{FC} is 0)

where I_{FC} is the fuel cell reference current.

3.2.2 *parameters and results on the hybrid electric truck*

fuzzy logic parameters

The parameters of the battery state of charge and fuel cell current references functions are given in TABLE. 11 and TABLE. 12 :

TABLE 8. Battery state of charge membership function parameters

Description	Notation	SoC Value
Emergency case	SoC_{limit}	0.1
state of charge is considered to be low	$SoC_{low_{min}}$	0.2
	$SoC_{low_{max}}$	0.5
state of charge is considered to be good (optimal)	$SoC_{good_{min}}$	0.6
	$SoC_{good_{max}}$	0.85
state of charge is considered to be high (the system can work in charge depleting mode in this case : only the battery is working)	$SoC_{high_{min}}$	0.95
	$SoC_{high_{max}}$	1

TABLE 9. Fuel cell current membership function parameters

Description	Notation	Current (A)
Fuel cell maximum current allowed	$FC_{current_{max}}$	130
Fuel cell current is considered to be low	$FC_{current\_low_{min}}$	50
	$FC_{current\_low_{max}}$	80
Fuel cell current for which the fuel cell has been designed (corresponding to the average power of the load)	$FC_{current\_opt_{min}}$	90
	$FC_{current\_opt_{max}}$	110
Fuel cell current is considered to be high (used in emergency cases when the battery state of charge is too low)	$FC_{current\_high_{min}}$	112
	$FC_{current\_high_{max}}$	120

results on different driving cycles

Three simulations are run :
- A simulation with a real driving cycle. Note that this driving cycle has not been used to determine the statistical distributions ;
- A simulation with a randomly generated driving cycle based on the statistical distributions.
- A simulation with the worst scenario case where the average power is the maximum of the statistical distributions.

For each simulations, it is assumed that the initial state of charge is 80 %. This will show if the vehicle can start with a state of charge different from 100 %, the controller can manage the recharge of the battery state of charge at the end of the cycle.

FIGURE. 66 and FIGURE. 67 shows respectively the results for the recorded and generated driving cycle : During the drive-away, the energy consumption is important (*i.e.*, the instantaneous power demand is higher than the fuel cell power), the speed and the driving time are relatively high. The fuel cell operates at its optimal power and the battery discharges significantly, it is clearly appear in FIGURE. 68 which described the worst scenario case which can be generated.

Once the drive-away ends, when the energy consumption is lower, the fuel cell recharges the battery and works beyond its optimal zone depending on the state of charge of the battery pack.

The charge of the power source therefore rises rapidly at the beginning of the collecting phase. During that phase, the fuel cell works most of the time in its optimal zone.

In some cases, the battery can provide all the required power as its state of charge is high (see FIGURE. 66) ; the fuel cell can be turned off during a long

time.

Finally, when the truck is back at the base after a drive-away back, the fuel cell continues to operate to recharge the battery until its optimal state of charge is reached. This operation could be avoided by plugging the vehicle to the grid which would reduce the vehicle's overall fuel consumption.

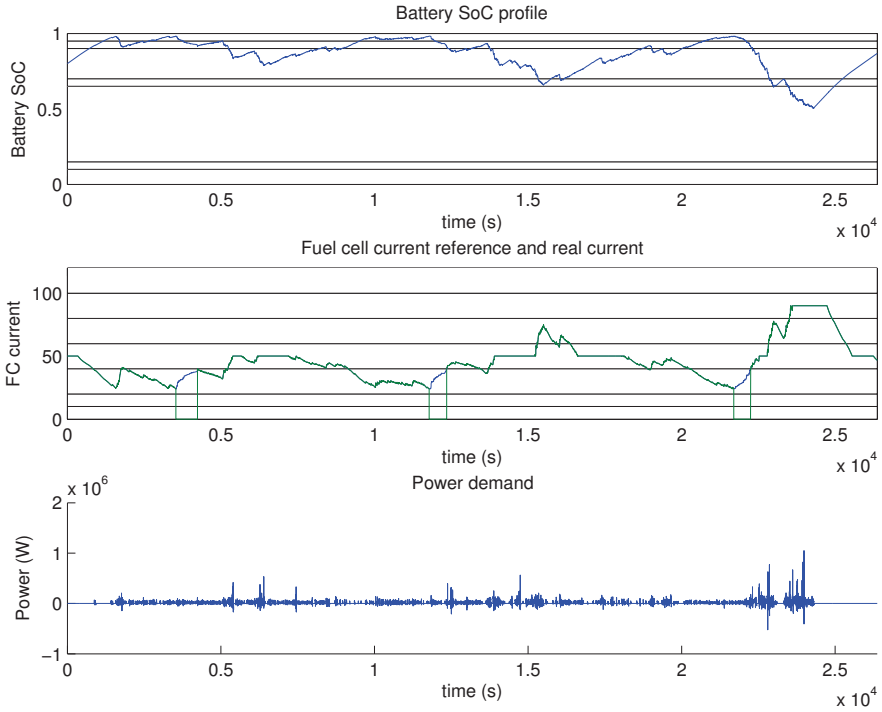

FIGURE 66. Real driving cycle

TABLE. 13 shows the hydrogen consumption along the real cycle, the randomly generated cycle and the worst case scenario of generated driving cycle. The hydrogen consumption with the fuzzy controller is around 4 kg which corresponds to the mass of hydrogen given in FIGURE. 47.

TABLE 10. hydrogen consumption

Type of driving cycle	Average power (kW)	Hydrogen consumption (g)
Real	14,3	3800
Random	9,1	3600
Worst case scenario	18,1	4600

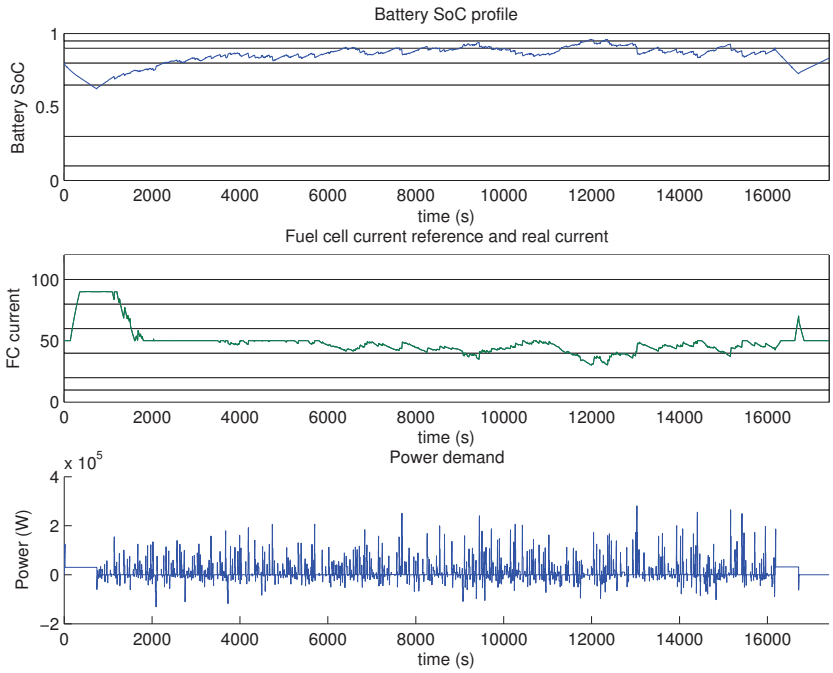

FIGURE 67. Randomly generated driving cycle

FIGURE 68. Worst case scenario of generated driving cycle

3.2.3 *parameters and results on the lightweight vehicle*

fuzzy logic parameters

The parameters of the battery state of charge and fuel cell current references functions are given in TABLE. 11 and TABLE. 12 : The vehicle has a fuel cell of 5 kW and a battery pack of 2880 Wh. The parameters are lower than the truck because of the vehicle weight : indeed, the accelerations phases of the vehicles require less power. Moreover, the urban profile of the vehicle allow a lot of start/stop phases, where the batteries can be refill (no drive-away compare to the trucks). Consequently, the all electric zone range is increased from 100 % to 80 % of the batteries state of charge.

TABLE 11. Battery state of charge membership function parameters

Description	Notation	SoC Value
Emergency case	SoC_{limit}	0.1
state of charge is considered to be low	$SoC_{low_{min}}$	0.15
	$SoC_{low_{max}}$	0.4
state of charge is considered to be good (optimal)	$SoC_{good_{min}}$	0.6
	$SoC_{good_{max}}$	0.7
state of charge is considered to be high (the system can work in charge depleting mode in this case : only the battery is working)	$SoC_{high_{min}}$	0.8
	$SoC_{high_{max}}$	1

TABLE 12. Fuel cell current membership function parameters

Description	Notation	Current (A)
Fuel cell maximum current allowed	$FC_{current_{max}}$	130
Fuel cell current is considered to be low	$FC_{current\_low_{min}}$	8
	$FC_{current\_low_{max}}$	20
Fuel cell current for which the fuel cell has been designed (corresponding to the average power of the load)	$FC_{current\_opt_{min}}$	30
	$FC_{current\_opt_{max}}$	40
Fuel cell current is considered to be high (used in emergency cases when the battery state of charge is too low)	$FC_{current\_high_{min}}$	80
	$FC_{current\_high_{max}}$	100

results : comparison between online and offline controller

The LA92 driving cycle has been used to run the fuzzy controller. It is a recorded driving cycle in the city of Los Angeles who described an urban pattern with a lot of acceleration/deceleration phases. FIGURE. 72 shows in red the results of the fuzzy controller and in blue the results of the dynamic programming optimization described in section FIGURE. 2.3. The dynamic programming strategy allows to find the optimum fuel economy while keeping the final state of charge at its initial value. Knowing the driving cycle allows the strategy to keep a constant fuel cell current value minimizing the hydrogen consumption and charging the battery during stop phases of the driving cycle. However, the online strategy cannot predict the power needed during the cycle and keep the state of charge in its optimal zone, decreasing the fuel cell when the state of charge is too high. This observation clearly appears at 400 and 900 seconds of the driving cycle where the speed increases and stays constant around 20 m/s. During this time, the power requested by the vehicle is higher than the power provided by the fuel cell and the batteries, which absorb the peak of power, has its state of charge decreasing. Consequently, the fuzzy logic controller up the reference of the fuel cell to keep the state of charge in the optimal zone. Therefore, the dynamic programming, knowing the entire driving cycle, lets the state of charge decreases because the end of the cycle does not require a lot of energy, and the fuel cell will be able to refill the batteries.
TABLE. 13 shows the hydrogen consumption for both strategies and for a stand alone fuel cell vehicle without batteries, assuming he is running the driving cycle. Hybridization and control strategy permit to improve the fuel cell economy up to 40 % for a fuzzy controller and up to 60 % for dynamic programming.

TABLE 13. hydrogen consumption for several architectures and controls

	Fuel cell power (kW)	Battery capacity (Ah)	H_2 consumption (g)
Stand alone fuel cell vehicle	13	0	102
Fuzzy logic controller	5	65	63
Dynamic programming	5	65	40

Conclusion

The fuzzy logic controller used here is not optimal : the final state of charge is higher than the initial, and the hydrogen consumption is also higher than the dynamic programing results. However, this strategy allows running

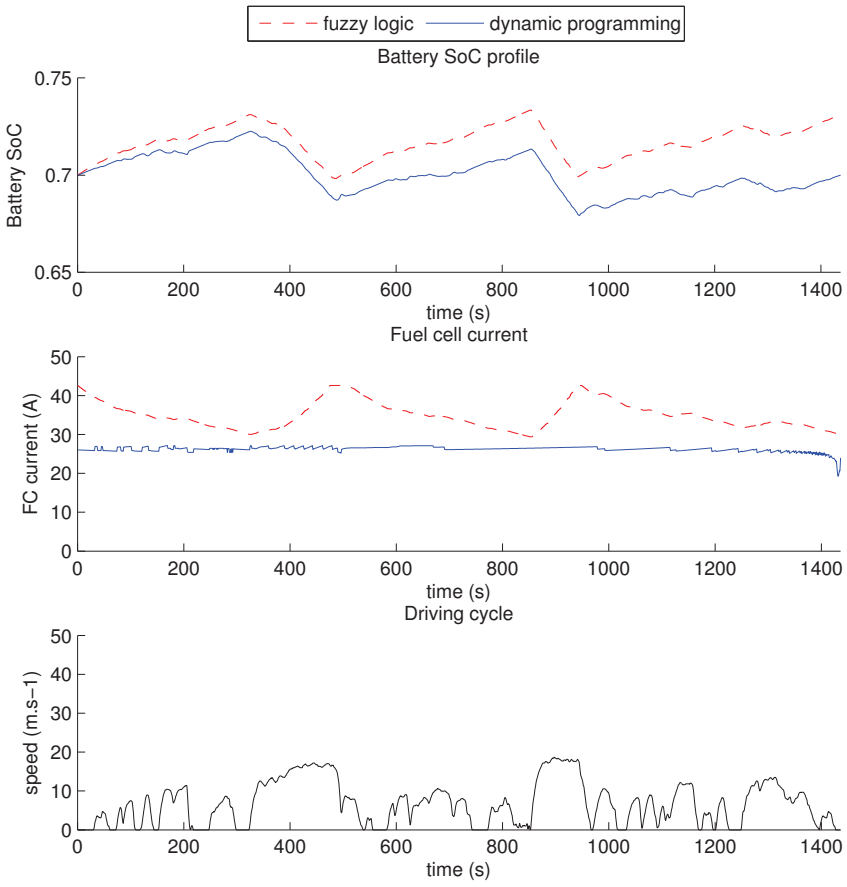

FIGURE 69. Fuzzy logic controller and dynamic programming results on LA92 driving cycle

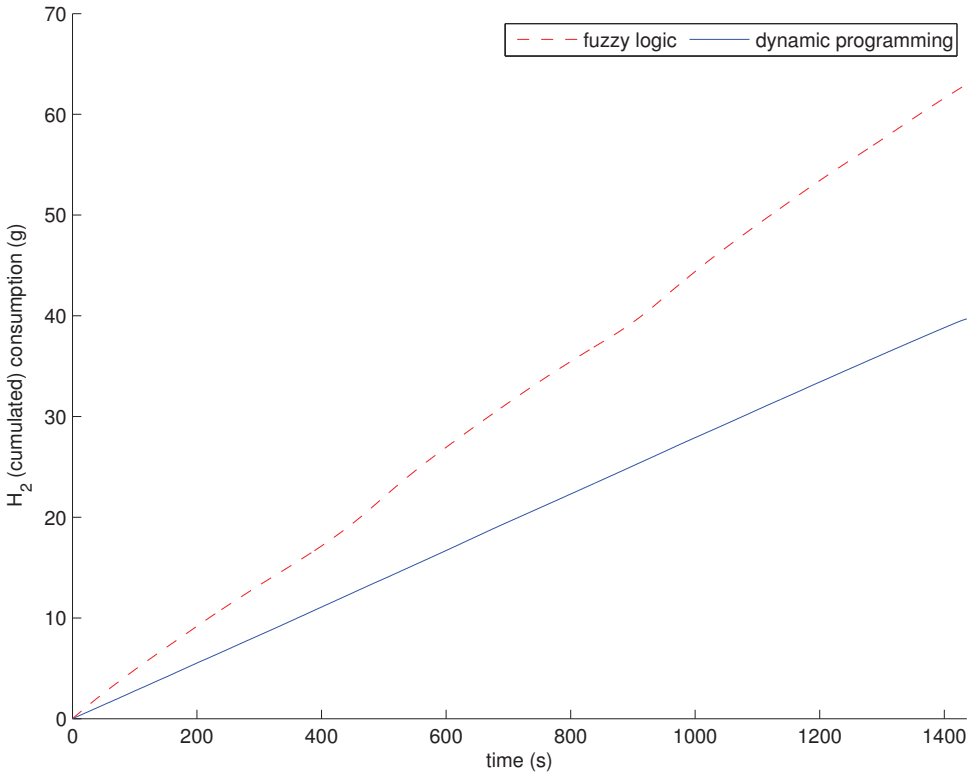

FIGURE 70. Fuzzy logic controller and dynamic programming results on LA92 driving cycle : hydrogen consumption

other driving cycles by the vehicle with the same results [59] (state of charge remaining in the optimal zone) compare to the off-line strategy which have to run the dynamic programing algorithm to find the optimal power split profile, which is not able to be done on real time. Consequently, the off-line strategy cannot be applied in vehicle if the driving cycle is not known or predicted [72]. In the next section, the membership functions of the fuzzy logic controller will be tuned in order to improve the hydrogen consumption and approach dynamic programming results.

3.3 FUZZY LOGIC CONTROLLER OPTIMIZATION

3.3.1 *Problem formulation*

The previously described fuzzy logic controller focused on maintaining the state of charge of the battery in the optimal zone (around 70 %) in order to respect the constraint given in (3.4). In order to reduce the hydrogen consumption, the memberships functions defining the fuel cell current (as described in FIGURE. 65), are tuned. Fig 71 gives an example of the configuration of the four membership functions. Each functions are trapezoidal and four variables $x(i,j)$ can be associated where i is the number of the function (1 for Ze, 2 for Low, 3 for Optimal and 4 for High) and j is the number of the variable, as described in the figure ($j \in [1,4]$).

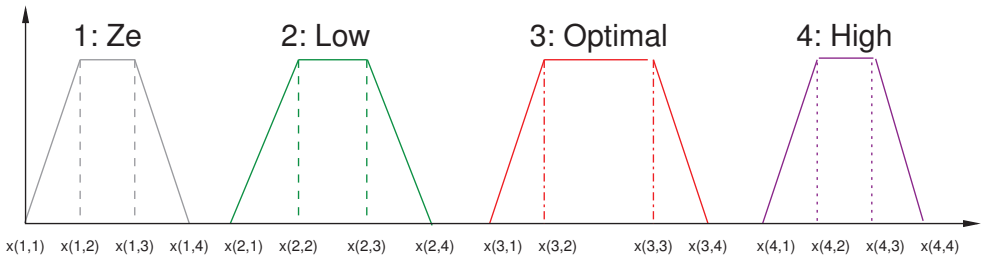

FIGURE 71. Fuzzy membership's variables

The optimization aims at reducing the hydrogen consumption by varying theses parameters while respecting the following constraint :

$$x(i,(j-1)) \leqslant x(i,j) \tag{3.1}$$
$$x((i-1),3) < x(i,2) \tag{3.2}$$
$$x(i,j) \in [0,130] \tag{3.3}$$
$$SoC_{final} = SoC_{init} \tag{3.4}$$

3.3.2 *Genetic algorithm*

To solve this optimization problem, a genetic algorithm is used. A candidate solution is composed of the sixteen variables $x(i,j)$ defined previously and the population is set to a hundred of candidate solutions. The population is randomly initialized, respecting the constraint given by (3.1) and the number of iterations is set to 10 000. The fitness function run the fuzzy logic controller tuned by each candidate solution on the LA92 driving cycle and return the hydrogen consumption and the SoC_{final}.
FIGURE. 72 shows the results of the optimized fuzzy logic controller by the best candidate solution compared to the fuzzy controller define in section FIGURE. 3.2.3. The optimized fuzzy is very close to the dynamic programming results, and did not increased the fuel cell current drastically on the two points of the driving cycle where the speed is high compare to the traditional fuzzy. Consequently, the fuel cell current is almost steady during all the driving cycle. TABLE. 14 shows the hydrogen consumption compare to results of the section 3.2.3. The consumption with the optimized fuzzy is reduce by 22 % compare to standard one, and is close to offline results.

TABLE 14. hydrogen consumption comparison with optimized fuzzy controller

	Fuel cell power (kW)	Battery capacity (Ah)	H_2 consumption (g)
Stand alone fuel cell vehicule	13	0	102
Fuzzy logic controller	5	65	63
Optimised Fuzzy logic controller	5	65	49
Dynamic programming	5	65	40

3.3.3 *Conclusion*

This section presented a methodology to improve the real time controller based on fuzzy logic for a specific driving cycle. It as been demonstrated that 22 % of hydrogen consumption can be saved by optimizing the membership function of the controller. Nevertheless, this optimized controller brings new issues : the control is aimed for a specific patterns, and can be less efficient on other patterns, as for example : highway roads.

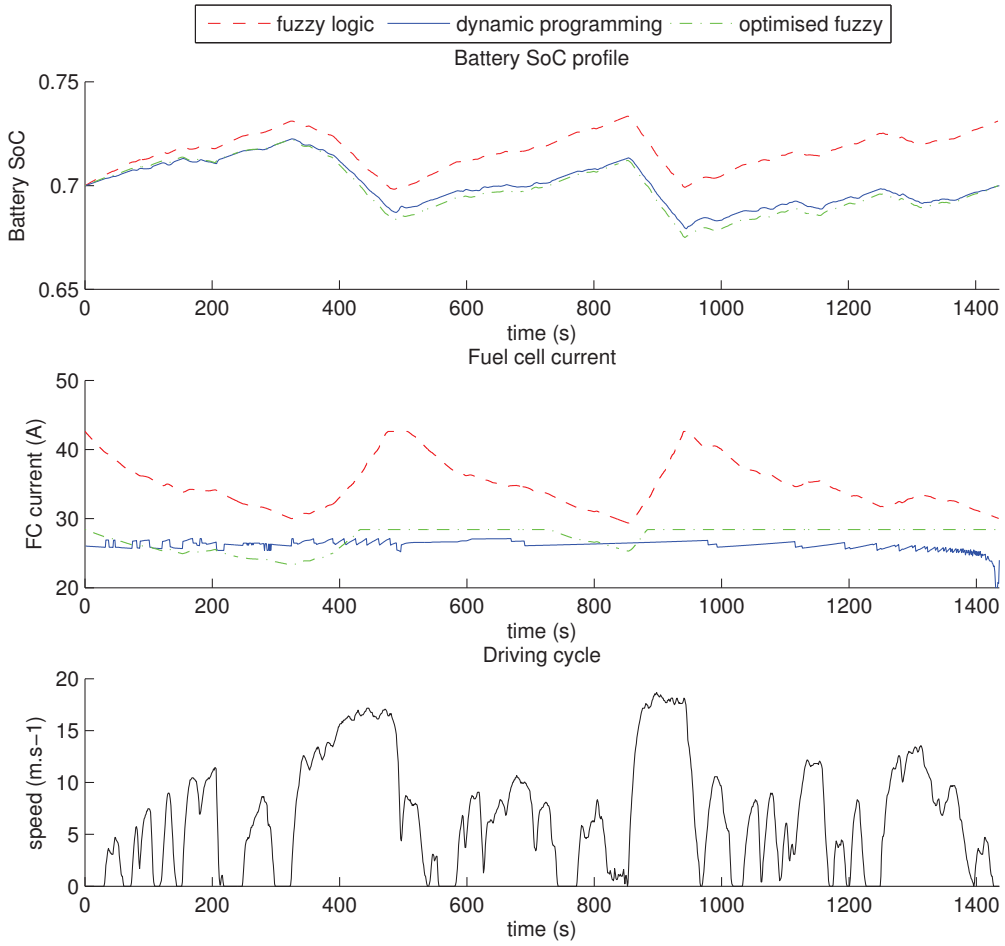

FIGURE 72. Optimized Fuzzy logic controller results compare to standard fuzzy and dynamic programming

3.4 EXPERIMENTAL VALIDATION ON A REAL FUEL CELL HYBRID ELECTRIC VEHICLE

The designed fuzzy logic controller presented in section 3.2.3 is implemented in the SeTcar vehicle described in 3. The vehicle has the following characteristics :

- *Vehicle mass* : 578 kg ;
- *Front surface* : 2 m^2 ;
- *Drag coefficient* : 0.7 ;
- *Rolling coefficient* : 0.015 ;
- *Battery technology* : Lead acid ;
- *Battery capacity* : 40 Ah ;
- *Battery cells number* : 6 ;
- *DC-bus voltage* : 72 V ;
- *Fuel cell power* : 5 kW.

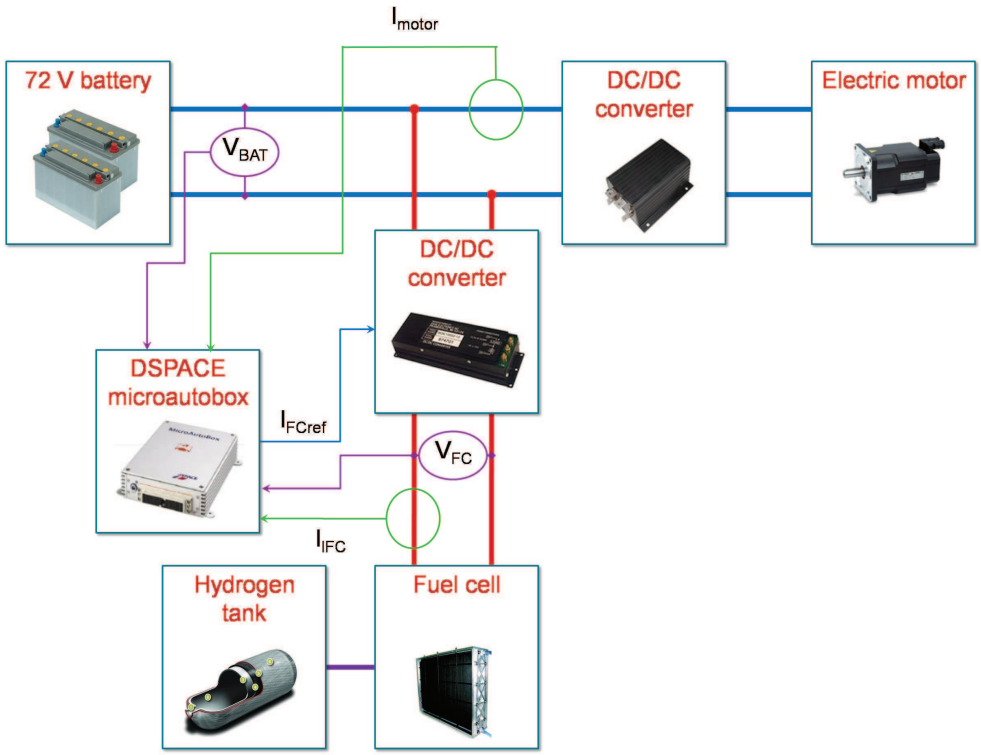

FIGURE 73. Vehicle architecture

FIGURE. 62 shows a picture of the vehicle and fig 73 shows the architecture of the vehicle. The fuel cell current is controlled using a buck DC-DC buck converter [73, 74] from 120 V to 72 V. The batteries are directly linked to the DC-bus. Current and voltage sensors give informations to the DSPACE Microautobox controller where fuzzy logic is implemented, and the analog

output controls the DC/DC converter. The power needed by the motor is emulated by an active load running the LA92 driving cycle with vehicle parameters.

Since lead acid batteries does not have battery management system [75], the state of charge needs to be evaluated using the current and voltage given by sensors.

3.4.1 *Experimental state of charge determination*

The state of charge of the batteries is given by (3.5) :

$$SoC(t) = \frac{C_{battery}}{\int_{x_0}^{t} i_{motor}(t) - i_{FC}(t)\ dt} \tag{3.5}$$

Where $SoC(t)$ is the state of charge at each time t, $C_{battery}$ is the battery capacity in Ah, i_{moto} and i_{FC} are the current needed by the motor (active load) and given by the fuel cell and x_0 is the initial battery capacity.
To determine the initial battery capacity, a charge/discharge experimentation is run in order to determine the relation between the state of charge and the open circuit voltage. FIGURE. 74 shows the results of this experimentation for a discharge at 50 Ah from 100 % to 0 %

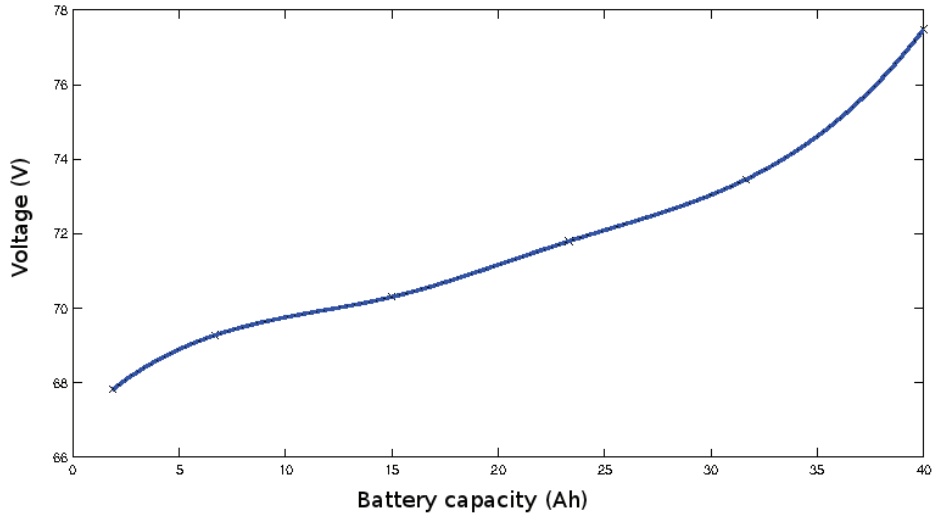

FIGURE 74. Remaining battery capacity as a function of open circuit voltage

When the vehicle start, open circuit voltage is given by the voltmeter and the initial state of charge is calculated. The state of charge is then computed at each time step t of the fuzzy controller.

3.4.2 *Fuzzy controller implementation*

The fuzzy controller is implemented in a DSPACE microautobox which is runs at 10kHz. As describe in FIGURE. 73, the fuzzy controller controls the DC-DC converter through analog output from 0 V to 10 V corresponding to a fuel cell current range between 0 A and 30 A. the fuzzy zone is defined as :

- *Low state of charge* : Below 50 % state of charge, fuel cell is running at maximum power (5 kW) ;
- *Optimal state of charge* : from 60 % to 70 % state of charge, fuel cell is running at optimal point (3,4 kW) ;
- *High state of charge* : from 70 % to 60 % state of charge, fuel cell is low (1.7 kW) ;
- *Very high state of charge* : up to 80 % state of charge, fuel cell is switched off.

3.4.3 *Results : comparison of simulation and experimentation*

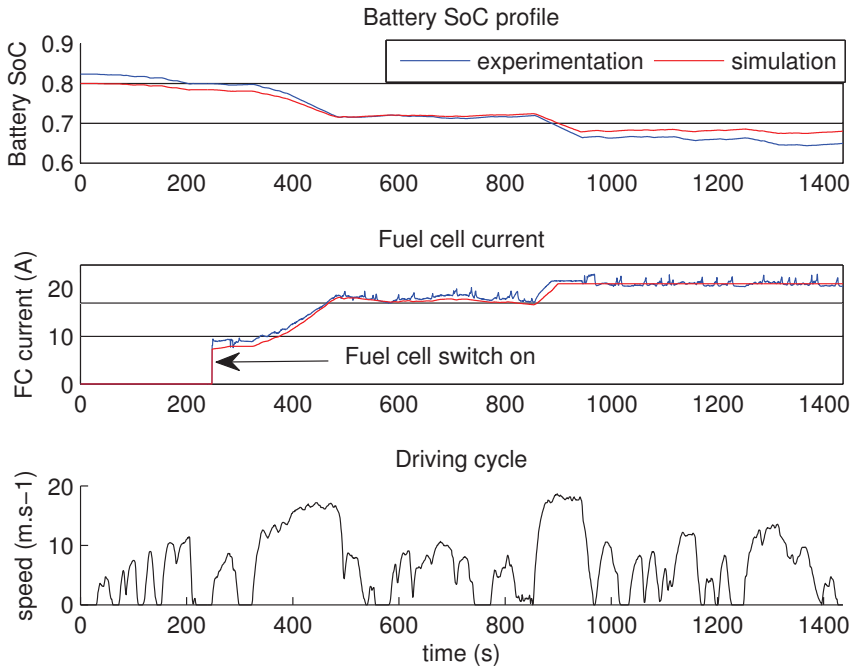

FIGURE 75. Experimental results for fuzzy logic controller with LA92 driving cycle

FIGURE. 75 shows the results for LA92 driving cycle emulated by the active load for the experimentation and the results for the simulation with the same fuzzy logic parameters. The initial state of charge is 80 %. In a first part, the

fuel cell is switched off in order to decrease the state of charge in its optimal zone. The state of charge is then in the High zone, the fuel cell running point (20 A) is under the optimal working point (where the efficiency is the best) and the state of charge keep decreasing steadily to reach the optimal zone. Finally the fuzzy logic controller maintains the state of charge in this zone (between 60 % and 70 %). The simulation results fit with the experimentation : the fuel cell current is almost the same during all the cycle, but the state of charge shows some small differences : in fact, the experimental state of charge determination amplify the measurement errors. However, this error is acceptable. The hydrogen consumption is 31 g for experimentation and 25 g for simulation. this gap can be explain by the granularity of the fuel cell model : Indeed, the model used for the simulation does take into account the system auxiliaries by subtracting a constant power to the output power of the fuel cell system. Nevertheless, this approximation does not take into account transient phases like hydrogen purge for example or the increase of the blower if the fuel cell runs at an high temperature points. This issues appears in the experimentation and explain the excess of hydrogen consumption compare to simulation.

3.4.4 *Conclusion*

The fuzzy logic controller has been implemented and validated in a real hybrid electric vehicle based on fuel cell. The results show that the simulated hydrogen consumption is equivalent to experimentation, minus the errors on the model. This study on the conception of the fuzzy controller, its optimization and comparison with an offline method has been presented on a conference : IEEE Vehicle Power and Propulsion Conference in 2011, Chicago, USA [76], and a journal article has been made : Control Strategies for Fuel-Cell-Based Hybrid Electric Vehicles : From Offline to Online and Experimental Results : IEEE Transaction on Vehicular Technology, 2012 [77].

3.5 DRIVING CYCLE RECOGNITION

As discussed in section 3.3.3, an optimized controller aims to reduce the hydrogen consumption for a specific patterns, but can be less efficient in others ones. In this way, driving cycle recognition can be a good source of information if an algorithm is able to recognize a driving patterns. Consequently, the real time control can adapt his parameters in order to fit with the patterns. In the literature, some papers studied driving cycle recognition or learning algorithm such as : [72, 78, 35]. But all of this studies bring at offline method, knowing the driving cycle in the control process. The proposed Driving Cycle Recognition Algorithm (DCRA) is a real time algorithm which define a driving patterns and give the information to the control strategy.

3.5.1 *Driving cycle recognition algorithm*

The algorithm principle is described in FIGURE. 76 : the algorithm's input is based on severals parameters :

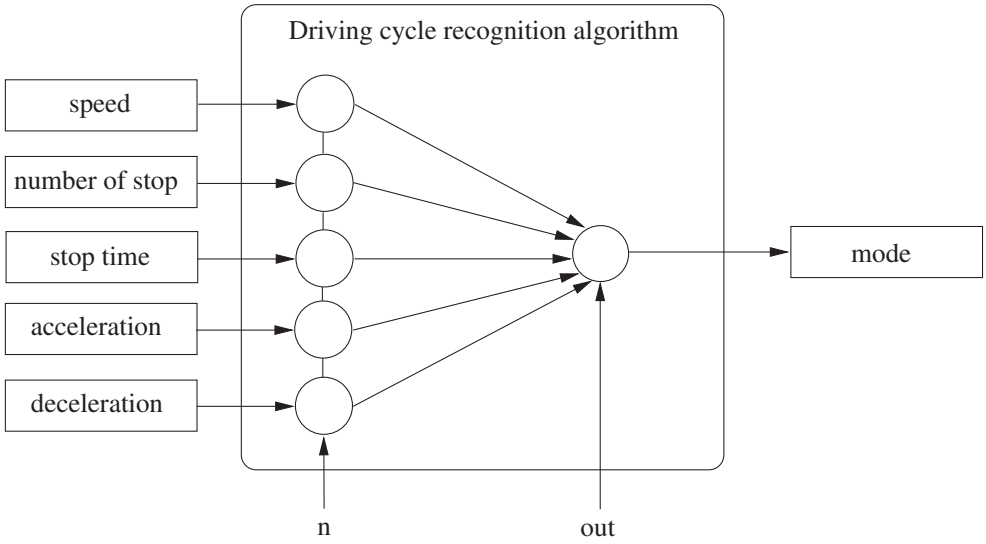

FIGURE 76. Driving cycle recognition algorithm principle

- *Vehicle speed* ;
- *Number of stop* ;
- *Stop time* ;
- *Acceleration* ;
- *Deceleration* ;

the output : mode is composed of three states :

- *Urban* : The mean speed of the vehicle is low (around 30 km/h) but the dynamic is very high. There are a lot of start/stop, acceleration/deceleration phases. Nevertheless, due to long stop durations, the mean acceleration/deceleration is average ;
- *Suburban* : The mean speed is medium/high (around 60 km/h) and the dynamic of the vehicle is average due to the low number of start/stop.
- *Highway* : The mean speed is high (up to 100 km/h) and the number of start/stop phases is zero. The dynamic is low because the vehicle is constantly running at high speed.

For each mode, a specific driving cycle is used to determine the limits of all inputs to determine the output.
FIGURE. 77 shows the speeds distribution of different modes for the specific driving cycle. Each parameters (speed, acceleration, deceleration, stop time and number of stops) are statistically described and each DCRA boundary is set to 70 % of the total occurrences.

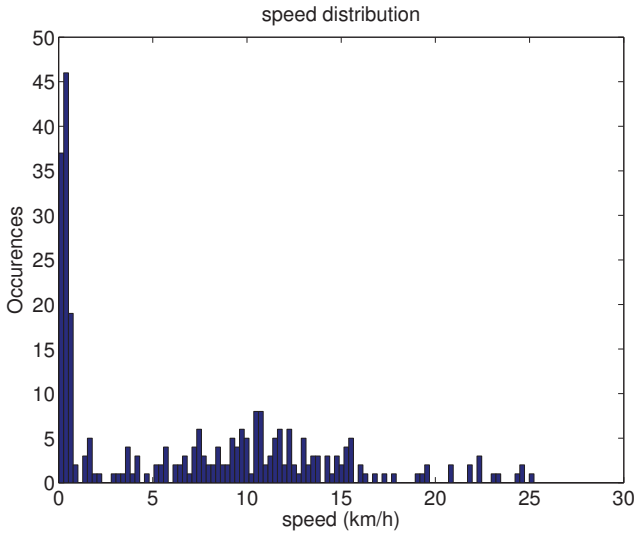

(a) Urban speeds distribution

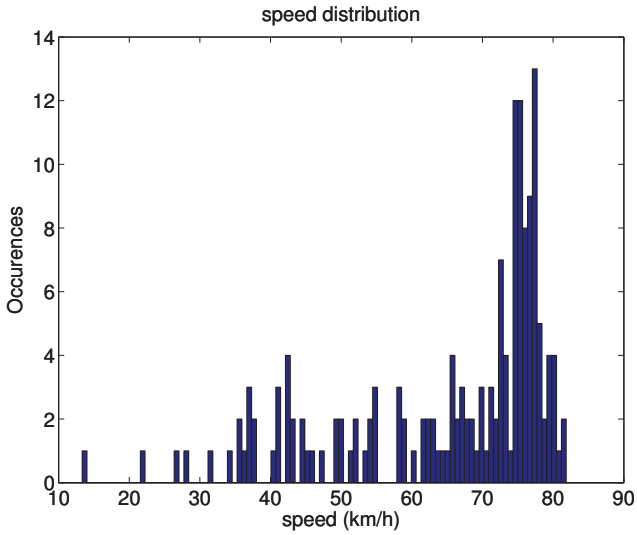

(b) Suburban speeds distribution

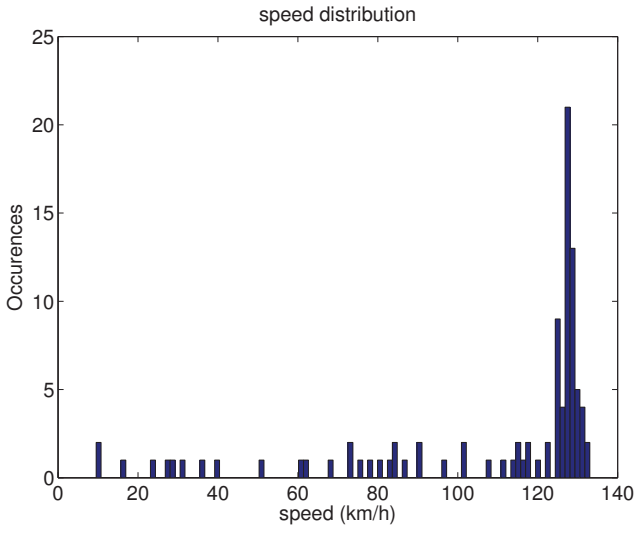

(c) Highway speeds distribution

FIGURE 77. Statistical distributions of speeds

The output is given by (3.6) :

$$M = \sum_{k=1}^{5} n_k i_k \tag{3.6}$$

$$mode = 1 \quad if \quad 0 < M < out_1 \tag{3.7}$$

$$mode = 2 \quad if \quad out_1 < M < out_2 \tag{3.8}$$

$$mode = 3 \quad if \quad M > out_2 \tag{3.9}$$

where i_k is the input vector of the DCRA (average speed, number of stops, etc), n_k is the weight factor of the input vector, M is the sum of all input, out_1 , out_2 are the outputs triggers and $mode$ is 1 for urban, 2 for suburban and 3 for highway.

3.5.2 *Results*

FIGURE. 78 shows the results of DCRA for a custom driving cycle. The driving cycle is composed of urban trips, highway roads and mixed parts. The DCRA switches between modes with a good reactivity, recognizing the type of the road. The algorithm has a window of time of 30 s, which is a good response time for this cycle. Reducing the time frame allows to increase the response time of the algorithm but decreases the precision.

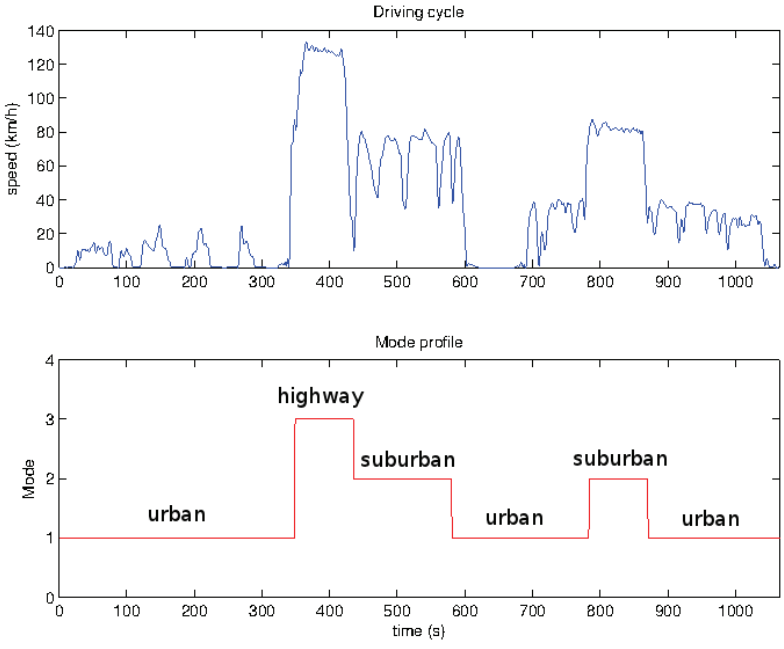

FIGURE 78. Driving cycle recognition results on a custom driving cycle

3.5.3 *Fuzzy logic controller including driving cycle recognition*

The controller used in section 3.2.3 is modified to get dcra results : FIGURE. 79 described the input of the controller : the DCRA information is added to the fuzzy to modify the optimal power zone (i.e, the fuel cell current working range) based on the value of mode :

$$mode = 1 \quad , \quad I_{FC_{opt}} \in [20\,,30] \tag{3.10}$$

$$mode = 2 \quad , \quad I_{FC_{opt}} \in [40\,,60] \tag{3.11}$$

$$mode = 3 \quad , \quad I_{FC_{opt}} \in [80\,,90] \tag{3.12}$$

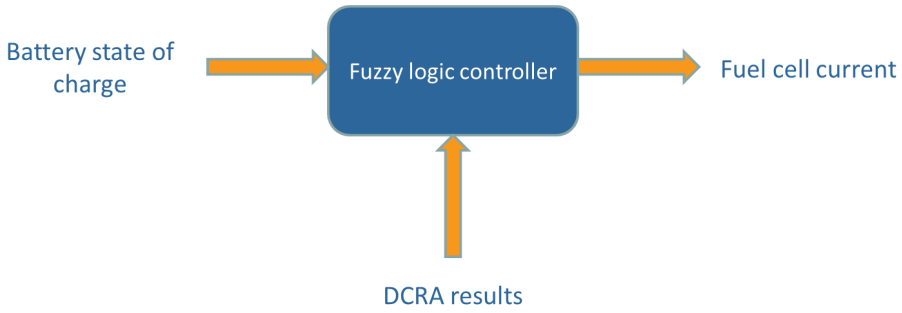

FIGURE 79. Fuzzy controller with DCRA principle

3.6 SIMULATION OF DIFFERENT SCENARIOS

FIGURE. 80 shows the fuzzy logic controller results for the same driving cycle used for the DCRA. The batteries's state of charge is kept in the optimal zone (around 70 %) during all the cycle due to the switch of mode. In order to compare results, two fuzzy logic controllers without DCRA are parametrized :

- Urban fuzzy logic controller : The fuel cell membership functions are parametrized for a specific urban driving cycle : LA92.
- Highway fuzzy logic controller : The fuel cell membership functions are parametrized to run with a highway driving cycle.
- DCRA fuzzy logic : The results of DCRA mode are used to define the three types of fuzzy : urban, suburban and highway. The urban and highway parts have the same parameters as the previously defined fuzzy controllers.

A first simulation is carried out with LA92 driving cycle : FIGURE. 82 shows the comparison for the fuzzy logic tuned for urban and highway. Since the driving cycle is urban, the DCRA fuzzy logic controller has the same results than fuzzy logic with urban parameters. The fuzzy controller with highway parameters aims to run the fuel cell at the optimal points for highway driving style : between 80 and 90 A, which is too high compare to the power needed

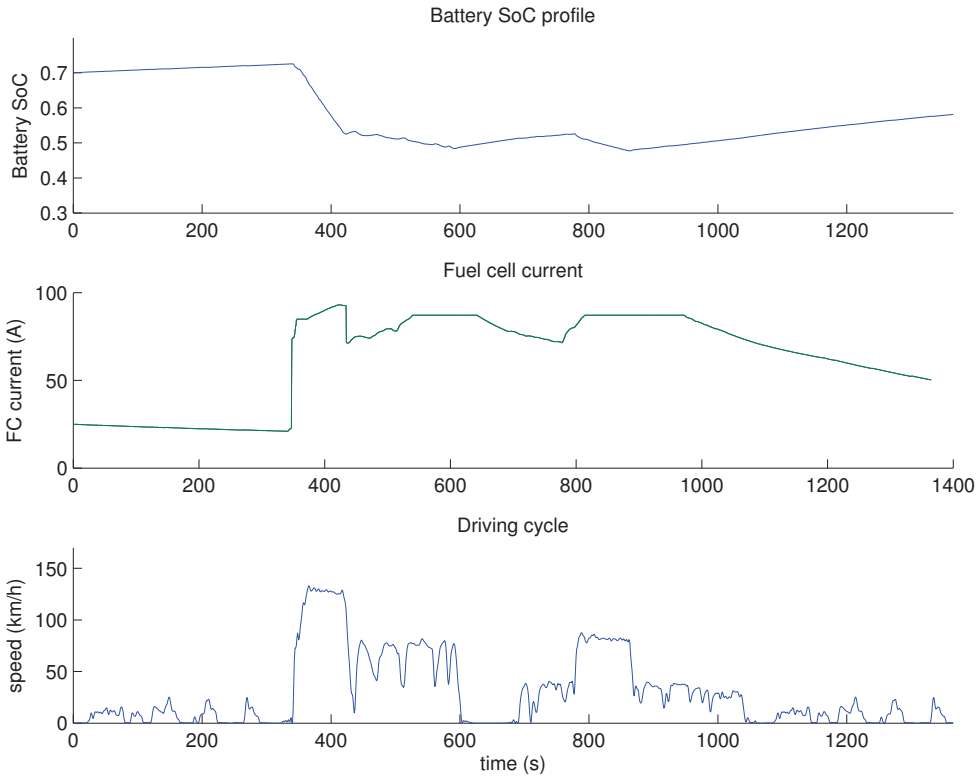

FIGURE 80. Fuzzy controller with DCRA results

by the vehicle. Consequently, the SoC increases and the fuel cell is switched off several times during the cycle in order to maintain the SoC in the optimal zone. Therefore, the urban fuzzy controller operates the fuel cell to the best running point for this driving cycle, allowing to keep the fuel cell current constant to save hydrogen consumption.

TABLE 15. Simulations results

Driving cycle	Parameters of fuzzy controller	Final SoC	Hydrogen consumption (g)
LA92 cycle	Urban	0.72	73
	Highway	0.7	98
	DCRA	0.72	73
Custom cycle	Urban	0.56	168
	Highway	0.62	212
	DCRA	0.6	179
Custom cycle ran 5 times	Urban	0.28	1015
	Highway	0.6	1252
	DCRA	0.45	1143
Custom cycle ran 10 times	Urban	Not finished	Not finished
	Highway	0.6	2556
	DCRA	0.4	2365

A second simulation is carried out to point out the interest of fuzzy logic with DCRA : FIGURE. 82 shows the simulations of the mixed driving cycle presented in FIGURE. 80 run ten times. Results are drawn for fuzzy logic with DCRA (with red color) and fuzzy logic with urban parameters (with blue color). The fuzzy logic controller with urban parameters aim to run the fuel cell in its optimal zone : between 20 and 30 A, but the power needed by the cycle is greater. The SoC decreases quickly and the controller response time is too low. After five cycles, the SoC goes under 20 %, and the simulation stops automatically (20 % SoC is the lower limit in order not to damage the batteries). Therefore, the fuzzy logic with DCRA anticipates the power needed during the highway phases and increases the fuel cell current, allowing to carry out the driving cycle ten time with a final state of charge of 40 %.
TABLE. 15 shows the final SoC and hydrogen consumption of both simulations with different scenarios. On the one hand, the fuzzy controller with DCRA maintains the final SoC close to the initial during the custom driving cycle, allowing to carry out it ten times. On the other hand, the results of fuzzy with DCRA on urban cycle are the same as the optimized urban fuzzy logic, allowing to save hydrogen consumption compared to the fuzzy tuned for

highways.

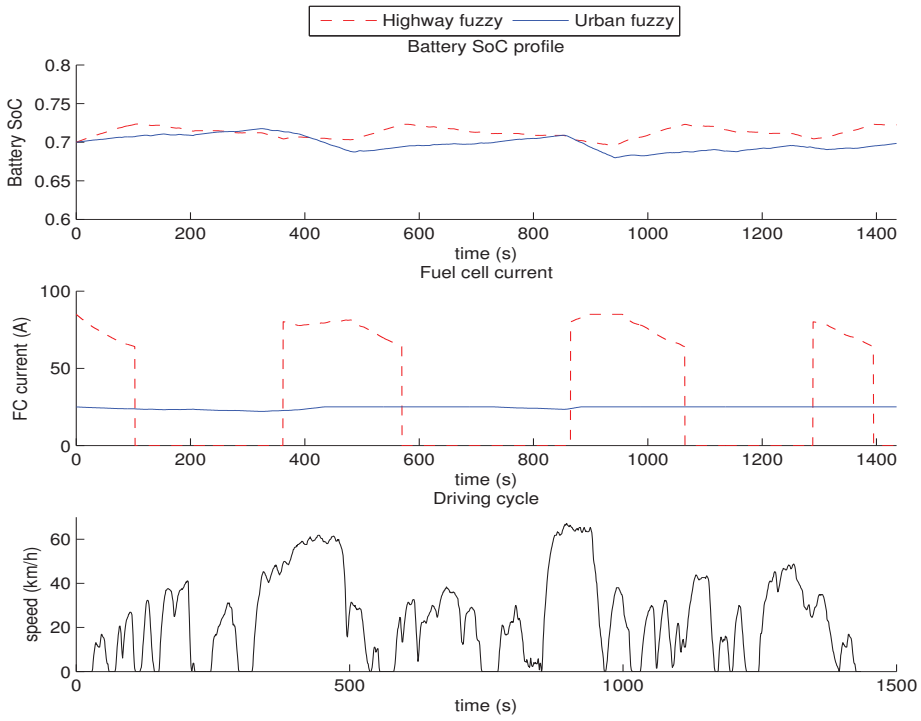

FIGURE 81. Comparison of fuzzy logic controller with urban optimisation and highway

3.6.1 *Conclusion*

A driving cycle recognition algorithm has been presented. The proposed method allows to optimize a fuzzy logic control for a specific driving pattern (for instance urban), and still runs other patterns (highway) without dropping to low the battery's state of charge. This study has been presented on a conference : IEEE Transportation Electrification Conference and Expo (ITEC), 2012, Dearborn, USA [79].

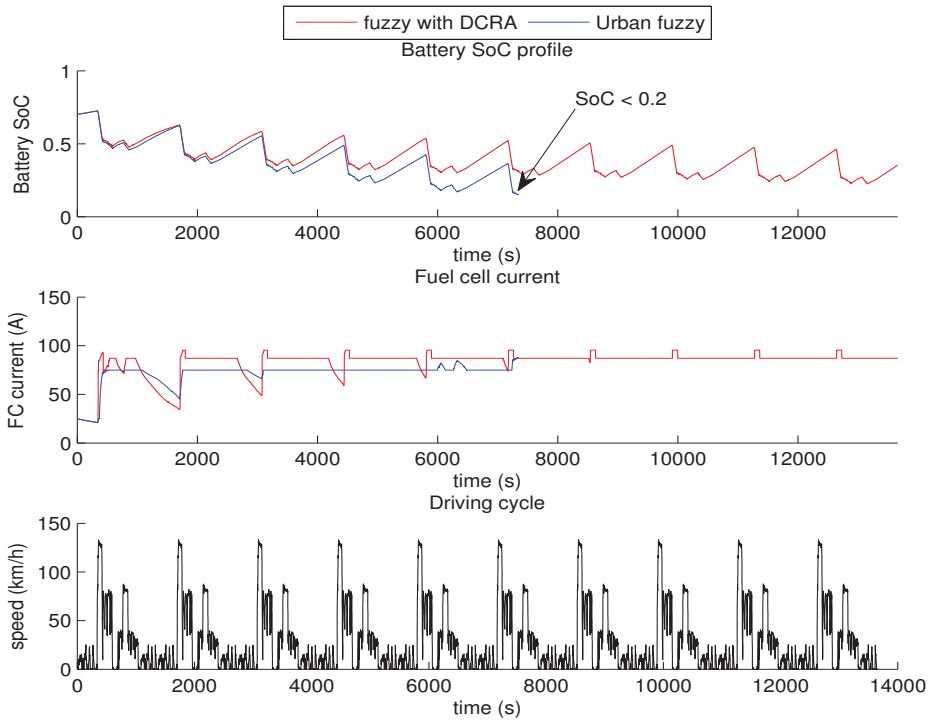

FIGURE 82. Comparison of fuzzy logic controller with DCRA and urban for a custom mixed driving cycle

3.7 CONTROL STRATEGY OF PLUG IN HYBRID ELECTRIC VEHICLE BASED ON DESTINATION PREDICTION

3.7.1 *Problematic : control strategy on standard hybrid electric vehicle versus plug in hybrid*

As discuss in section 3.2.3, the main constraint of a standard hybrid electric vehicle composed of a primary source (internal combustion engine or fuel cell) and batteries is to keep the state of charge of the batteries at a good level. Indeed, no matter of the architecture used : series, parallel or combined ; the batteries can only be charged using recovery power by the vehicle brake or by the primary source [80]. This constraint is a big issue for the control strategy : the battery's role is limited to absorb the peak of power in order to run the primary source at is best efficiency point. Therefore, in a plug in hybrid electric vehicle, the battery can be charged by the grid. It adds a new degree of freedom in the control strategy : the state of charge at the end of the driving cycle is not a constraint anymore and can be lowered as most as possible, assuming that the vehicle will be plugged to the grid. It allows to focus the control strategy in fuel consumption economy rather than trying to keep the state of charge in a good zone using the best efficiency point of the primary source. Moreover, the vehicle can run in pure electric mode when the batteries energy is enough to run the driving cycle.

To illustrate this, FIGURE. 83 and FIGURE. 84 show an example of two different control strategies for the vehicle studied in section 3, based on a 5 kW fuel cell and 2880 Wh batteries considering two scenarios :

- A standard hybrid electric vehicle : the state of charge of the batteries need to be keep in a good zone.
- A plug in hybrid electric vehicle : the batteries can be plug to the grid at the end of the driving cycle.

LA92 driving cycle is used to simulate both scenario : FIGURE. 83 shows the control strategy for the first scenario based on fuzzy logic : the fuel cell runs at a good efficiency point allowing the batteries state of charge to be kept in around 70%. FIGURE. 84 shows the control strategy for the same vehicle assuming that it is plug in. The vehicle runs in pure electric mode during all the driving cycle, and the state of charge decreases to reach 50%. The results shows that 49 g are of hydrogen are consumed for the standard hybrid electric vehicle and 0 g for the plug in.

This new degree of freedom in the control strategy for plug-in vehicle bring also new problems :

- *The all electric mode range :* In a charge depleting / charge sustaining control strategy (section 1.3.3), the range of the electric mode is a big issue when running a specific driving cycle. for instance, in FIGURE. 84, the batteries's energy is big enough to runs in all electric mode during all the driving cycle. However, some more dynamic driving cycle require

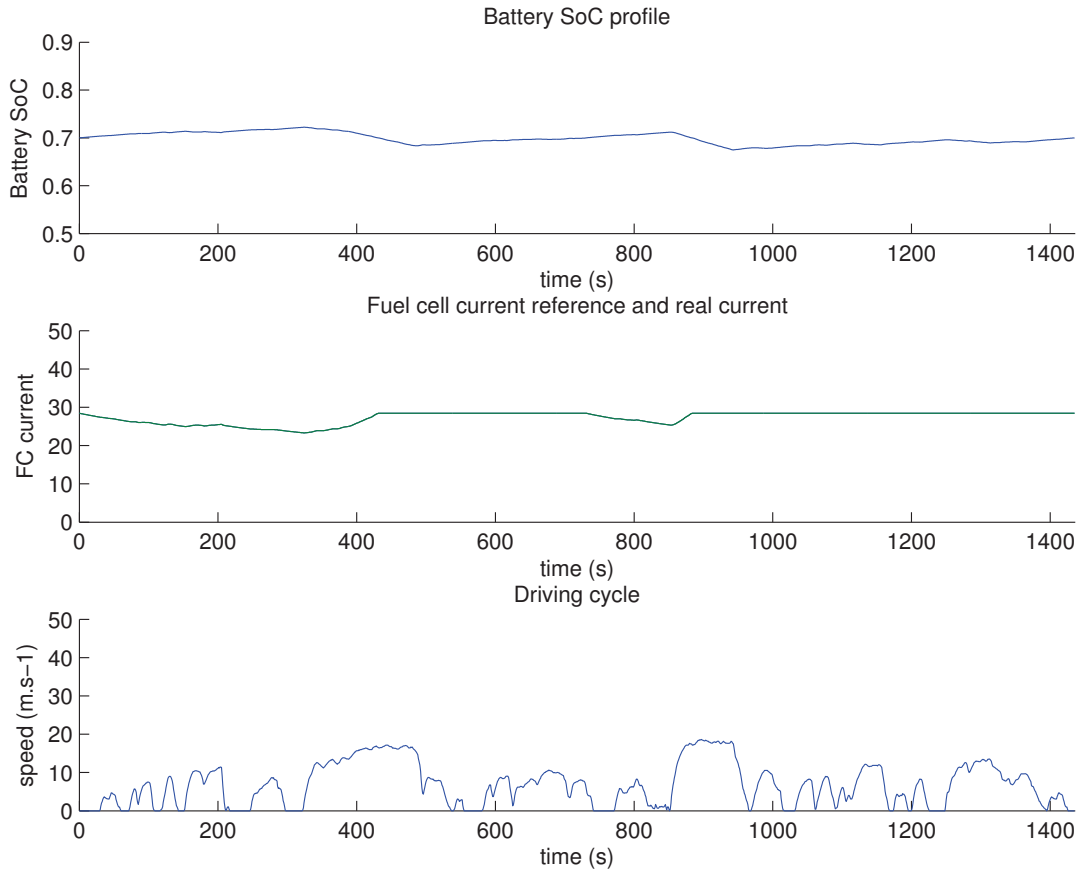

FIGURE 83. Control strategy based on fuzzy logic on a plug in hybrid electric vehicle

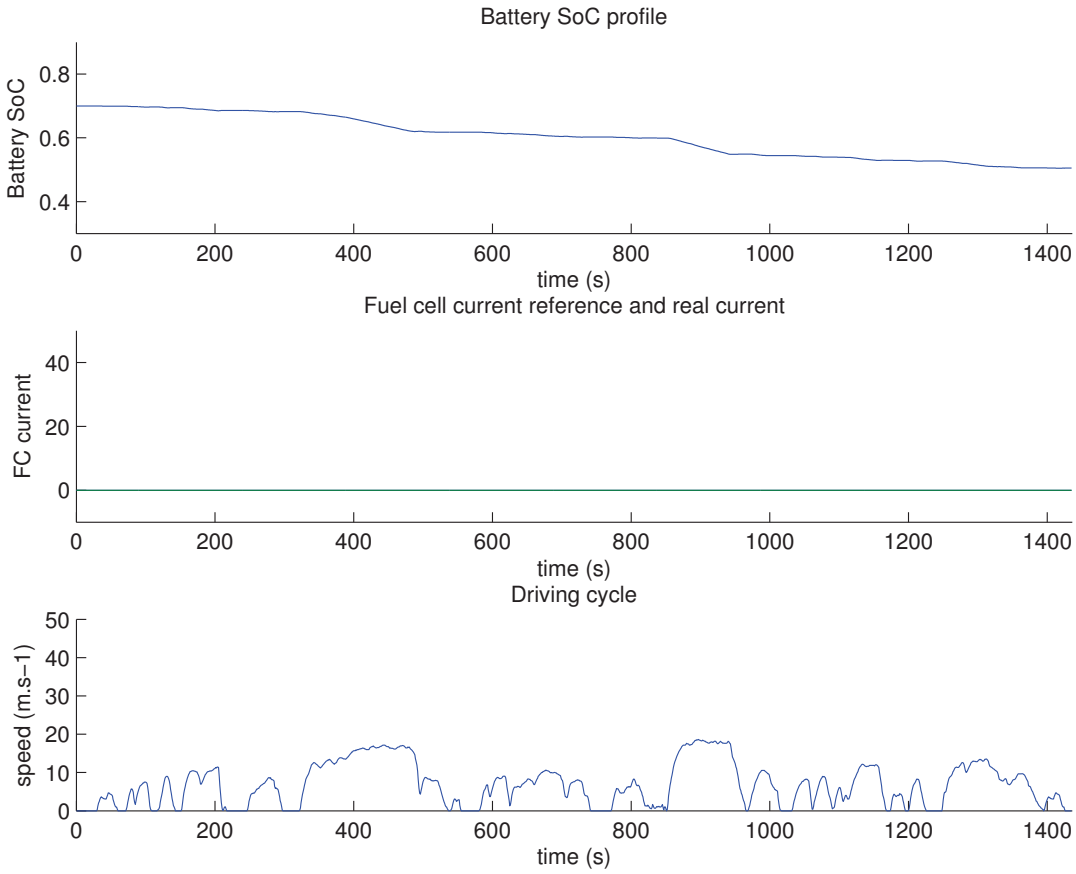

FIGURE 84. Control strategy based on fuzzy logic on a plug in hybrid electric vehicle

more energy than the batteries's can provide, and the primary source of energy must be turned on to maintain the batteries's state of charge. During this charge sustaining phase, either the primary source of energy is big enough to provide all the power required by the cycle while running at its efficiency point ; either the source must runs on high power point in order to provide the power and recharge the batteries.

– *The dynamic of discharge :* if the control strategy aim to reach the minimal state of charge at the end of the driving cycle without entering in charge sustaining phase, the dynamic of the state of charge is the main problem : The control must predict the remaining energy in order to control the coefficient of discharge of the state of charge.
In this section, the second point is developed : Firstly, a destination prediction algorithm is presented in order to determine the remaining distance of the driving cycle. Then a control strategy is built based on the results of the destination prediction. Finally, results are drawn and shows the improvement of the methodology compared to the charge traditional charge depleting / charge sustaining control strategy.

3.7.2 *Destination prediction algorithm*

As shown in section 3.7.1, the control strategy in a plug in hybrid electric vehicle which focus to minimize the state of charge of batteries at the end of a trip mainly depend on the prediction of the distance remaining. In order to determine this distance, a destination prediction algorithm was created.
In the litterature, several studies focus on the distance prediction, where two major parts can be distinguished :

– The prediction of the destination point [81, 82, 43, 83, 84, 85] : Based on the past experiences of trips, the algorithm determine the most prorable final point (where the vehicle will stop at the end of the driving cycle). Theses studies are based on a learning algorithm which fill memory with pasts driving cycle and destination point reached. Mainly of them are composed of a Markov model in order to statistically choose the best probable destination point knowing the initial point of the trip.
– The prediction of the distance knowing the final point [86, 87, 88, 89, 90, 81, 91] based on Global Positioning System informations and knowing the actual and final point, an algorithm calculates the distance remaining by crossing GPS points with a map database containing roads segments, intersections and traffic flow.

Both parts have its own pros and cons : the prediction of the destination point allows to determine the most probable point that the vehicle can reach but since its based on probabilities, the real results can diverge and leads to huge difference between the predicted distance and the real one. The prediction of the distance knowing the final point is very accurate, since its based on a GPS database including all roads that the vehicle can runs, but the information of the final point must be given by the driver before doing

the trip. Also, this solution is very memory consuming, since all the database needs to be embedded in the system, assuming that the algorithm will be embedded in the vehicle, which is a big constraint in the conception of the control strategy system. Indeed, the destination prediction algorithm not the main part of the control strategy, and need to stay as small as possible in term of memory and time consuming for the system.

In both scenario, GPS points are used as input of the simulation : this system is necessary in order to determine final point and distance between actual point and destination.The proposed solution has a learning capability from past experiences based on a Markov model which build a matrix of probable points for a given initial position. Each probable points has its own probability to be reached. Then theses probabilities are updated has the vehicle moves. The results is a mean distance of each points by probabilities.

Driving cycle survey

In order to simulate the learning part of the algorithm, a survey has been conducted on 5 drivers in the city of Raleigh in North Carolina, USA. Each driver's trip has been logged during 2 months, and each driver was chosen because of the driving style and the variety of driving cycle that they create. A GPS logger has been put in each cars of drivers. The logger used is GPS Tracking System 3100-INT made by LandAirSea, and is described in FIGURE. 85.

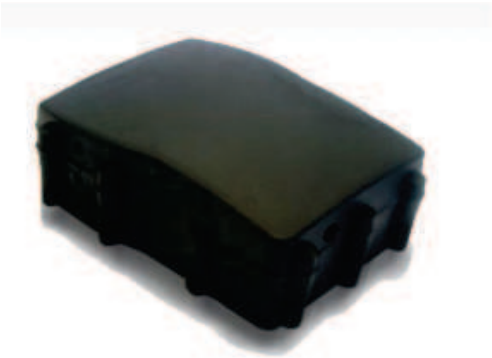

FIGURE 85. GPS Tracking System 3100-INT by LandAirSea

The GPS logger has the following characteristics :
- Internal Antenna.
- External 12 Volt power input option.
- Powered by 4 regular AA Batteries which will last up to 1 month with average driving.
- Records 100 hours of driving data.
- 12 Channel GPS receiver.

- Horizontal Accuracy : 2.5 meters.
- Memory Type : Flash Memory.
- Data Output : USB.
- Sleep Mode Entry : 3.5 minutes of no movement.
- Cold Start GPS Acquisition Time 90 seconds.
- Warm Start 50 seconds.

The logger is autonomous with AA batteries and can be stored in a vehicle for one month. It also have a sleep mode which is enable when the vehicle is stop more than 3.5 minutes. This sleep mode is a good way to save batterie's life but bring an issue for the survey : Indeed, the Cold start of GPS acquisition (when leaving sleep mode) is 90 second. Some errors can appear during this cold start time resulting by missing GPS point. Nevertheless, since the vehicle stop is recorded, missing points can be interpolated.
The logger has a 4 Gb of memory and come with a software to download the data from memory to PC. The software can also display the trip traveled with stops. FIGURE. 86 shows the software results for a 15 days of record of a driver : The blue line represent the vehicle's driving cycle with low speed (lower than 50 km/h) and the pink lines high speeds (more than 50 km/h).

Extraction of destination and initial points

The algorithm is working with points where the vehicle start or stop. From the data recorded, the initial point (beginning of the driving cycle) and destination point (last point of the driving cycle) are extracted by comparing each time step with a trigger :

$$\text{If } t(k) - t(k-1) > T_{trig} \text{ then} \tag{3.13}$$

$$Dest_{GPS_{lat}} = GPS_{lat}(k) \tag{3.14}$$

$$Dest_{GPS_{long}} = GPS_{long}(k) \tag{3.15}$$

Where Ttrig is the time trigger, GPS_{lat} is the latitude GPS point, GPS_{long} is the GPS longitude point and $Dest_{GPS}$ is the new destination GPS point. If the comparison between the time of a step minus the time of last step is superior to the trigger, the point is define as a Destination point. For our study, the trigger has been set to 10 minutes. This time has been set to avoid to get some stop as define as Destination point (for example : stops due to traffic light/jams).
FIGURE. 87 shows a report of all destination and initial point for 15 days of recorded data.

Clustering the points

The principle of the destination prediction algorithm is to determine the point where the vehicle stop in order to deduce the probability to go from an initial point to a final point. Since the GPS technology allows the logger to get GPS points with a precision of 10 meters, every time the vehicle reaches a final point several times, the GPS coordinates can be different. The most

FIGURE 86. LandAirSea software displaying trip recorded

usually scenario to describe this situation is when the vehicle stop at a parking lot : The vehicle does not park every time on the same spot, and the GPS coordinates can vary for more than 100 m. As the number of time when a final point is reached count in the algorithm, a cluster algorithm has been made : The principle is described in FIGURE. 88 : where P_n is a new final point detected, t is a index of the database (from $t = 0$ to $t = tmax$, $tmax$ depends of the number of final point already recorded) $Dist_{long}$ and $Dist_{lat}$ are respectively the longitude and the latitude distance between the two point P_n and $P(t)$, and $Trigger$ is the trigger distance which define if the point is within the range to be considered as the same point as the final point compared. In our study, the Trigger distance has been set to 200 m, corresponding to the mean surface of a parking lot.

When a new final point P_n is recognized as the same as another one, a new center is calculated. A center is defined as the GPS coordinate of the center describing all recorded point considered as the same final point. These coordinates are linked to the final point and will be used by the destination prediction algorithm to determine the distance between this point and the vehicle's position.

Build the probability matrix

All clustered initial and final points (and their GPS center coordinates) are recorded in a database. The algorithm create a probability matrix which is updated every time a new point is added or updated (a new final point is found corresponding to an already recorded one).The probability matrix has the following characteristics :

– Each rows represents an initial point, and each columns a final point :

Daily Driving Report
Date Span : Wednesday, April 18, 2012 ~ Tuesday, May 01, 2012

Wednesday, April 18, 2012
Departed From: 2379 Lilley Ct, Raleigh, NC 27606
Arrived At : 3033 Ligon St, Raleigh, NC 27607
Total Driving Time : 27 minutes, 5 seconds
Total Mileage Driven : 9.3 miles
Maximum Speed : 59.7 mph

Departed	Driving Time	Arrived	Location Arrived	Distance (Miles)	Stopped Time
16:35:40	04m:28s	16:40:08	3033 Ligon St, Raleigh, NC 27607	1.6	13m:05s
16:53:13	10m:42s	17:03:55	1699 Lethbridge Ct, Raleigh, NC 27606	3.4	1h:15m:41s
18:19:36	11m:55s	18:31:31	3033 Ligon St, Raleigh, NC 27607	4.4	14h:35m:38s

Thursday, April 19, 2012
Departed From: 3033 Ligon St, Raleigh, NC 27607
Arrived At : 3039 Ligon St, Raleigh, NC 27607
Total Driving Time : 1 hours, 35 minutes, 57 seconds
Total Mileage Driven : 39.7 miles
Maximum Speed : 63.4 mph

Departed	Driving Time	Arrived	Location Arrived	Distance (Miles)	Stopped Time
09:07:09	27m:51s	09:35:00	894 Main Campus Dr, Raleigh, NC	12.3	2h:52m:14s
12:27:14	27m:00s	12:54:14	3601 Cum Laude Ct, Raleigh, NC 27606	15.8	14m:58s
13:09:12	08m:33s	13:17:45	3045 Ligon St, Raleigh, NC 27607	3.2	39m:33s
13:57:18	01m:32s	13:58:50	3999 Lexington Dr, Raleigh, NC 27606	0.5	22m:56s
14:21:46	24m:51s	14:46:37	894 Main Campus Dr, Raleigh, NC	6.1	3h:32m:22s
18:18:59	06m:10s	18:25:09	3039 Ligon St, Raleigh, NC 27607	1.7	14h:49m:39s

Friday, April 20, 2012
Departed From: 3009 Ligon St, Raleigh, NC 27607
Arrived At : 3039 Ligon St, Raleigh, NC 27607
Total Driving Time : 1 hours, 46 minutes, 6 seconds
Total Mileage Driven : 38.1 miles
Maximum Speed : 66.5 mph

Departed	Driving Time	Arrived	Location Arrived	Distance (Miles)	Stopped Time
09:14:48	29m:05s	09:43:53	894 Main Campus Dr, Raleigh, NC	12.5	2h:09m:58s
11:53:51	00m:01s	11:53:52	890 Main Campus Dr, Raleigh, NC	0.0	22m:23s
12:16:15	32m:23s	12:48:38	3033 Ligon St, Raleigh, NC 27607	12.4	31m:43s
13:20:21	09m:04s	13:29:25	894 Main Campus Dr, Raleigh, NC	2.0	3h:44m:19s
17:13:44	05m:15s	17:18:59	3037 Ligon St, Raleigh, NC 27607	1.7	2h:24m:49s
19:43:48	21m:19s	20:05:07	1805 Walnut St, Cary, NC 27518	5.5	1h:13m:46s
21:18:53	08m:59s	21:27:52	3039 Ligon St, Raleigh, NC 27607	4.0	14h:04m:32s

Saturday, April 21, 2012
Departed From: 3039 Ligon St, Raleigh, NC 27607
Arrived At : 3039 Ligon St, Raleigh, NC 27607
Total Driving Time : 1 hours, 32 minutes, 44 seconds
Total Mileage Driven : 91.7 miles
Maximum Speed : 88.2 mph

Departed	Driving Time	Arrived	Location Arrived	Distance (Miles)	Stopped Time
11:32:24	01m:54s	11:34:18	991 Method Rd, Raleigh, NC 27607	0.5	28m:53s
12:03:11	01m:56s	12:05:07	3037 Ligon St, Raleigh, NC 27607	0.5	1h:20m:37s
13:25:44	53m:59s	14:19:43	Arrowhead Blvd, Mebane, NC	47.7	4h:03m:37s
18:23:20	34m:55s	18:58:15	3039 Ligon St, Raleigh, NC 27607	43.0	22h:01m:08s

Sunday, April 22, 2012
Departed From: 3037 Ligon St, Raleigh, NC 27607
Arrived At : 3037 Ligon St, Raleigh, NC 27607
Total Driving Time : 5 minutes, 45 seconds
Total Mileage Driven : 1.4 miles
Maximum Speed : 38.5 mph

Departed	Driving Time	Arrived	Location Arrived	Distance (Miles)	Stopped Time
16:59:23	04m:22s	17:03:45	3866 Jackson St, Raleigh, NC 27606	0.8	1h:09m:10s
18:12:55	01m:23s	18:14:18	3037 Ligon St, Raleigh, NC 27607	0.6	15h:06m:57s

Monday, April 23, 2012
Departed From: 3030 Ligon St, Raleigh, NC 27607
Arrived At : 3037 Ligon St, Raleigh, NC 27607
Total Driving Time : 1 hours, 27 minutes, 1 seconds
Total Mileage Driven : 31.1 miles
Maximum Speed : 69.0 mph

Departed	Driving Time	Arrived	Location Arrived	Distance (Miles)	Stopped Time

FIGURE 87. LandAirSea software report of 15 days of record

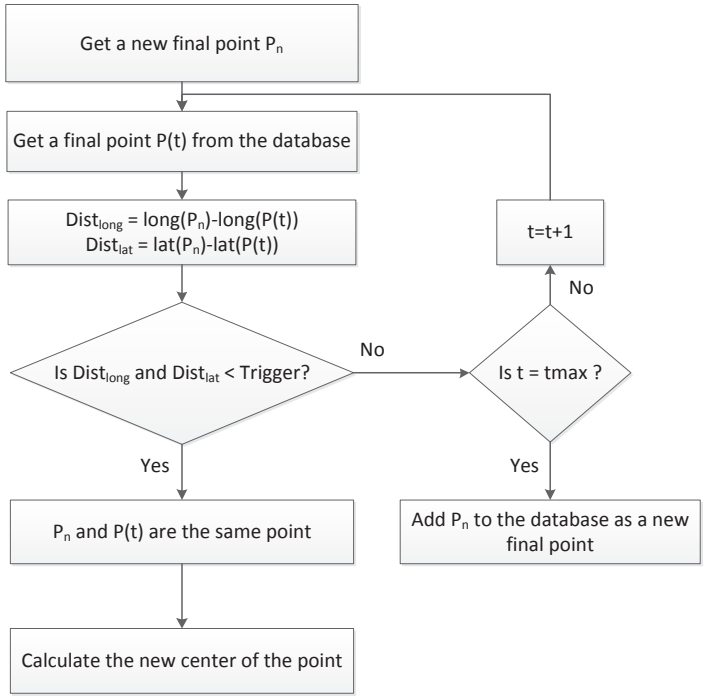

FIGURE 88. Clustering algorithm principle

the probabilities are filled in the matrix. Consequently reading a row correspond to : From a initial point, each final points (column) have x% probability to be reached.

– A probability is calculated by (3.16) :

$$P(F_i) = \frac{V_{F_i}}{V_i} \tag{3.16}$$

$$P(F_i) = 0 \text{ if } V_{F_i} < V_{trigger} \tag{3.17}$$

Where $P(F_i)$ is the probability to reach the final point F starting from initial point i, V_{F_i} is the number of visits recorded starting from i and ending to F, V_i is the number of visits recorded starting from i and $V_{trigger}$ is the minimal number of visits where the probabilities calculation is take into account. For our study $V_{trigger}$ is set to 5, meaning that under 5 number of visits from point i to point F, the probability $P(F_i)$ is set to 0. This prevent error on the destination prediction algorithm when the matrix does not have enough sample to determine a representative probability. Moreover, since the probability calculation is based on the total number of visit from i V_i, even if the number of visit for a given final point does not reach the trigger, theses visits count into the other probability point. Consequently, the sum of all probabilities $\sum P(F_i(y))$, with y the index of the column in the matrix, can be not equal to 100 %. Thus allow to keep a degree of incertitude in the destination prediction when the matrix has a low amount of informations. Consequently, the control strategy linked to the destination prediction will not decrease the state of charge of the battery to reach the minimum level for a given final point.

Oblivion algorithm

The matrix built is updated every time a new final point is created or its visit number is updated. Its leads to huge use of memory since the matrix grows constantly and informations can become wrong if for instance the driver change is habits (work, home...) In order to solve these both issues, a oblivion algorithm is created. Is principle is to simple keep the last 1000 lasts visits into the matrix. Every time a new visit $V(k)$is found (corresponding to either a new final point (first visit) or an update of the number of visit of a final point), the matrix will delete the $V(k-1000)$ visit. Final and initial points are then automatically deleted when their visit number is null. The choice of the number 1000 has been determined by the memory of the system used to runs the simulation. Reducing these number allow the matrix to be more adaptation to the change of habits of the driver but leads to more errors in the probabilities calculation.

Update probabilities as the vehicle moves

The probability matrix described in section 3.7.2 is updated every time a new final or initial point is found. Moreover, at each start of the vehicle, the matrix is parsed to find the corresponding initial point, and collect all

probable final points regarding the initial one. The probabilities and distance linked are calculated from this point. But when the vehicle will move, the results are not valid and need to be updated : At each time step, the GPS position of the vehicle is measured and the probabilities are updated from initial point by 3.18 :

$$P(F_t) = P(F_i)\left(\frac{d(F_t)}{d(F_i)}\right)^n \tag{3.18}$$

Where $P(F_t)$ is the probability starting at point t to go at final point F, $P(F_i)$ is the probability starting at initial point i to go at final point F, $d(F_t)$ is the distance between points t and F, $d(F_i)$ is the distance between points i and F and n is a coefficient allowing the probability update to converge faster on the final results.

Distance prediction

The final step of the algorithm is the distance prediction : from the probabilities updated linked with the distance for each probable final point, the mean distance can be determined 3.19 :

$$d_{final} = \sum_{k=0}^{nb_{fpoints}} P(F_t)d(F_t) \tag{3.19}$$

Where d_{final} is the output of the algorithm, the probable distance remaining and $nb_{fpoints}$ is the total number of final points in the probability matrix.

Results

To illustrate the algorithm, 3 scenarios has been simulated :
- *Scenario 1* : the vehicle start at initial point A, two final points B and C have initial 50 % probability each.
- *Scenario 2* : the vehicle start at initial point A, two final points B and C have initial 80 % and 20 % probability each.
- *Scenario 3* : the vehicle start at initial point A, six final points have random probabilities.

SCENARIO 1 FIGURE. 89 represents the probability update as the vehicles moves for scenario 1. The vehicle move from initial point A to point B : The probabilities are equal (50 %) at start. Since the vehicle runs from point A to point B, the probability of point B quickly increased to reach almost 100 % at the end of the cycle. Thus allow to have a better precision of the distance prediction rather than initial probabilities from matrix.

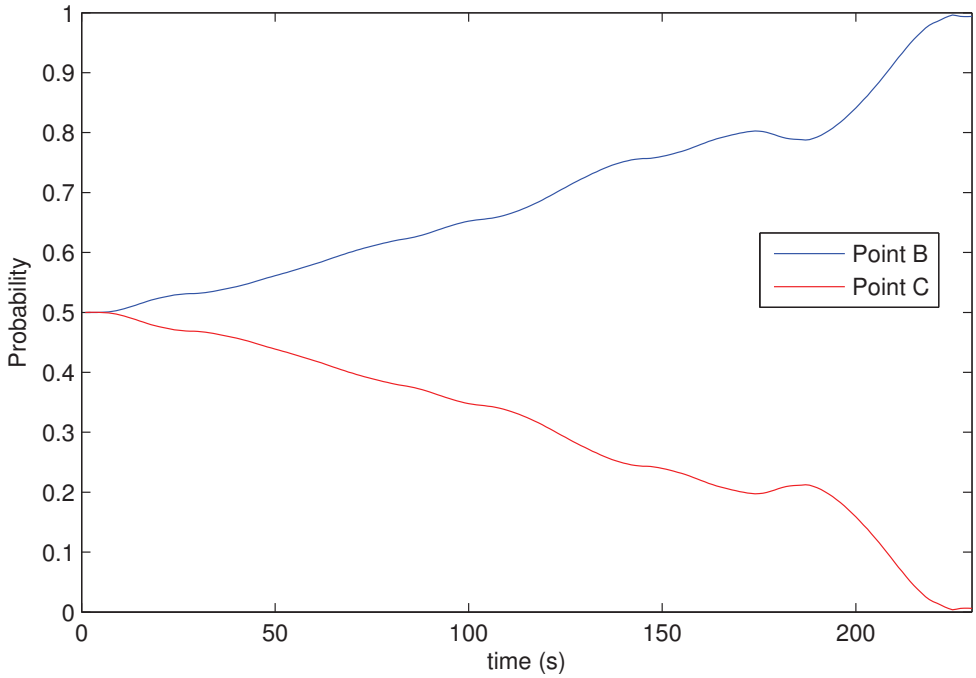

FIGURE 89. Probability updates as the vehicle moves for scenario 1

SCENARIO 2 FIGURE. 90 represents the probability update as the vehicles moves for scenario 2. The vehicle move from initial point A to point B. This scenario reflects the interest to update the probabilities as the vehicle moves : The initial probability was 80 % to go from point A to C, but since the vehicle goes from A to B, the probability to C drastically decreases during the driving cycle.

SCENARIO 3 FIGURE. 91 represents the probability update as the vehicles moves for scenario 3. The vehicle move from initial point A to point E

DISTANCE PREDICTION FIGURE. 92 represents the distance prediction as the vehicle moves for scenario 1 versus the real distance remaining (from point A to B). The estimated distance is very close to the real one. An error can be observed at the end of the cycle : Indeed the estimated distance increase instead of decreasing close to 0. It can be explain by looking at the clustering algorithm : Each same final point in a radius of 200 m are clustered and a new center is calculated : the matrix calculate the probability and the distance from the clustered center. The 200 m radius error clearly appear in the figure.

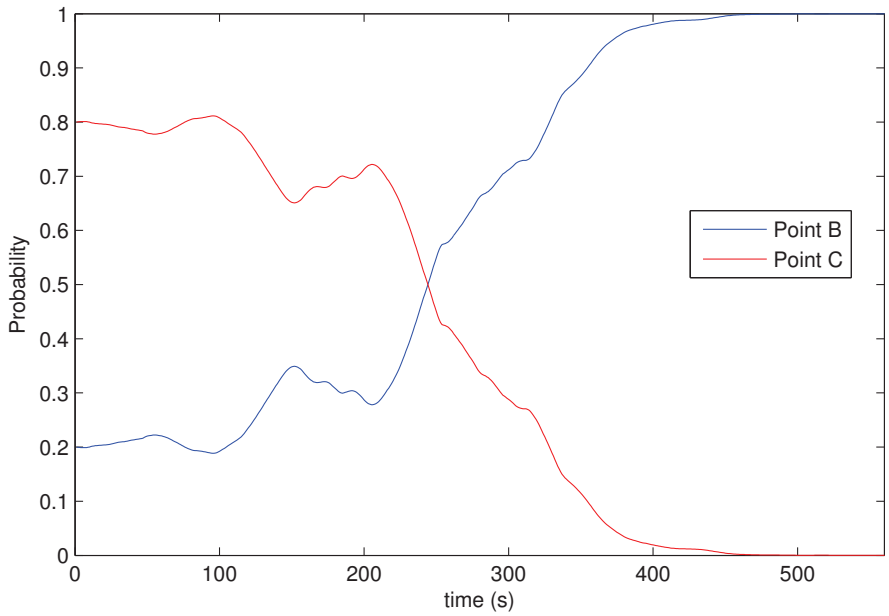

FIGURE 90. Probability updates as the vehicle moves for scenario 2

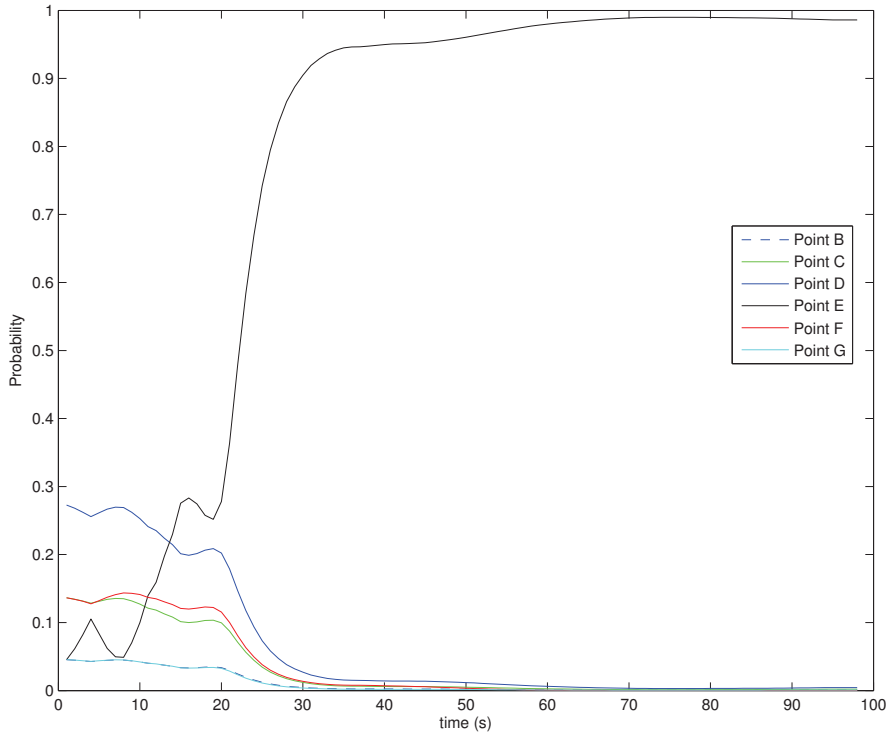

FIGURE 91. Probability updates as the vehicle moves for scenario 3

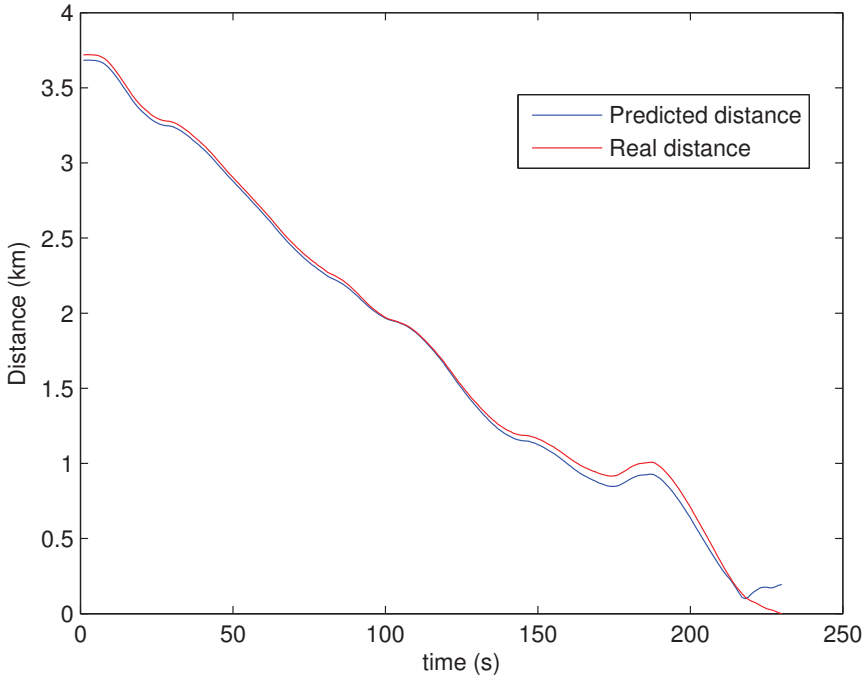

FIGURE 92. Distance remaining prediction as the vehicle moves for scenario 1

3.7.3 *Conclusion*

A destination prediction algorithm has been presented : By combining a learning part with a Markov probability matrix and a real time algorithm which update theses probabilities as the vehicle moves, the destination of the vehicle and the distance remaining can be predicted. these informations allow the control strategy to be adaptively and control the depth of discharge of the battery state of charge in a plug in hybrid electric vehicle. Futures works will aim to build a real time controller based on Equivalent Consumption Management Strategy including the remaining distance for a series hybrid electric vehicle based on ICE and battery. This works has been realized in collaboration with the North Carolina State University (NCSU) and Dr Srdkan Lukic.

3.8 CONCLUSION

In this chapter, real time control strategy has been presented for several hybrid electric vehicle configuration. It has been proven than optimized and adaptive control allows to save fuel consumption. A real time controller based on fuzzy logic designed for fuel cell hybrid electric vehicle has been presented, allowing the fuel cell to run at bests efficiency points while keeping the vehicle able to runs different driving patterns. The controller has been experimented into a lightweight hybrid series vehicle and simulations results are been validated. Moreover, a destination prediction algorithm aiming to determine the remaining distance of a vehicle trip has been presented. The results allows to build real time control strategy for plug in hybrid vehicle controlling the depth of discharge of the battery.

GENERAL CONCLUSION

The objectives of this thesis was to investigate the new methodologies of conception of an hybrid electric vehicle and its associate control strategy. A focus on series architecture has been done, and a new methodology of sizing regarding the literature and the manufacturer conception process has been presented. This methodology analysis a family of generated driving cycle rather than a single one to size the power train component.
Different designs of control strategy regarding the power train built has been then proposed : An offline strategy based on Dynamic programming optimization in order to determine the best power split between the two sources of an hybrid electric vehicle : In the case of the thesis's study subject : a fuel cell hybrid electric truck. Then a real time controller based on fuzzy logic has been presented and validated. Moreover, optimization and adaptation algorithm has been created in order to optimize the hydrogen consumption while keeping the controller adaptive to all driving patterns.
Finally, a control strategy on plug in hybrid electric vehicle has been presented, focusing on a destination prediction algorithm which increase greatly the fuel economy.

CONTRIBUTIONS

Regarding the literature, this thesis brought new contributions on the sizing and controls of hybrid electric vehicles :

- *Driving cycle generation* : A driving cycle generator has been created, allowing to create random driving cycle which have the same patterns as calibrated one.
- *Energy sources sizing methodology* : based on statistical description of a driving cycle family, this methodology gives specific informations about the power and capacity of energy sources in an hybrid electric vehicle.
- *Real time controller for fuel cell hybrid electric vehicle and its optimization for a specific pattern* : The fuzzy logic controller presented has been validated on a real fuel cell hybrid electric vehicle and its optimization by genetic algorithm allow to save 22 % of hydrogen consumption. Moreover, the driving cycle recognition algorithm allows to implement this optimization while keeping good results on other patterns like highway.
- *Destination prediction algorithm and its associate control strategy* : The destination prediction algorithm allow to precisely define the remaining distance to run by the vehicle and gives useful informations to the control strategy in order to decrease steadily the state of charge of the battery, saving fuel consumption.

PUBLICATIONS

The thesis's contributions leads to severals publications :

– *International Journal with proceeding* :

A. Ravey, N. Watrin, B. Blunier, D. Bouquain, and A. Miraoui : **Energy sources sizing methodology for hybrid fuel cell vehicles based on statistical description of driving cycles**. *Vehicular Technology, IEEE Transactions on* - 2011.

A. Ravey, B. Blunier, and A. Miraoui : **Control strategies for fuel-cell based hybrid electric vehicles : From offline to online and experimental results**. *Vehicular Technology, IEEE Transactions on* - 2012.

– *International Conference with proceeding* :

A. Ravey, N. Watrin, B. Blunier, and A. Miraoui : **Energy sources sizing for hybrid fuel cell vehicles based on statistical description of driving cycles**. *Vehicle Power and Propulsion Conference (VPPC), IEEE* - Lille, France - 2010.

A. Ravey, B. Blunier, and A. Miraoui : **Control strategies for fuel cell based hybrid electric vehicles : From offline to online**. *Vehicle Power and Propulsion Conference (VPPC), IEEE*- 2011.

A. Ravey, R. Roche, B. Blunier, and A. Miraoui : **Combined optimal sizing and energy management of hybrid electric vehicles**. *International Transportation Electrification Conference (ITEC)* - 2012.

A. Ravey, B. Blunier, S. Lukic, and A. Miraoui. **Control strategy of fuel cell hybrid electric vehicle based on driving cycle recognition**. *International Transportation Electrification Conference (ITEC)* - 2012

– *National conference with proceeding* :

A. Ravey, B. Blunier and A. Miraoui. **Dimensionnement et contrôle d'un véhicule hybride électrique basé sur une pile à combustible**. *Electrotechnique du Futur* - Belfort, France - 2011.

FUTURE WORKS

This thesis opened prospers to new improvement in hybrid electric vehicles domains : Firstly, the new sizing methodology including the driving cycle generator is applied to a real application, the Mobypost project : This project

aims to build a fuel cell hybrid vehicle for postal delivery services. The hydrogen is produce with renewable energy by electrolysis water with the help of photo voltaic panels. The power train design of the vehicle is build with the sizing methodology described in section 2.2 by analyzing the postal deliver driving cycle, using the generator based on recorded data ; to generate a family of cycle. The sizing methodology is then applied to define the power of the fuel cell and the battery pack size. This project leads to the conception of 10 vehicle which will be used by French postal delivery in 2013.
The destination prediction algorithm will be implemented into a real application to validate it. Moreover, a new study starting from this control strategy adding the vehicle to grid layer will be investigated : the control strategy will adapts the depth of discharge of the battery with taking into account the cost of electricity charging.

BIBLIOGRAPHY

[1] D. Calef and R. Goble. The allure of technology : How france and california promoted electric and hybrid vehicles to reduce urban air pollution. *Policy sciences*, 40(1) :1–34, 2007.

[2] CC Chan. An overview of electric vehicle technology. *Proceedings of the IEEE*, 81(9) :1202–1213, 1993.

[3] D.A. Kirsch. The electric vehicle and the burden of history. 2000.

[4] K. Rajashekara. History of electric vehicles in general motors. *Industry Applications, IEEE Transactions on*, 30(4) :897–904, 1994.

[5] S. Beggs, S. Cardell, and J. Hausman. Assessing the potential demand for electric cars. *Journal of econometrics*, 17(1) :1–19, 1981.

[6] M. Ehsani, Y. Gao, and A. Emadi. Modern electric, hybrid electric, and fuel cell vehicles : fundamentals, theory, and design. 2009.

[7] K. FUJIWARA, T. KOGURE, and T. BABA. Series hybrid electric vehicles. July 29 2005. WO Patent 2,005,068,244.

[8] S.M. Lukic and A. Emadi. Effects of drivetrain hybridization on fuel economy and dynamic performance of parallel hybrid electric vehicles. *Vehicular Technology, IEEE Transactions on*, 53(2) :385–389, 2004.

[9] J. Liu and H. Peng. Modeling and control of a power-split hybrid vehicle. *Control Systems Technology, IEEE Transactions on*, 16(6) :1242–1251, 2008.

[10] S.G. Wirasingha and A. Emadi. Classification and review of control strategies for plug-in hybrid electric vehicles. *Vehicular Technology, IEEE Transactions on*, 60(1) :111–122, 2011.

[11] Benjamin Blunier and Abdellatif Miraoui. *20 Questions sur la pile à combustible*. Technip, 2008. (in French).

[12] Benjamin Blunier and Abdellatif Miraoui. *Piles à combustible, Principe, modélisation et applications avec exercices et problèmes corrigés*. Technosup. 2007. (in French).

[13] DOE. Hydrogen, fuel cells and infrastructure technologies program, multi-year research, development and demonstration plan. U.S. Department of Energy, May 2007. Available online : www1.eere.energy.gov/hydrogenandfuelcells/mypp/.

[14] JC Amphlett, RF Mann, BA Peppley, PR Roberge, and A. Rodrigues. A model predicting transient responses of proton exchange membrane fuel cells. *Journal of Power Sources*, 61(1-2) :183–188, 1996.

[15] Benjamin Blunier and Abdellatif Miraoui. Proton exchange membrane fuel cell air management in automotive applications. *Journal of Fuel Cell Science and Technology*, 7(4) :041007, 2010. doi : 10.1115/1.4000627. URL http://link.aip.org/link/?FCT/7/041007/1.

[16] Benjamin Blunier and Abdellatif Miraoui. Air management in pem fuel cell : State-of-the-art and prospectives. In *ACEMP'07, Electromotion*, pages 245–253. IEEE-PES-MSC, sep 2007. doi : 10.1109/ACEMP.2007.4510510. Invited paper.

[17] Jay T. Pukrushpan, Anna G. Stefanopoulou, and Huei Peng. *Control of Fuel Cell Power Systems : Principle, Modeling Analysis and Feedback Design*. Advances in Industrial Control, 2004. ISBN : 1852338164.

[18] A. Sciarretta and L. Guzzella. Control of hybrid electric vehicles. *Control Systems Magazine, IEEE*, 27(2) :60–70, 2007.

[19] F.R. Salmasi. Control strategies for hybrid electric vehicles : Evolution, classification, comparison, and future trends. *Vehicular Technology, IEEE Transactions on*, 56(5) :2393–2404, 2007.

[20] Q. Gong, Y. Li, and Z.R. Peng. Trip based optimal power management of plug-in hybrid electric vehicle with advanced traffic modeling. *SAE International Journal of Engines*, 1(1) :861–872, 2009.

[21] Q. Gong, Y. Li, and Z.R. Peng. Optimal power management of plug-in hev with intelligent transportation system. pages 1–6, 2007.

[22] G. Paganelli, S. Delprat, TM Guerra, J. Rimaux, and JJ Santin. Equivalent consumption minimization strategy for parallel hybrid powertrains. 4 : 2076–2081, 2002.

[23] P. Pisu and G. Rizzoni. A supervisory control strategy for series hybrid electric vehicles with two energy storage systems. pages 8–pp, 2005.

[24] S. Stockar, V. Marano, M. Canova, G. Rizzoni, and L. Guzzella. Energy-optimal control of plug-in hybrid electric vehicles for real-world driving cycles. *Vehicular Technology, IEEE Transactions on*, (99) :1–1, 2011.

[25] L. Xu, G. Cao, J. Li, F. Yang, L. Lu, and M. Ouyang. Equivalent consumption minimization strategies of series hybrid city buses.

[26] Y. Zhu, Y. Chen, and Q. Chen. Analysis and design of an optimal energy management and control system for hybrid electric vehicles. 2002.

[27] G. Paganelli, TM Guerra, S. Delprat, JJ Santin, M. Delhom, and E. Combes. Simulation and assessment of power control strategies for a parallel hybrid car. *Proceedings of the Institution of Mechanical Engineers, Part D : Journal of Automobile Engineering*, 214(7) :705–717, 2000.

[28] G. Paganelli, M. Tateno, A. Brahma, G. Rizzoni, and Y. Guezennec. Control development for a hybrid-electric sport-utility vehicle : strategy, implementation and field test results. 6 :5064–5069, 2001.

[29] Scott Fish and Troy B. Savoie. Simulation-based optimal sizing of hybrid electric vehicle components for specific combat missions. *IEEE Transaction On Magnetics*, 37(1) :485–488, 2001.

[30] A. Sciarretta, M. Back, and L. Guzzella. Optimal control of parallel hybrid electric vehicles. *Control Systems Technology, IEEE Transactions on*, 12(3) :352–363, 2004.

[31] P. Tulpule, V. Marano, and G. Rizzoni. Effects of different phev control strategies on vehicle performance. pages 3950–3955, 2009.

[32] S. Li, S. Sharkh, F. Walsh, and C. Zhang. Energy and battery management of a plug-in series hybrid electric vehicle using fuzzy logic. *Vehicular Technology, IEEE Transactions on*, (99) :1–1, 2011.

[33] J. Moreno, M.E. Ortúzar, and J.W. Dixon. Energy-management system for a hybrid electric vehicle, using ultracapacitors and neural networks. *Industrial Electronics, IEEE Transactions on*, 53(2) :614–623, 2006. ISSN 0278-0046.

[34] C. Zhang and A. Vahid. Real-time optimal control of plug-in hybrid vehicles with trip preview. pages 6917–6922, 2010.

[35] T. Yi, Z. Xin, Z. Liang, and Z. Xinn. Intelligent energy management based on driving cycle identification using fuzzy neural network. In *Computational Intelligence and Design, 2009. ISCID'09. Second International Symposium on*, volume 2, pages 501–504. IEEE, 2009.

[36] J. Bernard, S. Delprat, FN Buchi, and T.M. Guerra. Fuel-cell hybrid powertrain : Toward minimization of hydrogen consumption. *Vehicular Technology, IEEE Transactions on*, 58(7) :3168–3176, 2009.

[37] B. Geng, J. Mills, and D. Sun. Two stage energy management control of fuel cell plug-in hybrid electric vehicles considering fuel cell longevity. *Vehicular Technology, IEEE Transactions on*, (99) :1–1, 2011.

[38] M. Zandi, A. Payman, J.P. Martin, S. Pierfederici, B. Davat, and F. Meibody-Tabar. Energy management of a fuel cell/supercapacitor/battery power source for electric vehicular applications. *Vehicular Technology, IEEE Transactions on*, 60(2) :433–443, 2011.

[39] D. Ambuhl and L. Guzzella. Predictive reference signal generator for hybrid electric vehicles. *Vehicular Technology, IEEE Transactions on*, 58(9) : 4730–4740, 2009.

[40] C. Musardo, G. Rizzoni, Y. Guezennec, and B. Staccia. A-ecms : An adaptive algorithm for hybrid electric vehicle energy management. *European Journal of Control*, 11(4-5) :509, 2005.

[41] C. Zhang, A. Vahidi, P. Pisu, X. Li, and K. Tennant. Role of terrain preview in energy management of hybrid electric vehicles. *Vehicular Technology, IEEE Transactions on*, 59(3) :1139–1147, 2010.

[42] C. Zhang and A. Vahidi. Route preview in energy management of plug-in hybrid vehicles. *Control Systems Technology, IEEE Transactions on*, (99) : 1–8, 2011.

[43] B.D. Ziebart. *Modeling Purposeful Adaptive Behavior with the Principle of Maximum Causal Entropy*. PhD thesis, 2010.

[44] Tian Yi Zhang Liang, Zhang Xin and Zhang Xinn. Intelligent energy management based on the driving cycle sensitivity identification using svm. *Second International Symposium on Computational Intelligence and Design*, pages 513–516, 2009.

[45] Jeffrey Raymond Kenworthy. Driving cycles, urban from and transport energy. 1986.

[46] EPA Dynamometer Driving Schedules. Cycles routiers. URL `http://www.epa.gov/nvfel/testing/dynamometer.htm`.

[47] R. Joumard, M. André, R. Vidon, P. Tassel, and C. Pruvost. Influence of driving cycles on unit emissions from passenger cars. *Atmospheric environment*, 34(27) :4621–4628, 2000.

[48] W.T. Hung, K.M. Tam, C.P. Lee, L.Y. Chan, and C.S. Cheung. Comparison of driving characteristics in cities of pearl river delta, china. *Atmospheric Environment*, 39(4) :615–625, 2005.

[49] M. Jain, C. Desai, N. Kharma, and S.S. Williamson. Optimal powertrain component sizing of a fuel cell plug-in hybrid electric vehicle using multi-objective genetic algorithm. In *Industrial Electronics, 2009. IECON'09. 35th Annual Conference of IEEE*, pages 3741–3746. IEEE.

[50] D. Browningb Q. Caia, D.J.L. Bretta and N.P. Brandona. A sizing-design methodology for hybrid fuel cell power systems and its application to an unmanned underwater vehicle. *Journal of Power Sources 195*, 2010.

[51] Lino Guzzella and Antonio Sciarretta. *Vehicle Propulsion Systems, Introduction to modeling and optimization*. Springer, 1 edition, 2005.

[52] H.L. Husted. A comparative study of the production applications of hybrid electric powertrains. *SAE paper*, pages 01–2307, 2003.

[53] M. Westbrook. *The electric and hybrid electric car*. Society of Automotive Engineers, 400 Commonwealth Dr, Warrendale, PA, 15096, USA, 2001.

[54] E. Schaltz, A. Khaligh, and P.O. Rasmussen. Influence of battery/ultracapacitor energy-storage sizing on battery lifetime in a fuel cell hybrid electric vehicle. *Vehicular Technology, IEEE Transactions on*, 58(8) :3882–3891, 2009.

[55] R. Apter and M. Prathaler. Regeneration of power in hybrid vehicles. In *Vehicular Technology Conference, 2002. VTC Spring 2002. IEEE 55th*, volume 4, pages 2063–2069. IEEE, 2002.

[56] David Linden and Thomas B. Reddy. *Batteries Handbook (3rd Edition)*. McGraw-Hill, 2002.

[57] K. Kawashima, T. Uchida, and Y. Hori. Development of a novel ultracapacitor electric vehicle and methods to cope with voltage variation. In *Vehicle Power and Propulsion Conference, 2009. VPPC'09. IEEE*, pages 724–729. IEEE, 2009.

[58] Alexandre Ravey, Nicolas Watrin, Benjamin Blunier, and Abdellatif Miraoui. Energy sources sizing for hybrid fuel cell vehicles based on statistical description of driving cycles. In *Vehicle Power and Propulsion Conference, 2010. VPPC '2010. IEEE*, 2010.

[59] A. Ravey, N. Watrin, B. Blunier, D. Bouquain, and A. Miraoui. Energy sources sizing methodology for hybrid fuel cell vehicles based on statistical description of driving cycles. *Vehicular Technology, IEEE Transactions on*, (99) :1–1, 2011.

[60] J. Santin, C.H. Onder, J. Bernard, D. Isler, P. Kobler, F. Kolb, N. Weidmann, and L. Guzzella. *The world's most fuel efficient vehicle*. 2007.

[61] J. Bernard, S. Delprat, F. Buechi, and TM Guerra. Global Optimisation in the power management of a Fuel Cell Hybrid Vehicle (FCHV). In *Vehicle Power and Propulsion Conference, 2006. VPPC'06. IEEE*, pages 1–6. IEEE, 2007. ISBN 1424401585.

[62] Rimaux J. Delprat S., Guerra T. Control strategy for hybrid vehicles : synthesis and evaluation. In *IEEE Vehicular Technology Conference, Orlando, USA*, 2003.

[63] S. Kermani, S. Delprat, TM Guerra, and R. Trigui. Predictive control for HEV energy management : experimental results. pages 364–369, 2009.

[64] S. Delprat, TM Guerra, and J. Rimaux. Optimal control of a parallel powertrain : from global optimization to real time control strategy. 4 : 2082–2088, 2002.

[65] O. Sundstrom and L. Guzzella. A generic dynamic programming Matlab function. pages 1625–1630, 2009. ISSN 1085-1992.

[66] A. Ravey, B. Blunier, and A. Miraoui. Dimensionnement et contrôle d' un véhicule hybride électrique basé sur une pile à combustible. In *Electrotechnique du Futur*, 2011.

[67] D.E. Goldberg. *Genetic algorithms in search, optimization, and machine learning*. Addison-wesley, 1989.

[68] A. Ravey, R. Roche, B. Blunier, and A. Miraoui. Combined optimal sizing and energy management of hybrid electric vehicles. pages 1–6, 2012.

[69] MH Hajimiri and FR Salmasi. A fuzzy energy management strategy for series hybrid electric vehicle with predictive control and durability extension of the battery. pages 1–5, 2006.

[70] Benjamin Blunier, David Bouquain, and Abdellatif Miraoui. *Alternative Propulsion Systems for Automobiles*, chapter Fuel cells, Energy Management using Fuel Cells and Supercapacitors, pages 97–116. Number 2. Expert Verlag, 2008. ISBN-13 : 978-3-8169-2835-5.

[71] Benjamin Blunier, Marcelo G. Simoes, and Abdellatif Miraoui. Fuzzy logic controller development of a hybrid fuel cell-battery auxiliary power unit for remote applications. *IEEE International Conference on Industry Applications*, 2010.

[72] R. Wang and S.M. Lukic. Review of driving conditions prediction and driving style recognition based control algorithms for hybrid electric vehicles. In *Vehicle Power and Propulsion Conference (VPPC), 2011 IEEE*, pages 1–7. IEEE, 2011.

[73] M. Kabalo, B. Blunier, D. Bouquain, and A. Miraoui. Comparaison analysis of high voltage ratio low input current ripple floating interleaving boost converters for fuel cell applications. In *Vehicle Power and Propulsion Conference (VPPC), 2011 IEEE*, pages 1–6. IEEE, 2011.

[74] M. Kabalo, B. Blunier, D. Bouquain, and A. Miraoui. State-of-the-art of dc-dc converters for fuel cell vehicles. In *Vehicle Power and Propulsion Conference (VPPC), 2010 IEEE*, pages 1–6. IEEE, 2010.

[75] S.M. Lukic, J. Cao, R.C. Bansal, F. Rodriguez, and A. Emadi. Energy storage systems for automotive applications. *Industrial Electronics, IEEE Transactions on*, 55(6) :2258–2267, 2008.

[76] A. Ravey, B. Blunier, and A. Miraoui. Control strategies for fuel cell based hybrid electric vehicles : From offline to online. In *Vehicle Power and Propulsion Conference (VPPC), 2011 IEEE*, pages 1–4. IEEE, 2011.

[77] A. Ravey, B. Blunier, and A. Miraoui. Control strategies for fuel-cell-based hybrid electric vehicles : From offline to online and experimental results. *Vehicular Technology, IEEE Transactions on*, 61(6) :2452–2457, 2012.

[78] C.C. Lin, S. Jeon, H. Peng, and J.M. Lee. Driving pattern recognition for control of hybrid electric trucks. *Vehicle System Dynamics*, 42(1-2) :41–58, 2004.

[79] A. Ravey, B. Blunier, S. Lukic, and A. Miraoui. Control strategy of fuel cell hybrid electric vehicle based on driving cycle recognition. pages 1–5, 2012.

[80] B. Sareni C. R. Akli, X. Roboam and A. Jeunesse. Energy management and sizing of a hybrid locomotive. *Power Electronics and Applications*, pages 1–10, 2007.

[81] R. Hariharan and K. Toyama. Project lachesis : parsing and modeling location histories. *Geographic Information Science*, pages 106–124, 2004.

[82] J. Krumm and E. Horvitz. Predestination : Inferring destinations from partial trajectories. *UbiComp 2006 : Ubiquitous Computing*, pages 243–260, 2006.

[83] B.D. Ziebart, A.L. Maas, A.K. Dey, and J.A. Bagnell. Navigate like a cabbie : Probabilistic reasoning from observed context-aware behavior. pages 322–331, 2008.

[84] X. Kang. Vehicle-infrastructure integration (vii) enabled plug-in hybrid electric vehicles (phevs) for traffic and energy management. 2009.

[85] L. Liao, D.J. Patterson, D. Fox, and H. Kautz. Learning and inferring transportation routines. *Artificial Intelligence*, 171(5) :311–331, 2007.

[86] N. Persad-Maharaj, S.J. Barbeau, M.A. Labrador, P.L. Winters, R. Pérez, and N.L. Georggi. Real-time travel path prediction using gps-enabled mobile phones. 30413 :16–20, 2008.

[87] N. Marmasse and C. Schmandt. Location-aware information delivery with commotion. pages 361–370, 2000.

[88] T. Cheong and CC White. Dynamic traveling salesman problem : Value of real-time traffic information. *Intelligent Transportation Systems, IEEE Transactions on*, (99) :1–12.

[89] S. Barbeau, M.A. Labrador, A. Perez, P. Winters, N. Georggi, D. Aguilar, and R. Perez. Dynamic management of real-time location data on gps-enabled mobile phones. pages 343–348, 2008.

[90] D. Ashbrook and T. Starner. Using gps to learn significant locations and predict movement across multiple users. *Personal and Ubiquitous Computing*, 7(5) :275–286, 2003.

[91] R. Simmons, B. Browning, Y. Zhang, and V. Sadekar. Learning to predict driver route and destination intent. pages 127–132, 2006.

[92] D. Calef and R. Goble. The allure of technology : How france and california promoted electric and hybrid vehicles to reduce urban air pollution. *Policy sciences*, 40(1) :1–34, 2007.